5-2018

Development of Microdialysis Probes in Series Approach Toward Eliminating Microdialysis Sampling Calibration: Miniaturization into a PDMS Microfluidic Device

Randy Espinal Cabrera
University of Arkansas, Fayetteville

Citation

Development of Microdialysis Probes in Series Approach Toward Eliminating Microdialysis Sampling
Calibration: Miniaturization into a PDMS Microfluidic Device

A dissertation submitted in partial fulfillment
of the requirements for the degree of
Doctor of Philosophy in Chemistry

by

Randy Francisco Espinal Cabrera
Autonomous University of Santo Domingo
Bachelor of Science in Chemistry, 2004
University of Arkansas
Master of Science in Chemistry, 2012

May 2018
University of Arkansas

This dissertation is approved for recommendation to the Graduate Council.

_____
Dr. Julie A. Stenken
Dissertation Director

_____   _____
Dr. Ingrid Fritsch   Dr. Christa Hestekin
Committee Member   Committee Member

_____   _____
Dr. Colin Heyes   Dr. David Paul
Committee Member   Committee Member

_____
Dr. Steve Tung
Committee Member

ABSTRACT

A new microdialysis sampling method and microfluidic device were developed in vitro. The method consisted of using up to four microdialysis sampling probes connected in series to evaluate the relative recovery (RR) of different model solutes methyl orange, fluorescein isothiocyanate (FITC)-dextran average mol. wt. 4,000 (FITC-4), FITC-10, FITC-20, and FITC-40. Different flow rates (0.8, 1.0, and 1.5 µL/min) were used to compare experimentally observed relative recoveries with theoretical estimations. With increasing the number of probes in series, the relative recovery increases and ~100% (99.7% ± 0.9%) relative recovery for methyl orange was obtained. For larger molecules such as fluorescein isothiocyanate (FITC)-dextran average mol. wt. 4,000 (FITC-4), FITC-10, FITC-20, and FITC-40, RR of 66.3% ± 0.0%, 39.4% ± 0.6%, 18.7% ± 0.1%, and 7.7% ± 0.1%, respectively, were obtained using four microdialysis sampling probes in series at 0.8 µL/min. Using theoretical estimations, the number of microdialysis probes in series needed to achieve 99% RR was determined for each solute. The theoretical estimations started deviating from experiments at mol. wt. 10,000 (FITC-10). For example, the deviations from experiments for FITC-10, FITC-20, and FITC-40 were +52%, +149%, and +179% respectively. On the other hand, methyl orange and FITC-4 theoretical estimations were closer to the experiments (-1%, underestimation, and +15%, overestimation). The method developed for this dissertation was miniaturized in a polydimethylsiloxane (PDMS) microfluidic device having a flat polyethersulfone membrane and seven micro-channels connected in series. Push-pull experiments determined that the optimal setting for this microfluidic device prototype during the collection of methyl orange was 0.2 µL/min-1.0 µL/min. The relative recovery of methyl orange using this setting was 78.8% ± 2.5%. This result indicated that a working microfluidic device prototype was developed. Further optimizations need to be performed to reach the same level as the microdialysis probes in series method. All the work conducted to achieve the development and miniaturization of the microdialysis probes in series approach is presented in this dissertation.

I feel very fortunate to have had an excellent group of professors as my advisors. Their help, guidance, and suggestions were very instrumental to complete my PhD.

DEDICATION

I want to dedicate this dissertation to my mother Luz M. Cabrera García. It always saddens me to think that she is no longer here with me. However, I am always going to remember her as a happy person. She was always smiling and being positive even in the direst of circumstances. She made sure that my siblings and I were well fed and healthy. Even as an adult she told us not to drink or eat unhealthy food and stay away from bad habits. I am very lucky and proud of my mom. She was a very creative and hardworking person always trying different business ventures. She moved heaven and earth to make sure that her children were well educated and healthy. Her selflessness is something that I am always going to remember.

TABLE OF CONTENTS

LIST OF TABLES

LIST OF FIGURES

GLOSSARY

Abbreviations:

ANOVA	Analysis of variance
ELISA	Enzyme-linked immunosorbent assay
EE	Extraction efficiency
ECF	Extracellular fluid
FR	Fluid recovery
FEP	Fluorinated ethylene propylene
ICF	Intracellular fluid
FITC	Isothiocyanate-dextran
MWCO	Molecular weight cutoff
PAES	Polyarylethersulfone
PC	Polycarbonate/Polyether
PDMS	Polydimethylsiloxane
PES	Polyethersulfone
RR	Relative recovery

Symbols:

A	Extracellular fluid concentration of biomolecules
a	Aspect ratio of rectangular channel
c	Concentration of perfusate
C_{outlet}	Dialysate concentration or outlet concentration
$C_{sample, \infty}$	Concentration of the analyte far away from the collection point
D	Hydraulic diameter
D_e	Diffusion coefficient in the extracellular space
D_q	Diffusion coefficient in the quiescent medium
f	Friction factor for fully developed laminar flow in noncircular pipes
f_Q	Ultrafiltration factor

K	Apparent diffusion constant across the membrane
k	mass transfer coefficient
L	Microchannel length
L_m	Effective membrane length
P	Overall probe-external medium permeability
Q	Flow rate
Q_d/ Q_{in}	Flow rate of the perfusion fluid
Q_{out}	Flow rate of the dialysate
ΔP	Pressure drop
$+\Delta P$	Positive pressure difference
$-\Delta P$	Negative pressure difference
Δp_a	Pressure drop within the annulus fluid
$\mathfrak{R}_a$	Annulus hydraulic resistance
r_{cann}	Outer radius of the cannula
r_i	Membrane inner radius
R_d	Mass transport resistance of the dialysate
R_e	Reynolds number
R_m	Mass transport resistance of the microdialysis probe membrane
R_q	Mass transport resistance of the quiescent medium external to the microdialysis probe
r_o	Membrane outer radius
S/A	Surface area of the microdialysis probe membrane
$\mathcal{S}_m$	Log mean surface area of membrane
t	Residence time
λ	Tortuosity factor
η	Perfusate viscosity
ς	Annulus radius ratio
V_{avg}	Average velocity

1 Chapter 1. Introduction to microdialysis sampling and microfluidic devices
1.1 Microdialysis sampling

1.1.1 History

Microdialysis sampling is a diffusion-based separation technique commonly used to sample biomolecules from fluid compartments (Figure 1.1) in mammals such as humans,[1, 2] monkeys,[3, 4] rodents,[5] and pigs.[6, 7] Microdialysis probes are composed of a concentric semi-permeable membrane, outer support membrane layer, inner cannula, and inlet and outlet tubing, see Figure 1.2. Microdialysis samples the extracellular fluid (ECF) or the fluid between the cells, because this is where chemical transport and chemical communication occurs. Proteins, electrolytes, and other chemicals travel in this region and are able to be collected during microdialysis sampling experiments.[8] The intracellular fluid (ICF), on the other hand, is the fluid inside the cell enclosed by plasma membranes. This region is closely regulated by the body and makes up ~60% of the total water in the human body.[8] The amount of water present in the human body varies depending on the type tissue from 8% in the teeth to 80-85% in the brain.[8] Microdialysis sampling has been widely used to collect many different classes of molecules from extracellular fluid (ECF) space with more than 15,000 publications documenting the collection of various solutes of biomedical interest.[9, 10] Like many separation techniques microdialysis sampling went through an evolutionary usage and development process.
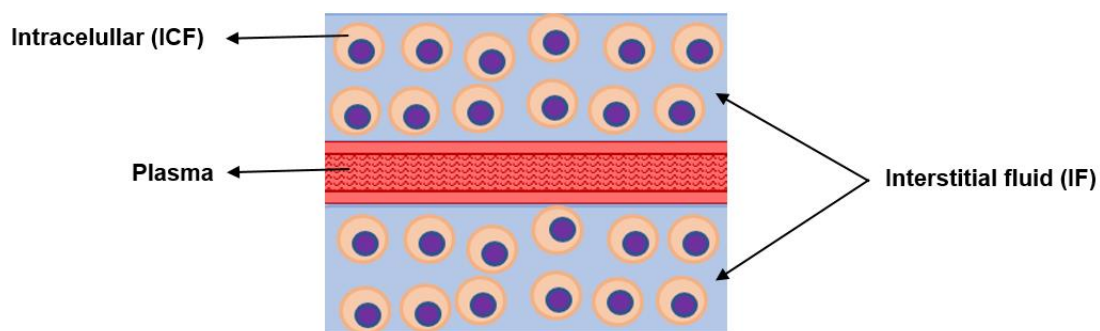
Figure 1.1. Schematic representation of fluid compartments in the human body (Redrawn from reference [11]).
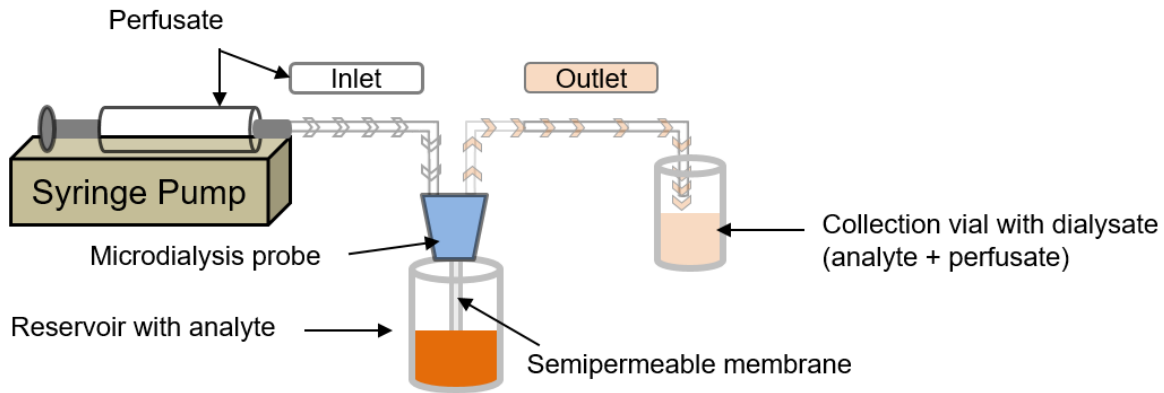
Figure 1.2. Schematic representation of traditional microdialysis sampling experiment setup.

Prior to microdialysis sampling, push-pull technique and dialysis bags were the preferred methods to collect biomolecules from living systems. Briefly, push-pull technique consists of pushing a solution through a cannula into a sampling site and pulling the solution by an adjacent cannula.[12] Push-pull technique fell out favor due to the fact that it was difficult to operate and caused a significant amount of tissue damage.[12] In 1966 Bito et al. were the first to propose the use of dialysis bags, sometimes called sacs for the collection of biomolecules from the brain of dogs.[9, 12, 13] One of the problems with this approach was that you could only take one sample per dialysis bag implanted.[13] Moreover, these dialysis bags were implanted for more than two months in order to study concentration changes of the biomolecules of interest.[12] As it is well-known, longer implantation periods lead to encapsulation of any implanted device by living systems foreign body response, when the immune system is unable to destroy it and try to isolate it.[14, 15] Foreign body response is outside of the scope of this dissertation and it is not going to be addressed in detail here.

Another improvement towards to what we nowadays called microdialysis sampling was demonstrated by Delgado et al. six years later (1972). Delgado and colleagues further developed the dialysis bag technique and called it dialytrode.[9, 13, 16] The dialytrode worked by perfusing a solution into a dialysis bag and moving it to an area where it could be collected and analyzed.[9] This process mirrored today's microdialysis sampling in which a solution is infused into a microdialysis probe and then collected from an outlet tubing.[13]

Finally, Ungerstedt et al. replaced the dialysis bags with hollow fibers and successfully measured neurochemicals in the brain of rats.[9, 12] Since then, microdialysis sampling became the preferred sampling technique to study biomolecules in living systems.

Commercially available microdialysis probes, as shown on Figure 1.3, consist of two fluorinated ethylene propylene (FEP) pieces of tubing (inlet and outlet) and a cylindrical hollow fiber semipermeable membrane of 0.5 mm in diameter. Semipermeable membranes are typically made of either polyarylethersulfone (PAES) or polyethersulfone (PES). Other materials such as polycarbonate/polyether (PC), polyamide[17] and cellulose acetate are used as microdialysis probe membranes as well. Microdialysis probes of different membrane lengths to sample from subcutaneous (10 mm) and brain (4 mm) spaces can be purchased from different vendors.[18] Also, microdialysis probes having membranes of different molecular weight cutoffs (e.g. 100 kDa and 1000 kDa) are commercially available.
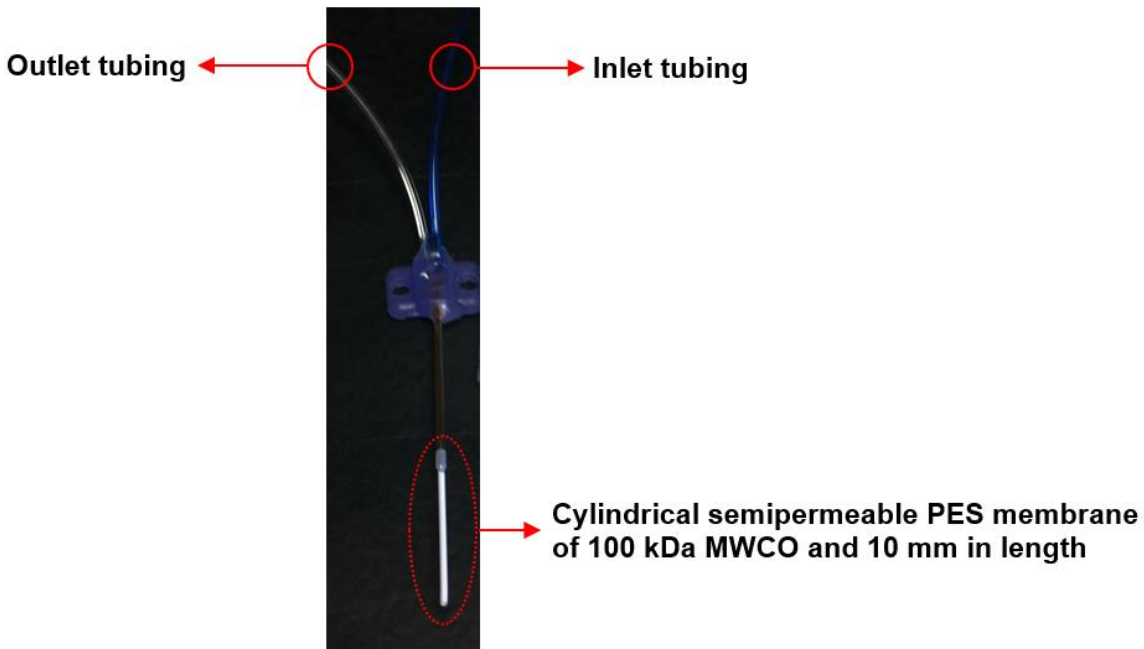
Figure 1.3. Picture of a commercially available CMA 20 microdialysis probe from Harvard Apparatus.

1.1.2   Mechanism

As previously mentioned, microdialysis sampling is a diffusion-based separation technique. Traditionally, microdialysis experiments require a microdialysis probe, gas-tight syringe, syringe pump, and perfusion fluid (Figure 1.2). During microdialysis sampling the perfusion fluid or perfusate is selected so that its chemical composition matches the chemical properties of their *milieu* (ECF) such as a pH and ionic strength.[19] Matching the chemical properties of the perfusion fluid to the environment in which it is perfused in is important to avoid disrupting the biology of the collection site or tissue.

Microdialysis sampling experiments can be conducted either *in vivo* or *in vitro*. *In vitro* microdialysis sampling experiments are conducted to gain information about the efficiency of the microdialysis probes and transport behavior of biomolecules. For example, microdialysis sampling has been used *in vitro* to sample peptides and proteins in highly complex bioprocesses.[20] However, most application are conducted *in vivo*. During *in vivo* microdialysis the sampling site is a living system's fluid compartment (e.g. ECF). On the other hand, the sampling site during *in vitro* microdialysis sampling experiments is a synthetic reservoir aimed to mimic the physicochemical conditions of living system's fluid compartments. In some cases, a small plastic vial or any other reservoir is used as sampling site. This causes several issues when correlating *in vitro* experiments to *in vivo* since the concentration of analyte in fluid compartments is never precisely known and can change rapidly overtime. Moreover, the tortuous path that biomolecules diffuse through during *in vivo* collections is significantly larger than *in vitro* collections, see Figure 1.4.[21] A new approach in which several or four microdialysis sampling probes are connected in series was developed for this dissertation. This microdialysis in series approach seeks to address the problem of never knowing the concentration of analyte in fluid compartments by getting to an equilibrium concentration as the surface area of the microdialysis probe increases as well as the residence time. This issue will be addressed in more detail later in the chapter.

The main driving forces acting on microdialysis sampling technique are hydraulic and concentration gradient. In order to create a hydraulic force during microdialysis sampling, a positive pressure (flow rate) is generated by a pump, typically a syringe pump. The flow rate generated by the syringe pump must be high enough to overcome the pressure at the outlet tubing and push the perfusion fluid.
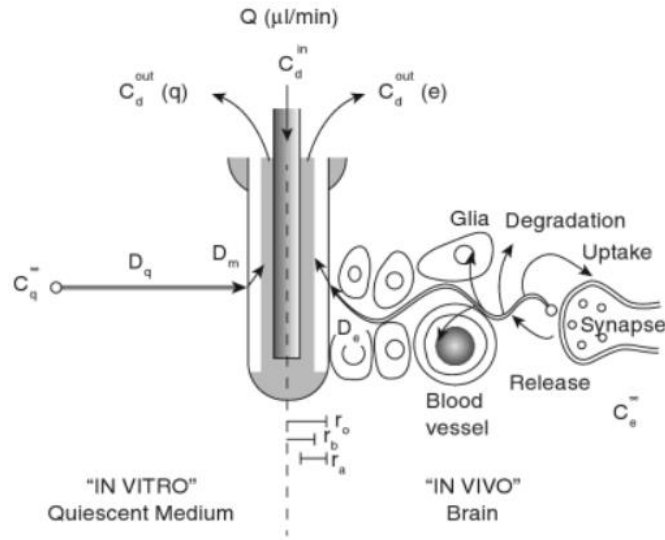
Figure 1.4. Comparison of *in vivo* and *in vitro* diffusion pathways during microdialysis sampling.[21] Adapted from reference 21, Copyright 2017, with permission from Elsevier.

The pressure at the outlet tubing is atmospheric (1 atm), since the outlet is open to the room where experiments are conducted. The resultant of pressure difference (ΔP) generated during microdialysis sampling experiments is called flow rate (Q). Flow rate represents the amount of volume that travels in the tubing as a function of time and its units are volume/time (μL/min). This is much like electric current which represents the amount of electric charge flowing in an electric circuit when a voltage difference in generated. Engineers take advantage of the latter to study flow behavior using electric circuits. This is very useful for prototyping. The mathematical approach used to accomplish this is called equivalent circuit theory.[22]

The pressure difference is typically positive (+ΔP) in traditional microdialysis, or negative (-ΔP), push-pull and vacuum ultrafiltration. It is good to point out that a +ΔP can be generated during push-pull microdialysis, but not during vacuum ultrafiltration, see Figure 1.5. As stated on section 1.1.1, the push-pull perfusion technique was one of the first microdialysis sampling techniques developed. The technique consists of pushing a solution through a cannula into a sampling site and pulling the solution by an adjacent cannula.[12] One of the problems with this technique was that it causes a significant amount of tissue damage and fluid loss.[12]

5
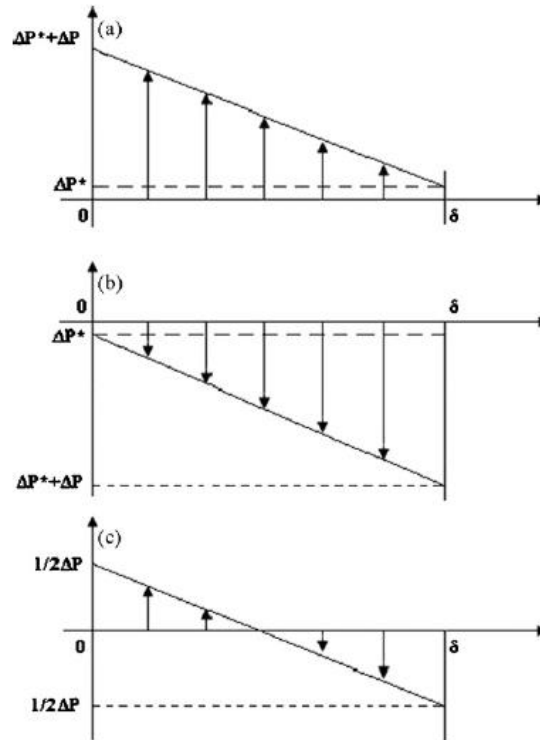
Figure 1.5. Schematic representation of pressure profile along microdialysis probe.[23] (a) push; (b) pull; (c) push and pull. Adapted from reference 23, Copyright 2017, with permission from Elsevier.

In contrast, push-pull microdialysis was developed to eliminate fluid loss. In push-pull microdialysis technique the perfusion fluid is normally pushed at a lower pressure into the inlet of the microdialysis probe and pulled at a higher pressure from the outlet (dialysate). The negative pressure difference ensures that the perfusion fluid is not loss across the microdialysis probe membrane. According to Polak, "push-pull was the most effective method for the elimination of fluid loss or gain during the sampling by probes of high MWCO [e.g. 100 kDa]."[24] On other hand, microdialysis sampling probes of 15 kDa MWCO or smaller were not influenced by pumping methods.[24] This could be due to the fact that membranes of smaller pore size are least susceptible to imbalance between the hydrostatic and osmotic pressure or fluid loss due to osmotic flux.[25]

Normally, during a microdialysis sampling experiment the perfusion fluid lacks the analyte of interests. This type of experiment is called relative recovery experiment. A concentration gradient is generated across the microdialysis probe membrane, during this experiment, and analytes diffuse from outside the membrane to the inner part of it, see Figure 1.6.

6

To explain, the solution located outside the microdialysis probe membrane must have a higher concentration than the perfusion fluid located inside the microdialysis probe membrane. This allows the target biomolecules to diffuse from outside of the membrane to the inside and be carried by the perfusate to the microdialysis sampling probe outlet. The solution composed of perfusate and analyte is called dialysate. The dialysate is the solution that is collected and analyzed during microdialysis sampling experiments, see Figure 1.6. Unlike the perfusion fluid, the dialysate contains the analyte of interest during microdialysis sampling collections. On the other hand, during pharmacokinetic studies, for example, in which drugs need to be delivered in situ to study their interactions with their milieu, the perfusate concentration is not zero. This microdialysis sampling mode is called delivery. Delivery is essentially the reverse process of collection mode.

The efficiency of microdialysis sampling is represented as either relative recovery (RR) or extraction efficiency (EE).[26, 27] Relative recovery is defined as the ratio of dialysate concentration or outlet concentration (C_{outlet}) and the concentration of the analyte far away from the collection point ($C_{sample,\infty}$).[27] This ratio, relative recovery, for an *in vitro* system is defined as: [28]

$$RR = \frac{C_{outlet}}{C_{sample,\infty}}$$
Equation 1.1
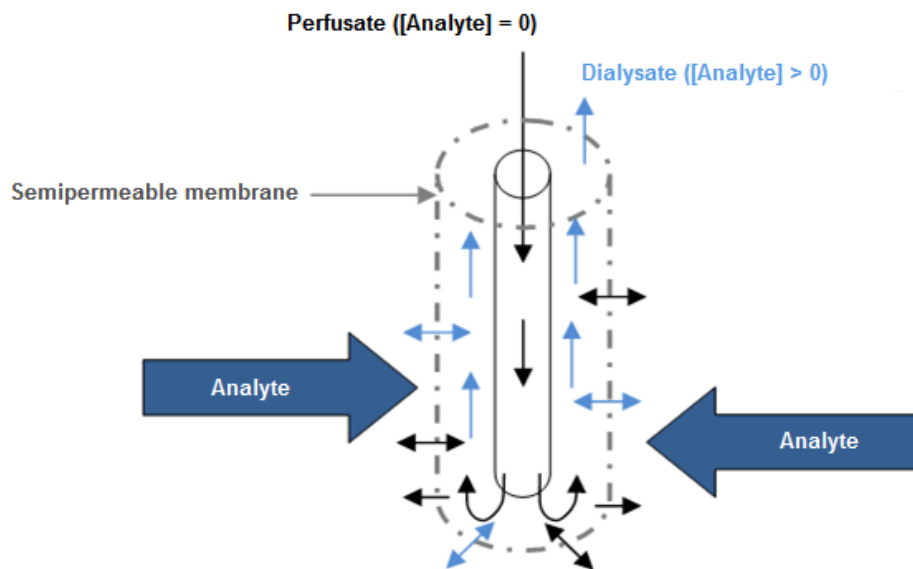
Figure 1.6. Schematic representation of the diffusion-based microdialysis process.

Relative recovery can also be expressed as: [28]

$$RR = 1 - \exp\left\{\frac{-1}{Q_d(R_d+R_m+R_q)}\right\}$$ Equation 1.2

The terms of equation 1.2 have been defined in detail by Bungay et al. as shown in Figure 1.7.[29] In Equation 1.2, Q_d represents flow rate, R_q mass transport resistance of the quiescent medium external to the microdialysis probe, R_d mass transport resistance of the dialysate, and R_m mass transport resistance of the microdialysis probe membrane. The difference between Equation 1.1 and Equation 1.2 is that Equation 2 includes the resistances involve in the microdialysis sampling process and its flow rate. These resistances in term include all the different diffusivity and kinetic processes involved in overall mass transport.[22]

$$RR = 1 - \exp\left(\frac{-1}{Q_d(R_d + R_m + R_q)}\right)$$

$$R_d = \frac{13(r_i - r_\alpha)}{70\pi L r_i D_d}$$

Mass transport resistance of the dialysate

Negligible relative to other regions at > 0.25 μL/min

$$R_m = \frac{\ln\left(\frac{r_o}{r_i}\right)}{2\pi L D_m \Phi_m}$$

Mass transport resistance of the membrane

Mass transport resistance of the quiescent medium external to the microdialysis probe

$$R_q = \frac{1}{2\pi D_q \Phi_q \sqrt{2r_o L}}$$

In well-stirred solutions $R_q \to 0$

$R_m \gg R_d$, R_q in *in vitro* experiments
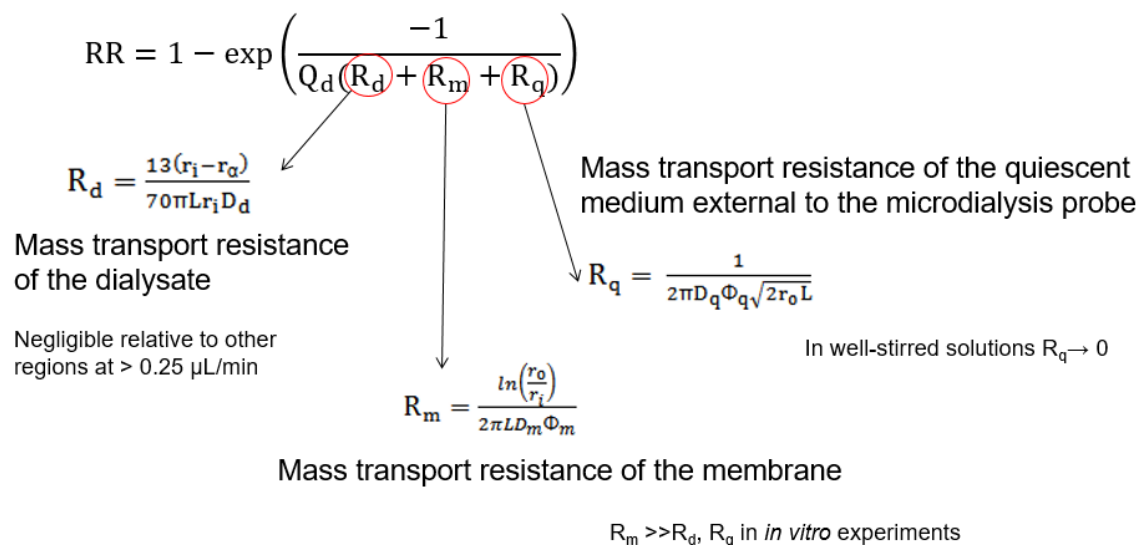
Figure 1.7. Bungay microdialysis sampling mass transport model and strategies to minimize the influence of mass transport resistances on the relative recovery (RR).[26, 29]

Equation 1.1 is more commonly used during microdialysis sampling experiments. For experiments in which a deeper understanding of the sampling site is needed, Equation 1.2 is used. However, the resistance values are often hard to get. Equation 1.2 is mostly used for microdialysis sampling modeling and theoretical work. Relative recovery differs from absolute recovery or recovery, a term commonly used in analytical chemistry separation processes, in that the relative recovery is concentration based and absolute recovery is mass based, see Figure 1.8.[12, 21]
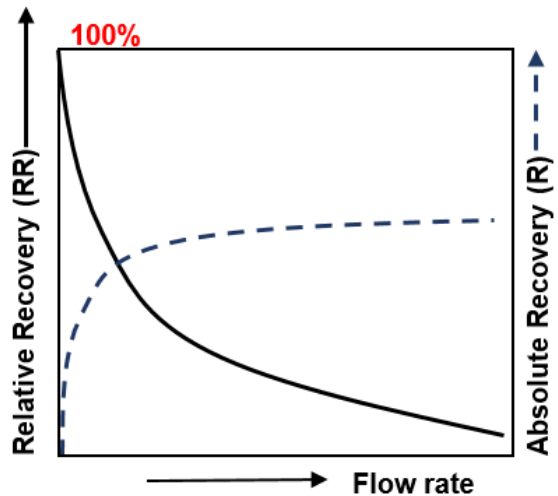
Figure 1.8. Relationship between relative recovery, absolute recovery, and flow rate.[12] (Redrawn from reference 12)

As the flow rate increases more mass overall is collected, absolute recovery, but a larger volume and smaller mass of analyte or lower concentration relative to the concentration outside the membrane is collected (relative recovery). Relative recovery is commonly used during microdialysis experiments, because the concentration of analyte outside the membrane is unknown during *in vivo* experiments. Sometimes this causes confusion among researchers that are not familiar with microdialysis sampling relative recovery. Figure 1.7 illustrates that the resistances denoted in this equation depend on the effective membrane length (L), which in terms is directly related to relative recovery. This means that a microdialysis probe with a membrane of large surface area will have a higher relative recovery than a probe with a membrane of small surface area (all other parameters being equal). The membrane length is a key feature useful to reduce the influence of resistances on relative recovery. Microdialysis sampling technique has several advantages and drawbacks as shown in Table 1.1, modified from the Kloft and Plock's review about microdialysis implementation in applied life-science.[30]

Table 1.1. Advantages and drawbacks of microdialysis sampling.[30]

Advantages	Drawbacks
Collection of biomolecules at site of action	Size limitation for molecules of interest
Direct delivery to target tissue	Determination of mean concentrations overtime interval
On-line measurements	Calibration necessary as recovery does not reach 100%
"Analytically clean" samples	Requires an analytical method with a low limit of quantitation capable of dealing with small volumes
Simultaneous sampling at multiple sites	Risk of tissue trauma [9]
Applicability to almost every organ	Limited time resolution ≥1 min; typically 10 min [9]
Applicability in conscious animals	

1.1.3 Limitations

1.2 Calibration methods

A common issue that continues to frustrate many microdialysis sampling users is that of *in vivo* calibration. There are numerous reasons why calibration of implanted microdialysis probes *in vivo* is extremely challenging. The primary reason for this has been recognized for decades is that tissues are not homogeneous structures and there are typically numerous inputs and outputs that can be difficult to model *in vitro*.[31, 32] *In vivo* microdialysis calibration methods have different problems associated with their use and in many cases can be quite cumbersome from an experimental perspective. It is good to point out that the term calibration in this context means to determine the concentration of the target analyte outside the probe or from the sampling site. This cannot be confused with the more commonly used definition of calibration, in which instruments must go through during experiments. These calibration methods used for *in vivo* calibration require steady-state concentrations for measurements.[33]

1.2.1 In vitro

The first calibration method used to correlate C_{outlet} to $C_{sample,\infty}$ was the *in vitro* calibration method.[34] The way how *in vitro* calibration method works is by determining the concentration (relative recovery) of a standard solution of the biomolecule of interest *in vitro* and relating it to the *in vivo* relative recovery.[12]

10

This method assumes that the mass transport resistance of the membrane is greatest through the membrane and not the tissue.[34] The problem with this assumption is that, as stated before, the tortuosity of *in vitro* experiments is almost non-existence compared to *in vivo* experiments. Nevertheless, the kinetic processes that drive the differences between *in vivo* and *in vitro* calibration are similar.

Another problem with this method and that few researchers have addressed, is that the pressure inside sampling sites (*in vivo*) is not constant, see Figure 1.9. Every time a microdialysis probe is implanted in any tissue the transmembrane pressure of the semipermeable membrane will increase. For example, the pressure in the cranium of humans or intracranial pressure can vary from 2 to 7 mmHg in healthy patients. The intracranial pressure of injured patients can be more than 50 mmHg.[35] Still several factors such as age, body posture, and clinical conditions can affect intracranial pressure.[36, 37]

This is far different than collections conducted *in vitro* in which only atmospheric pressure is present outside the microdialysis probe membrane. When the *in vitro* calibration method is used the relative recovery of the analyte of interest is off by a factor of two or three compared to the true concentration of the analyte in the sampling site.[34]
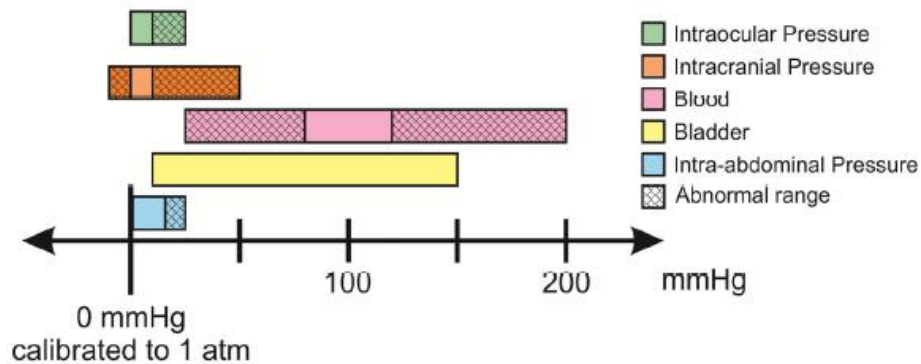
Figure 1.9. Variation of pressures within the human body.[37] (From reference 37 with permission from the Creative Commons Attribution License, open access, see appendices)

1.2.2 No-net flux or zero-net-flux

The method of zero-net-flux method requires steady-state concentrations and if they are present in the tissue flow rates can be sequentially changed.[12, 38]

This method requires a significant amount of experimental time to cycle through the concentrations necessary to straddle the suspected *in vivo* concentration. According to Hershey and Kennedy, no-net-flux is the most popular calibration method for *in vivo* microdialysis sampling experiments.[39] However, this method requires steady-state conditions and not all analytes are at steady-state during experiments.

1.2.3   Internal standards

The internal standards calibration method requires steady-state conditions as the no-net-flux method.[34] Stable-isotope labels or other suitable analogs for small molecules are used for this method, but can be problematic or prohibitively expensive for different solutes including drugs, peptides and proteins.

1.2.4   Slow perfusion

Like its name implies, the slow perfusion microdialysis sampling calibration method consists of the slow perfusion of a perfusion fluid into a microdialysis probe. This method takes advantage of the fact that, $RR \propto \frac{1}{Q_d}$. The slower the flow rate used, the higher the residence time of the perfusate. Higher residence times allow the perfusion fluid more time to interact with the fluid surrounding the microdialysis probe membrane. Hence, more time for the analyte to travel from outside the membrane into the perfusion fluid (inside the membrane). The aim of this method is to allow enough time for equilibrium to occur between the perfusion fluid and the fluid surrounding the microdialysis probe membrane. One of the problems with the slow perfusion method is that it requires very long collection times in order collect enough sample (e.g. 50 µL for some ELISA kits) to analyze it. Long collection times lead to sample evaporation.

1.3 Membranes

Another limitation of microdialysis sampling is that the relative size of semipermeable membrane pores is expressed as molecular weight cutoff (MWCO). Molecular weight cutoff is one of the factors that influence the relative recovery of biomolecules, according to Chaurasia (Table 1.2).[38] Snyder et al. stated that as the size of the analyte approaches to the size of the microdialysis probe pore size a reduction in the relative recovery of the analyte is observed due to an increase in the microdialysis membrane resistance.[40] The latter as compared with smaller analytes.[40] MWCO allows researchers to choose microdialysis probes based on the molecular weight of biomolecules.

However, there are several issues with using MWCO as an indication of the pore size of microdialysis probe membranes. First of all, there is not a standardized method to determine MWCO of semipermeable microdialysis probe membranes. Some companies do not disclose which method they use, and methods can vary from company to company.[41, 42, 43, 44] One method used to determine MWCO of microdialysis probe membranes is equilibrium dialysis, in which a semipermeable membrane is placed in between two enclosed chambers.[22] The membrane serves as a barrier to separate both chambers. Several chemical compounds of different molecular weights are placed in one chamber and the other chamber is filled with a buffer solution. This is done to generate a concentration gradient across the membrane "similar" to the microdialysis collection mode previously mentioned. Next, the enclosed chambers are incubated until equilibrium is reached.[42] The problem with using this method to determine MWCO of microdialysis probe membranes is that microdialysis sampling works differently than equilibrium dialysis.

Table 1.2. Chaurasia's list of factors influencing microdialysis sampling recovery.[38]

1)	Perfusion flow rate
2)	Sample flow rate
3)	Temperature of the tissue or dialysis target
4)	Diffusion of the substance within the sample medium
5)	Diffusion rate in dialysis membrane
6)	Molecular weight cutoff of the dialysis
7)	Chemical interaction between the analyte and the membrane
8)	Surface area of the dialysis membrane (length and diameter of the probe)
9)	Blood flow rate
10)	Metabolism rate
11)	Uptake into cells
12)	Extent of tissue vascularization

Microdialysis sampling is a dynamic process driven mainly by pressure differences or flow rates in which a perfusion fluid is continually being perfused, so equilibrium is never reached between inner and outer compartments of microdialysis probe membranes.[42, 45] Some companies define MWCO as the molecular weight of a molecule that is 90% retained by the membrane or 90% of the total molecules that diffuses across the membrane.[41, 43, 44] Depending on the company the percentage of retention can oscillate from 60 to 90%.[41, 44] Several approaches are used by researchers and companies to minimize this problem. For example, Li and Cui stated that, "Theoretically, the MWCO of microdialysis membrane three times greater than the molecular weight of the target molecule is sufficient to permit diffusion across the dialysis membrane."[46] This approach ensures that, on average, membrane pores are larger than target molecules. In contrast, CMA Microdialysis A Harvard Apparatus Company advises to choose a microdialysis probe membrane four times greater than the molecule of interest.[47] Another example, Bioanalytical Systems, Inc (BASi) claims on their tech note 1013 that their microdialysis probes have a molecular weight cutoff range of 30 to 38 kDa (kilodaltons), but during microdialysis experiments they would not expect to collect any chemical compounds higher than 6 to 7 kDa.[42] Compared to the other two examples, BASi would recommend to choose microdialysis probes five times greater than the analyte to be sampled. As can be seen there is not a consensus on what molecular weight cutoff really means adding more complexity to microdialysis sampling experiments. The ultimate goal would be to have a more robust microdialysis sampling probe with a minimal membrane transport resistance for analytes of different molecular weights.

1.4 Mathematical models

Many biomolecules have their concentrations changed during disease states. Microdialysis sampling technique allows researchers to monitor those changes in real-time. However, as mentioned before, microdialysis calibration methods can only give an approximate value of the concentration. For example, knowing the concentration of glucose is vitally important for people suffering from diabetes. This information facilities physicians regulate their glucose levels.

Several attempts to solve this problem have been made utilizing different strategies, see Table 1.3.[9, 21] According to Kehr, the first researchers to identify and try to quantify relative recovery during microdialysis sampling *in vivo* experiments were Ungerstedt and Zetterstrom.[21]

Their method assumes that microdialysis sampling *in vitro* recoveries, under quiescent conditions, were the same as *in vivo* recoveries.[21] This would allow them to determine the relative recovery of different biomolecules present in different tissue spaces. Their idea was that, if you used the same conditions (microdialysis sampling probe and flow rate) used to determine recoveries *in vitro*, when used *in vivo* they must be equivalent. However, there are a lot of problems with their assumption.[9] Some these problems were previously addressed in this chapter.

Firstly, the concentration of biomolecules is generally not static in living systems, they change rapidly which is not the case for *in vitro* microdialysis experiments. However, some studies have found that for some concentrations those changes are generally static and stable for long periods of time. Another problem, as stated before, is that the tortuosity for *in vivo* microdialysis is significantly different than *in vitro*, see Figure 1.4.

Table 1.3. Kehr's classification of microdialysis sampling mathematical and empirical models.[21]

Type of model	Author (s)	Year (s)
Empirical	Ungerstedt and Zetterstrom	1982
	Jacobson	1985
	Lerma	1986
	Lönnroth	1987
	Ekblom	1992
	Merlo Pich	1993
Mathematical	Lindefors and Amberg	1989
	Benveniste et al.	1989, 1990
	Bungay et al.	1990
	Morrison	1991

Benveniste et al. determined that microdialysis sampling recoveries of potassium (K^+) and calcium (Ca^{2+}) ions *in vitro* were higher than those measured *in vivo*.[31] They used ion-selective microelectrodes in order to measure the ions concentration in the dialysate.

Due to this observation a tortuosity factor, λ, was introduced to correct for the difference in tortuosity for *in vivo* and *in vitro* microdialysis experiments.[31] This factor was defined by Nicholson and Philips in 1981 and states that: [31, 48, 49]

$$\lambda^2 = \frac{D_q}{D_e} \qquad \text{Equation 1.3}$$

Where λ represents the tortuosity factor, D_q is the diffusion coefficient in the quiescent medium, and D_e the diffusion coefficient in the extracellular space. Benveniste and colleagues strategy worked well for microdialysis sampling collections of Ca^{2+}, but not so well for neurotransmitters such as glutamate and dopamine.[31]

An empirical method called flow rate method was developed by Jacobson et al. in 1985, see Figure 1.10.[9, 50, 51] According to Chefer et al.,"The flow rate method was one of the first empirical methods designed to determine extracellular concentration by determining the relationship between perfusate flow rate, the active area of the membrane, and the mass transfer coefficient and then extrapolating to the case of zero flow rate."[9] Jacobson et al. pointed out that the mass transfer coefficient (*k*) of any molecule can be determined experimentally during microdialysis sampling by measuring its relative recovery at different flow rates and plotting the results to find the slope or *k*, see Figure 1.10.[50, 51] Bungay et al., stated that the overall probe-external medium permeability, P, is equivalent to the mass transfer coefficient of Jacobson et al., *k*.[29] Thus:

$$PS = \frac{1}{R_d + R_m + R_q} \qquad \text{Equation 1.4}$$

In Equation 1.4, S or A is surface area of the microdialysis probe membrane, R_q mass transport resistance of the quiescent medium external to the microdialysis probe, R_d mass transport resistance of the dialysate, and R_m mass transport resistance of the membrane, see Figure 1.7. To determine the mass transfer coefficient, *k,* of any biomolecule using microdialysis sampling technique, Equation 1.2 and 1.4 are combined:

$$RR = 1 - \exp\left\{\frac{-1}{Q_d(R_d + R_m + R_q)}\right\} \qquad \text{Equation 1.2}$$

$$kA = \left(\frac{1}{R_d + R_m + R_q} \right)$$

Equation 1.4

Note that in Equation 1.4 P and S were replaced by *k* and A.

Thus:

$$RR = 1 - \exp\left(\frac{-kA}{Q_d} \right)$$

Equation 1.5

Rearranging Equation 1.5:

$$kA = [-\ln(1 - RR)]Q_d$$

Equation 1.6

Equation 1.6 can be used only if $(1 - RR) \neq 0$.
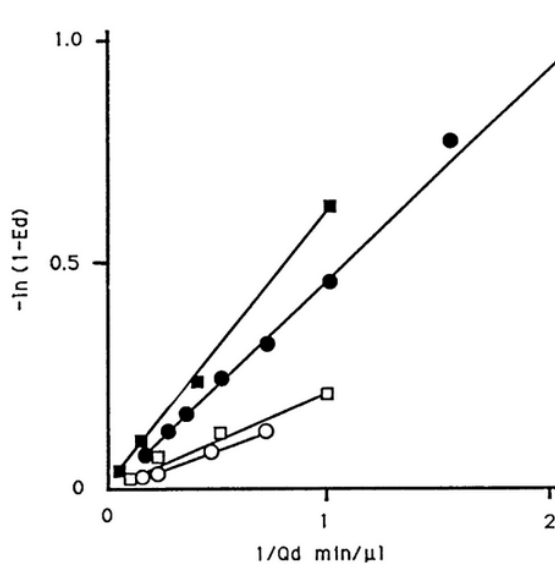
Fig. 3. Effects of flow rate on recovery (from Jacobson et al., 1985). Straight lines are regression fits of Eqn. 29 to the experimental data of Jacobson and Hamberger (1984), filled squares; Johnson and Justice (1983), filled circles; Sandberg and Lindstrom (1983), open circles; and Ungerstedt (1984), open squares.

Figure 1.10. Jacobson et al. microdialysis sampling method.[50, 51] Reprinted from reference 51, Copyright 2017, with permission from Elsevier. Original figure reference 50, Copyright 2017, with permission from Elsevier.

By plotting $-\ln(1 - RR)$ as a function of Q_d^{-1}, the product kA can be obtained from the slope, see

Figure 1.10. This is a very useful tool developed by Jacobson et al., but it assumes steady-state conditions.

Most microdialysis sampling mathematical methods make this assumption. This method was used to estimate the relative recovery of methyl orange and fluorescein isothiocyanate-dextrans (FITCs) during microdialysis probes in series approach as denoted in chapter 4.

1.5 Approaches to improve relative recovery

Microdialysis sampling relative recovery is a multifactorial problem which makes it a challenging problem. Chaurasia listed a number of factors such as flow rate, temperature, diffusion properties, molecular weight cutoff, and so on that influence the relative recovery of biomolecules during microdialysis sampling, see Table 1.3.[38] Researchers have developed several strategies to improve the collection of biomolecules such as cytokines using microdialysis sampling.[27, 52, 53]

1.5.1 Affinity agents

Duo et al. developed a method to improve cytokine relative recovery using affinity agents such as antibodies and heparin attached to polystyrene microspheres, see Figure 1.11.[53] Their method consists in perfusing polystyrene microspheres with affinity agents chemically attached to their surface. For example, they chemically attached antibodies to the surface of the microspheres and perfused them through the microdialysis probe during cytokines collection to increase cytokines diffusion across the membrane pores.[53, 54] Finally, cyclic oligosaccharides called cyclodextrins have also been used as affinity agents to improve microdialysis relative recovery of molecules.[55]

1.5.2 Mechanical approaches

1.5.2.1 Recycling or recirculation

Another way to improve the relative recovery of biomolecules during microdialysis sampling experiments is by increasing the residence time of the perfusion fluid at the microdialysis probe semipermeable membrane (inner site). As mentioned before this can be achieved by using slow flow rates; however, several issues arise when slow flow rates (< 0.5 μL/min)[56, 57] alone are used. Some of these issues are sample evaporation and longer collection time.
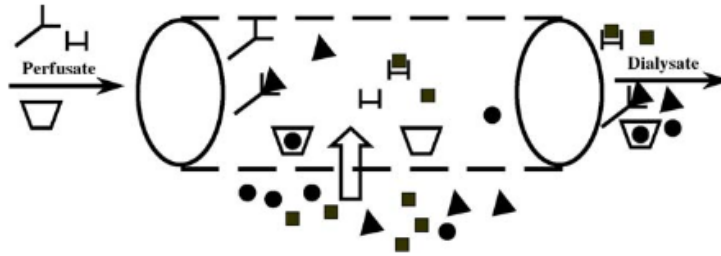
Fig. 1. A schematic of a microdialysis probe denoting different affinity-based trapping agents included in the perfusion fluid. The cone shape denotes cyclodextrins or other molecules with a cavity that serves as a host for host-guest chemical interactions. The "Y" denotes an antibody and the "H" shape denotes any other type of affinity agent. Analytes diffuse in (denoted by the arrow) and can be trapped by the affinity agent. The extent of bound and free material would be dictated by the equilibrium association constants between the affinity agent and the targeted analyte.

Figure 1.11. Microdialysis sampling using affinity agents approach.[53] Reprinted from reference 53, Copyright 2017, with permission from Elsevier.

Figure 1.7 shows that from a theoretical stand point increasing the surface area and length of the microdialysis sampling membrane will improve relative recovery. The problem with increasing the length of microdialysis probe membranes is that you are limited by the size of the sampling site. In other words, extracellular fluid compartments in living systems are very small relative to the current microdialysis sampling probes. Microdialysis sampling probe membranes of 4 or 10 mm in length are commonly used. However, depending on the need smaller membranes (1 mm) can be used. In general, the size of the sampling site dictates the length of the microdialysis probe membrane.

In 1986 Lerma et al. were the first to design a microdialysis sampling probe having a closed loop to recirculate perfusate (Figure 1.12) for *in vivo* measurements of amino acids in rat hippocampus.[58] They used this method to increase the residence time of the perfusate and predict the concentration of amino acids in the extracellular fluid space. Lerma and colleagues made a diffusion mathematical model for this system. The assumptions of their model were that simple diffusion guided biomolecules across the membrane, concentration was constant around the probe, and steady-state conditions.[58] Equation 1.7 summarizes their method. The concentration of perfusate is represented by *c, A* represents extracellular fluid concentration of biomolecules, *K* is apparent diffusion constant across the membrane, and *t* residence time.[58]

At $t = 0$ or beginning of perfusion, the concentration of the perfusate (c) is zero, but after sufficiently long times ($t \rightarrow \infty$) the concentration of the perfusate will be equal to the concentration of biomolecules in the extracellular fluid. In other words, the perfusate and extracellular fluid will be at equilibrium allowing to determine the concentration of the extracellular fluid for any biomolecule.

$$c = A \left(1 - e^{-Kt}\right)$$
<div align="right">Equation 1.7</div>
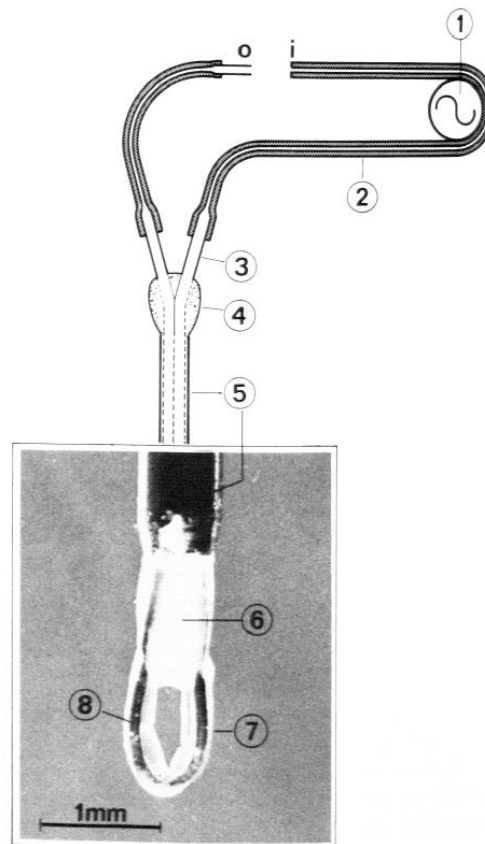
Fig. 1. Arrangement of perfusion lines and dialysis probe. i, liquid inlet; 1, peristaltic pump; 2, flow tube; 3, 26-gauge stainless-steel cannula; 4, dental cement; 5, 22-gauge stainless-steel cannula; 6, epoxy seal; 7, hollow fiber; 8, steel wire; o, perfusate outlet. Inset shows a magnification of the dialysis loop.

Figure 1.12. Lerma et al.'s microdialysis sampling circulation experimental set up.[58] Reprinted from reference 58, Copyright 2017, with permission from Elsevier.

Sternberg et al. eight years later, in 1994, developed a calibration method for glucose sensors using a microdialysis sampling recirculation device to determine subcutaneous concentrations of glucose in humans.[59]

Their method consisted on recirculating a perfusion fluid (phosphate saline), using a peristaltic pump, inside a microdialysis probe until a concentration equilibrium was reached between the glucose concentration outside the microdialysis probe membrane and the inside. Similar to Lerma et al.'s work, they increased the residence time of the perfusion fluid. This in terms helped them determine the glucose concentration present in the tissue. Sternberg et al. listed five reasons why their recirculation method was very effective, see Table 1.4.[59] One of the reasons was that a small amount of liquid is continuously in contact with the extracellular fluid preventing any adverse responses from the sampling site.[59]

Table 1.4. Sternberg et al. reasons why their calibration method is effective.[59]

a)	Microdialysis probe implantation does not interfere with results within 30 minutes after implantation
b)	Only a small amount of volume is in contact with the extracellular fluid continuously minimizing any adverse reaction
c)	The dialysate is constantly stirred
d)	Surface area and residence time allow for a total equilibrium to occur
e)	Blood contamination is avoided by using a semipermeable membrane

In 1995, Sternberg at al. published the same paper or similar than their 1994 recirculation paper, but this time they called their method "the recirculator".[60] In this work they estimated subcutaneous glucose concentration in humans and continuously monitored the concentration changes using a recycling system.[60] They found that fifteen cycles were needed to achieve equilibrium between recirculated phosphate buffer saline inside microdialysis probe and plasma glucose or standard solution of glucose outside of it.

One interesting observation about Lerma et al. work and Sternberg et al's is that as far as this author knows since 1995 no other work further investigating or improving this method have been published. Their recirculation method seems to be a very effective way to eliminate microdialysis sampling calibration methods. The preliminary work for this dissertation consisted of a similar method of recirculation or recycling microdialysis sampling to improve relative recovery and eliminate microdialysis sampling calibration methods, see Figure 1.13. This will be covered in chapter 2 in more detail.

1.5.2.2 Transmembrane pressure

Microdialysis sampling is not only driven by diffusion, but also by hydraulic pressure. According to Bungay et al.,"It is customarily assumed that no significant amount of the perfusate fluid is loss across the probe membrane and that solute exchange across the membrane occurs by diffusion."[61] This assumption causes errors during the interpretation of experiments conducted using microdialysis sampling probes of high molecular weight cutoff (e.g., 100 kDa) membranes. However, understanding how pressure influences the relative recovery of biomolecules during microdialysis sampling experiments can be very useful.

Bungay et al. demonstrated how relative recovery of biomolecules can be improved by changing the transmembrane pressure of microdialysis sampling probes, see Figure 1.14. Their experiment consisted on changing the height of the collection vial or the outlet tubing of a microdialysis sampling probe to change the transmembrane pressure. To explain, when the vial is elevated an increase in backpressure or hydraulic resistance is generated inside the microdialysis probe. This causes an increase in fluid loss across the membrane. On the other hand, when the vial is lowered a positive pressure is generated inside the microdialysis probe drawing liquid from outside the probe to inside. A fluid gain is observed.
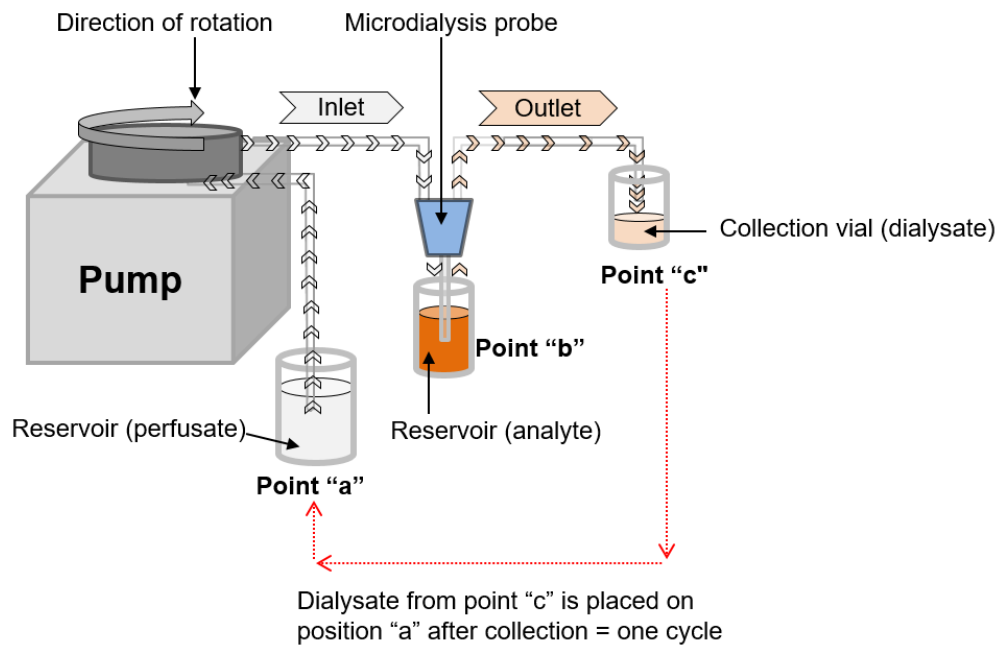
Figure 1.13. Diagram of setup used for microdialysis sampling recycling flow method experiments.

This gain or loss was defined by Bungay and colleagues as an ultrafiltration factor, see Equation 8. In this equation, Q_{in} and Q_{out} represent the flow rate of the perfusion fluid and the dialysate respectively. For fluid loss $Q_{out} < Q_{in}$ and for fluid gain $Q_{out} > Q_{in}$.[61]

$$f_Q \equiv \frac{Q_{in} - Q_{out}}{Q_{in}}$$
<div align="right">Equation 1.8</div>

Recently, Chu et al. found a direct relationship between fluid recovery (FR), and static pressure.[62, 63] They studied the importance of transmembrane pressure in fluid recovery by using a pressured chamber that they designed, see Figure 1.15.[64] Their work consisted on changing the pressure outside and inside the microdialysis probes systematically. They used four CMA 71 microdialysis sampling probes for their experiments having membranes of 100 kDa MWCO and 10 mm in length. These probes were placed inside a chamber and each probes were connected to syringe pumps.[62] It is good to point out that these probes were not connected in series. The chamber allowed them to control the pressure outside the microdialysis probes. It is a common practice to add osmotic agents during microdialysis sampling experiments that use microdialysis probes having membranes of 100 kDa or larger MWCO. These agents such as dextrans counterbalance the pressure inside the probe. This approach helps reduce fluid loss during microdialysis sampling experiments and improve relative recovery of biomolecules.
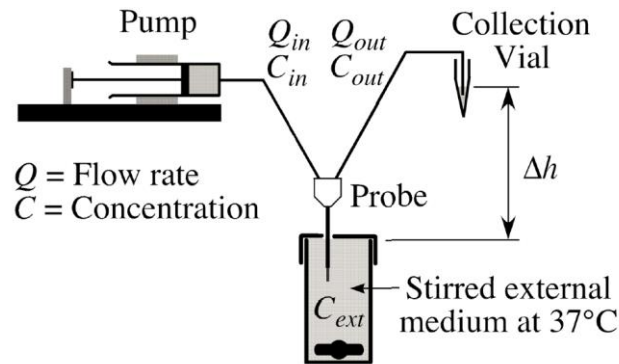
Fig. 4.
Schematic for *in vitro* experiments in which probes were immersed in a well-stirred aqueous solution maintained at 37°C. The extent of perfusate ultrafiltration was varied by two means. Changing the inflow rate, Q_{in}, alters the hydrodynamic contribution to the transmembrane pressure drop. This portion arises from resistance to flow of the retained fluid through the effluent tubing and the passages within the probe downstream of the membrane. Adjusting the height of the dialysate collection vial relative to the probe alters the effluent fluid hydrostatic contribution to the transmembrane pressure drop. That contribution is associated with the difference in elevation between the dialysate meniscus in the collection vial and the external medium surface denoted by Δh.

Figure 1.14. Transmembrane pressure experimental set up to improve microdialysis sampling recovery.[61] Reprinted from reference 61, Copyright 2017, with permission from Elsevier.

FIGURE 1 | Schematic drawing of a pressurized *in vitro* MD sampling system is shown. The chamber held four MD catheters and was used to study the impact of different pressures present in a MD sampling system on fluid recovery (42). Pressure parameters tested included perfusion flow rate, colloid osmotic additives in both perfusate and sample, and static outside pressure. The precision of the system was <0.5 mmHg and pressures could be set accurately in order to simulate different NIC conditions [adopted from Ref. (42)].

Figure 1.15. Pressure chamber engineered to study transmembrane pressure influence on recovery.[63, 64] (From reference 64, open access article, with permission to reuse under the terms of the Creative Commons License, see appendices for details)

The experiments described by Chu et al. were the first to study the influence of osmotic, transmembrane, hydraulic, and outside probe or sampling site pressure on fluid recovery during microdialysis.[62] Their work could lead to an automated microdialysis sampling system in which pressure sensors control the pressure in the system. For example, during *in vivo* experiments the pressure outside microdialysis probes changes depending on the sampling site internal pressure. This impacts the transmembrane pressure of the probes and the relative recovery. This will be addressed on chapters 3 and 4. By assuming that the pressure applied to the microdialysis sampling probe or hydraulic pressure (flow rate) is constant, we could measure the pressure change during *in vivo* experiments.

In other words, the pressure change would be the difference between the hydraulic pressure and the pressure outside the microdialysis sampling probe. Regulating this pressure change systematically could lead to higher relative recoveries.

1.5.2.3 Microdialysis probes in series

Microdialysis probes in series is a new approach that was developed during this dissertation to improve the relative recovery of biomolecules during microdialysis sampling and toward eliminating the need for microdialysis sampling calibration methods. Microdialysis probes in series approach optimizes membrane surface area and perfusion fluid residence time to increase relative recovery of macromolecules. As far as the author know nobody has done something similar. The new approach consisted of up to four microdialysis probes in series, see Figure 1.16.
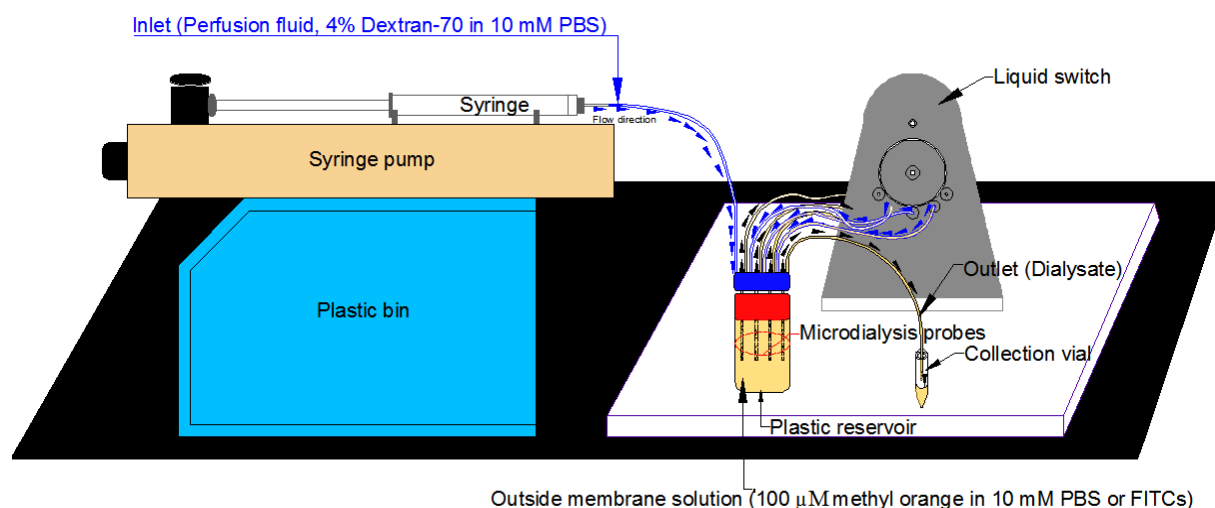
Figure 1.16. Four microdialysis probes in series system.

As far as this author knows there are not similar work published in the scientific literature. However, there is a patent[65] similar to the work of this dissertation. The aims of this dissertation and the patent were different, since four microdialysis probes were not going to be implanted in any living system. It is good to point out that this dissertation work was used to assess the difference between theory and experiment. Previously researchers have implanted four microdialysis probes in living systems in order to assay a larger sampling area and closely monitor concentration changes of biomolecules. This is done to have a higher resolution of concentration changes in a sampling area.

For example, Wei et al. implanted four microdialysis probes in the heart of dogs to study the enzymatic mechanism of angiotensin II in the interstitial fluid. Another example was the work done by Strouch et al. They implanted four CMA/20 microdialysis probes subcutaneously in swine to study the extracellular cyclic adenosine monophosphate.[66] It is good to point out that these microdialysis probes in both of those studies were not connected in series or parallel. Samples were taken from them independently. Wei's and Strouch's groups wanted to map the concentration of their analyte by using multiple microdialysis probes. The problem of implanting multiple microdialysis probes in any living system is the amount of damage that it causes to the tissue from which samples are been taken. Nevertheless, if the concentration changes of a biomolecule want to be studied in any organ, more than one microdialysis probe could be used to cover a larger area. Finally, Lu and colleagues glued four probes together to be implanted and used to sample biomolecules, see Figure 1.17. Their work showed that microdialysis probes could be arrayed in series and parallel.[65] The four microdialysis probes in series approach was used as the basis to develop a polydimethylsiloxane (PDMS) microfluidic-based microdialysis probe.

1.6 Microfluidic devices used or applied to microdialysis sampling

Manufacture of microfluidic devices is emerging as one the fastest growing research areas.[67] It is estimated that this year (2016), pharmaceutical & biomedical research will use $1 billion worth of microfluidic devices. The microfluidics market is expected to reach $4 billion this year.[68] The combination of microfluidic devices and microdialysis sampling in order to develop a diagnostic system able to monitor in real-time concentration changes of biomolecules and make faster diagnosis, unlike traditional methods, during disease states is needed. Researchers have developed different approaches to tackle this need. Finally, the number of publications related to microfluidics and membranes have had a substantial growth since 1996, see Figure 1.18.[69]
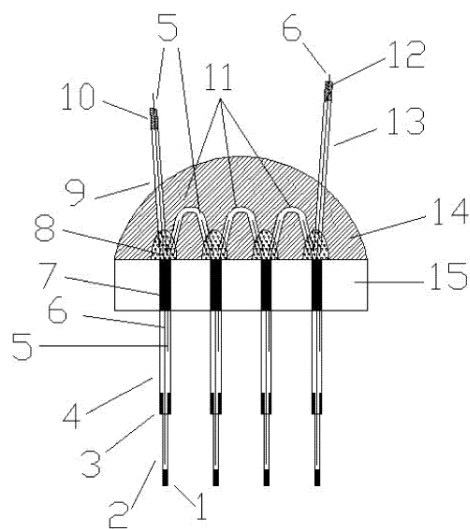
图 1

Figure 1.17. Four microdialysis probes approach by Lu et al.[65]
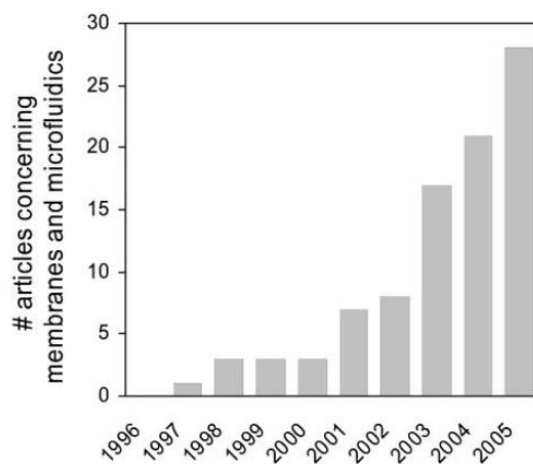
Fig. 1   Articles concerning membranes and microfluidics discussed in this review, categorized by year of publication. The graph shows substantial growth over the past 10 years.

Figure 1.18. Growth in the number of publications related to microfluidic and membranes.[69] Reproduced from reference 69 with permission of The Royal Society of Chemistry.

1.6.1   Microfluidic devices based on microdialysis sampling

1.6.1.1 Miniaturization

There is a growing interest in miniaturizing microdialysis sampling technique into microfluidic systems.[70, 71, 72] The advantages of achieving this are: a) Significant reduction in cost, b) smaller sample volume, and c) faster results. On other hand, according to Tüdős et al., "The large ratio of volume and flow rate between the microfluidic components and their associated conventional fluidics raises considerable system integration challenges when miniaturised devices are incorporated into instrumentation."[70] That is while the growing interest in miniaturizing microdialysis sampling into microfluidic systems and microfluidics in general, has created a need for engineering fundamental work.[70] Some of the engineering tools used to develop microfluidics are summarized in Table 1.5.[70] One of these tools is dialysis, used to separate biomolecules as previously mentioned in this chapter.

Since microdialysis sampling technique requires a membrane to allow the separation of analytes from complex matrices, choosing the appropriate fabrication approach is crucial for a successful microfluidic device. An in-depth review about membranes and microfluidics has been provided by de Jong et al.[69]

They divided several fabrication approaches used to integrate membranes in microfluidic systems into four categories, see Table 1.6.[69] 1) Direct incorporation of (commercial) membranes, 2) membrane preparation as part of the chip fabrication process, 3) *in-situ* preparation of membranes, and 4) use of membrane properties of bulk chip material were the four categories developed by de Jong and colleagues.[69]

Table 1.5. Summary of engineering tools used for microfluidics.[70] Reproduced from reference 70 with permission of The Royal Society of Chemistry.

Table 4 'Lab-on-a-chip' engineering tools

Engineering tool	Description
Channels	Etching, dry or wet
Dialysis	Separate liquid solutions with a diffusion barrier
Separators	μ-Channel electrophoresis (CE and CEC)
Extractors	Two-phase system
Mixers	Splitting or coiling of laminar flow
Filters	Porous silica or controlled devices
Valves	Mechanical, flowFET or by electrowetting
Detectors	T, P, flow, pH, electrochemical, optical, acoustical, MS

Table 1.6 shows more details about their categories. For the work done for this dissertation, the category one was used. To explain, commercially available polyethersulfone (PES) membranes were used to make the devices. PES was the membrane material of choice, since microdialysis probes having PES membranes were used. Chapter 5 is going to cover this in more detail. Finally, de Jong et al made a useful flow chart to help researchers choose membranes and fabrication approaches suitable for their needs, see Figure 1.19.[69]

1.6.1.2 Microfluidic microdialysis devices

Several researchers have designed and developed microdialysis devices to sample or monitor biomolecules. For instance, Hsieh and Zahn devised a microfluidic microdialysis biochip for glucose recovery.[71] They engineered an *in vitro* on-chip microdialysis system to study concentration changes of glucose. The key feature of their design was that for the microdialysis probe membrane they used thin-film fabrication technique and direct polymer bonding giving them a more efficient microdialysis system. This was due to the fact that high surface to volume ratio can be achieved with these techniques.[71]

Subrebost developed a similar microfluidic system for his PhD dissertation.[73] Subrebost's system consisted of a membrane at the tip of an a silicon chip. His device has an on-chip fraction collector and embedded platinum planar electrodes used as a membrane biofouling control.[73] However, Subrebost system was designed, but never tested experimentally.

Recently, Lee et al. published a work showing a new method to microfabricate microdialysis probes in silicon.[74] They were able to fabricate a microdialysis probe 79% smaller (160 μm) than the smallest conventional microdialysis probes' cross-sectional area, see Figure 1.20.[74] Lee and colleagues used a flow rate of 100 nL/min (0.1 μL/min).[74] As previously stated in this chapter and they stated in their conclusions, such as small flow rates are a drawback.

The main difference between Subrebost's design and this dissertation's design was that Subrebost's design focused on membrane biofouling. The design outlined in this dissertation was focused on miniaturizing the microdialysis probes in series approach. An approach developed to eliminate the need for microdialysis sampling calibration methods.

Table 1.6. Division of fabrication approaches by de Jong et al's.[69] Reproduced from reference 69 with permission of The Royal Society of Chemistry.

Table 1 Categorization of different approaches to integrate membrane functionality on-chip

Method	Approach
Direct incorporation of (commercial) membranes	Clamping or gluing of commercial flat membranes[9–33] —Similar, followed by functionalization[34–38] Incorporation of membrane during micro stereo lithography[39] Use of hollow fiber membranes between capillaries[35,40–44]
Membrane preparation as part of the chip fabrication process	Production of sieves with well-defined pores by etching[45] Thin metal film deposition[46–49] Growing of zeolite crystals[50,51] Preparation of porous silicon in wafers[52,53] Preparation of porous oxide layers[54–56] Creation of pores by ion track technology[57] Preparation of polymeric membranes by casting[58–60] Photo polymerization of ion-permeable hydrogels[61,62]
In-situ preparation of membranes	Local photo polymerization of acrylate monomers[63–65] Interfacial polymerization in two-phase flow[66] Liquid membranes by three-phase flow[2,67,68] Formation of lipid bilayers[69,70]
Use of membrane properties of bulk chip material	PDMS chips[71–85] Other polymeric chips[86–88] Hydrogel based chip[89] Fabrication of completely porous chips[90]
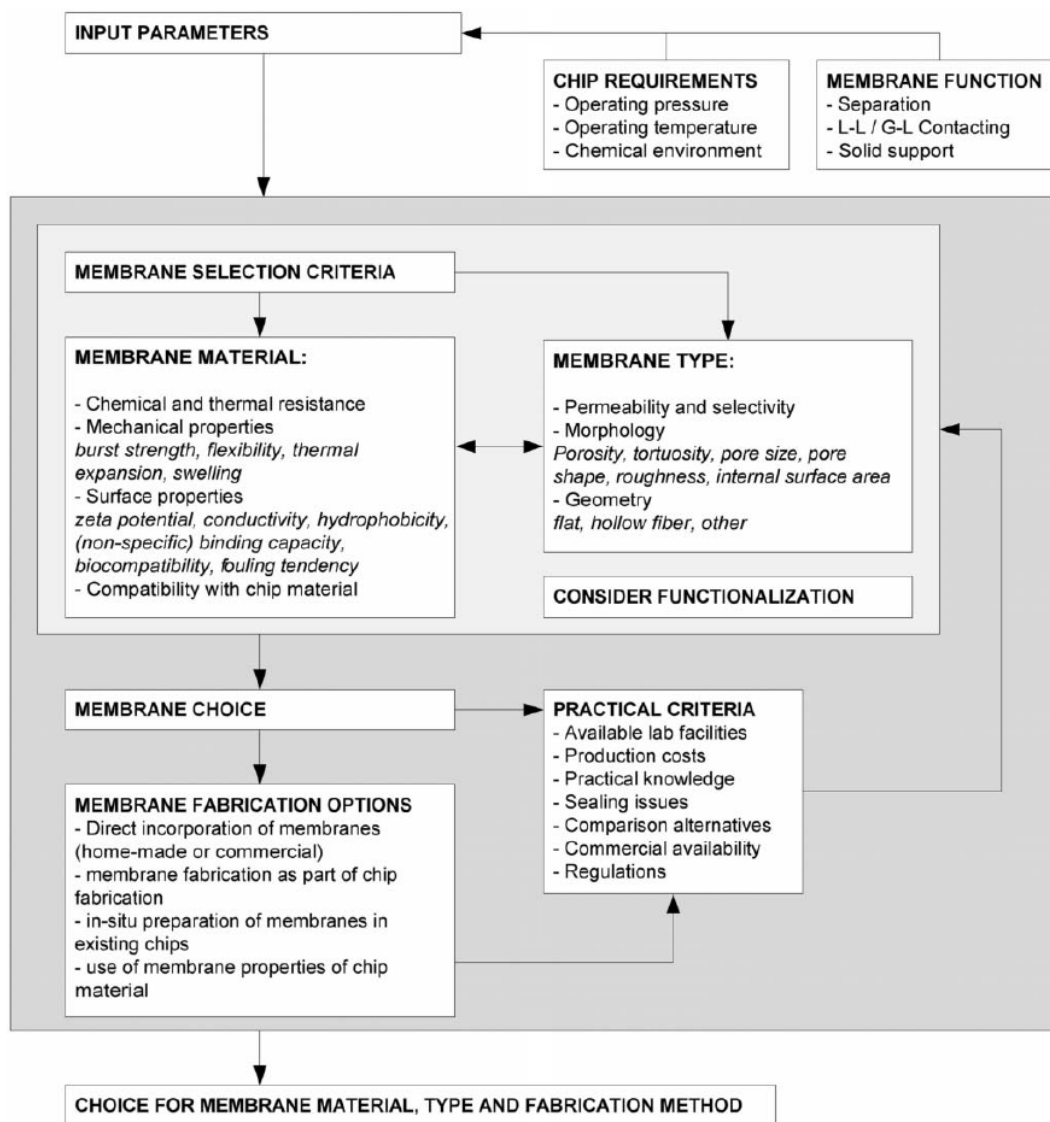
Fig. 6 Selection scheme for choice of membrane material, type and fabrication method.

Figure 1.19. Flow chart for membrane and fabrication selection made by de Jong et al.[69] Reproduced from reference 69 with permission of The Royal Society of Chemistry.
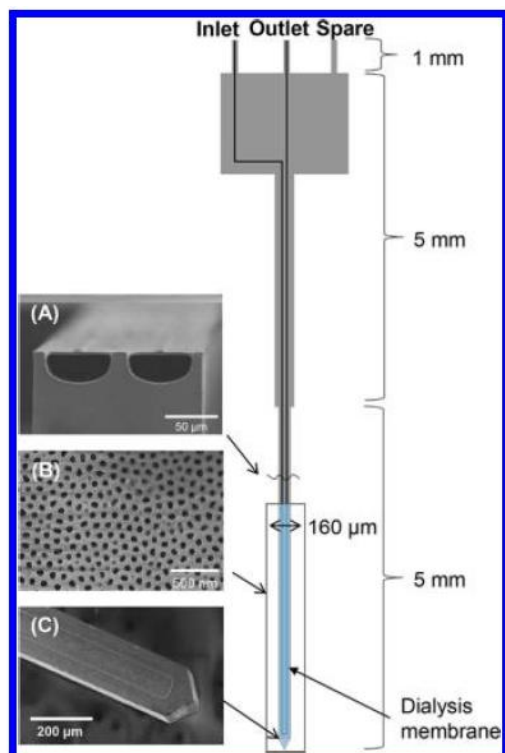
Figure 1. Layout of microfabricated microdialysis probe. A probe has three ports including inlet, outlet, and spare for other potential uses (it was not used at this probe). (A) SEM image of cross-section of channels showing semicircular shape and thin polysilicon top layer. (B) SEM image of of AAO membrane over sampling area. (C) SEM image of sampling probe tip showing the channel pattern.

Figure 1.20. Lee at al. small microdialysis probe.[74] Reprinted with permission from reference 74. Copyright 2017 American Chemical Society.

Hsieh and Zahn mentioned above, developed another device in 2007 to monitor glucose on a polydimethylsiloxane (PDMS) microfluidic system.[71] Their microdialysis on-a-chip system used platinum electrodes to measure the glucose concentration and a micromixer to avoid concentration gradients due to not well-mixed flows. Microdialysis type microfluidic systems have also been used for protein preconcentration. Kim et al. devised a microfluidic dialysis system to enrich protein samples by modifying the dialysis membrane with oxygen plasma.[75]They modified the dialysis membrane using oxygen plasma treatment to change the hydrophobicity of the membrane surface to improve flux and selectivity. They made serpentine channels on two PDMS substrates. These two PDMS substrates were used to sandwich a regenerated cellulose membrane. Fluid flows from either side of the microfluidic system.

The microfluidic system that was developed for this dissertation could be another step toward eliminating the need for microdialysis sampling calibration methods, due to the fact that the microdialysis probes in series approach was able to achieve ~100 % recovery of small molecules such as methyl orange in *in vitro* experiments. This means that the concentration of analyte collected would be approximately the same as the concentration in the sampling site, ideally, and microdialysis sampling calibration methods would not be necessary. Eliminating microdialysis sampling calibration methods, would be one of the greatest achievement of the field, if reached.

The PDMS microfluidic device was developed by miniaturizing the microdialysis probes in series method, see Figure 1.16. An external pump and analytical benchtop detection methods still need to be used. The main aim was to make a microdialysis probe-like device better, in terms of recovery, than the current commercially available. The idea was to mimic the four microdialysis probes in series approach by having four channels connected in series, but parallel to each other, see Figure 1.21. The number of probes required to achieve ~100% relative recovery of methyl orange was determined *in vitro*. A mathematical model based on Bungay's and Jacobson's work was devised to estimate the number of microdialysis probes in series necessary to achieve ~100% recovery of methyl orange and isothiocyanate-dextrans (FITCs), see Equation 1.6. By translating the number of probes necessary to achieve ~100% recovery of any analyte into number of channels, the microfluidic device could be tailored for wide range of biomolecules based on their mass transfer coefficient (k), see Equation 1.6. From a practical standpoint, this would be more like a calibration of the device. For example, several biomolecules could yield ~100% recovery for the same number of channels.
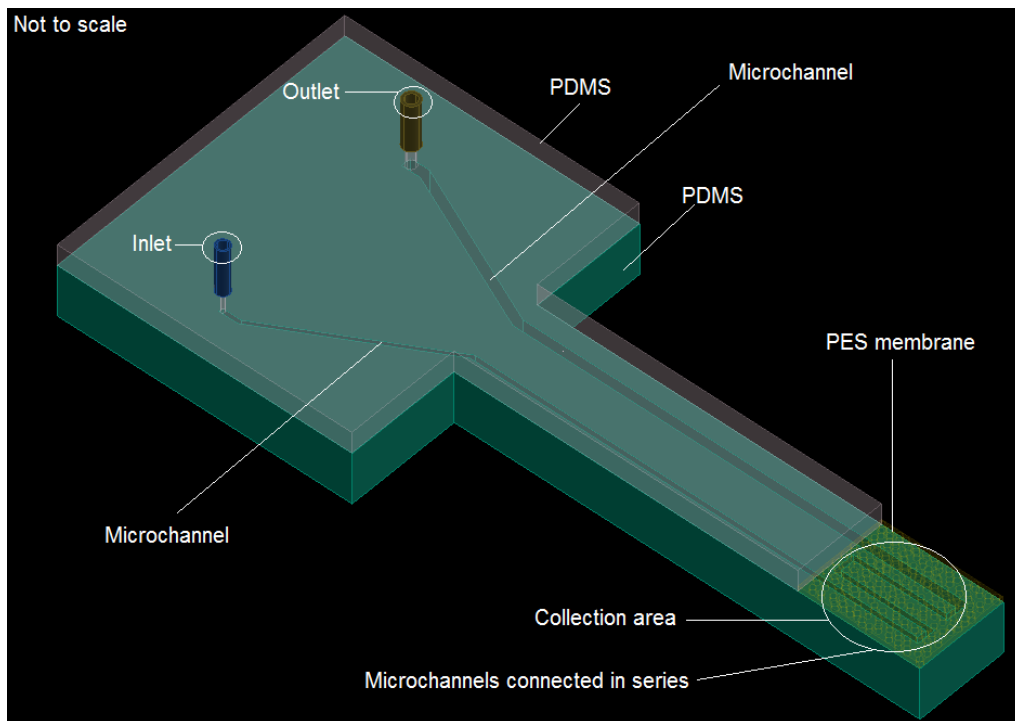
Figure 1.21. 3D model of the microdialysis in series microfluidic device engineered for this dissertation.

1.7 References

1. Stahl, M.; Bouw, R.; Jackson, A.; Pay, V., Human microdialysis. *Curr. Pharm. Biotechnol. FIELD Full Journal Title:Current Pharmaceutical Biotechnology* **2002,** *3* (2), 165-178.

2. May, M.; Batkai, S.; Zoerner, A. A.; Tsikas, D.; Jordan, J.; Engeli, S., Enhanced Human Tissue Microdialysis Using Hydroxypropyl-ß-Cyclodextrin as Molecular Carrier. *PLoS ONE* **2013,** *8* (4), e60628.

3. Boulet, S.; Mounayar, S.; Poupard, A.; Bertrand, A.; Jan, C.; Pessiglione, M.; Hirsch, E. C.; Feuerstein, C.; François, C.; Féger, J., Behavioral recovery in MPTP-treated monkeys: neurochemical mechanisms studied by intrastriatal microdialysis. *The Journal of Neuroscience* **2008,** *28* (38), 9575-9584.

4. Tsukada, H.; Nishiyama, S.; Fukumoto, D.; Ohba, H.; Sato, K.; Kakiuchi, T., Effects of acute acetylcholinesterase inhibition on the cerebral cholinergic neuronal system and cognitive function: functional imaging of the conscious monkey brain using animal PET in combination with microdialysis. *Synapse* **2004,** *52* (1), 1-10.

5. Zapata, A.; Chefer, V. I.; Shippenberg, T. S., Microdialysis in Rodents. *Current protocols in neuroscience / editorial board, Jacqueline N. Crawley ... [et al.]* **2009,** *CHAPTER,* Unit7.2-Unit7.2.

6. Valen, G.; Owall A Fau - Takeshima, S.; Takeshima S Fau - Goiny, M.; Goiny M Fau - Ungerstedt, U.; Ungerstedt U Fau - Vaage, J.; Vaage, J., Metabolic changes induced by ischemia and cardioplegia: a study employing cardiac microdialysis in pigs. (1010-7940 (Print)).

7. Wei, H.; Chen, Y.; Xu, L.; Zheng, J., Percutaneous penetration kinetics of lidocaine and prilocaine in two local anesthetic formulations assessed by in vivo microdialysis in pigs. *Biol. Pharm. Bull. FIELD Full Journal Title:Biological & Pharmaceutical Bulletin* **2007,** *30* (4), 830-834.

8. OpenStax College, Anatomy & Physiology. OpenStax College. 25 April 2013. http://cnx.org/content/col11496/latest/.

9. Chefer, V. I.; Thompson, A. C.; Zapata, A.; Shippenberg, T. S., Overview of brain microdialysis. *Current Protocols in Neuroscience* **2009**, 7.1. 1-7.1. 28.

10. Ballerstadt, R.; Schultz, J. S., Sensor methods for use with microdialysis and ultrafiltration. *Advanced Drug Delivery Reviews* **1996,** *21* (3), 225-237.

11. https://opentextbc.ca/anatomyandphysiology/chapter/26-1-body-fluids-and-fluid-compartments/.

12. Müller, M., *Microdialysis in Drug Development*. Springer: 2013; Vol. 4.

13. Robinson, T. E.; Justice, J. B., *Microdialysis in the Neurosciences: Techniques in the Behavioral and Neural Sciences*. Elsevier: 2013; Vol. 7.

14. Kyriakides, T. R.; Bornstein, P., Matricellular proteins as modulators of wound healing and the foreign body response. *Thrombosis and Haemostasis* **2003,** *90* (6), 986-992.

15. Hetrick, E. M.; Prichard, H. L.; Klitzman, B.; Schoenfisch, M. H., Reduced foreign body response at nitric oxide-releasing subcutaneous implants. *Biomaterials* **2007,** *28* (31), 4571-4580.

16. Myers, R., Development of Push-Pull Systems for Perfusion of Anatomically Distinct Regions of the Brain of the Awake Animala. *Annals of the New York Academy of Sciences* **1986,** *473* (1), 21-41.

17.   Torto, N.; Bang, J.; Richardson, S.; Nilsson, G. S.; Gorton, L.; Laurell, T.; Marko-Varga, G., Optimal membrane choice for microdialysis sampling of oligosaccharides. *J Chromatogr A* **1998,** *806* (Copyright (C) 2012 U.S. National Library of Medicine.), 265-78.

18.   http://www.microdialysis.se/us/products/products.

19.   Stenken, J. A.; Lunte, C. E.; Southard, M. Z.; Ståhle, L., Factors that influence microdialysis recovery. Comparison of experimental and theoretical microdialysis recoveries in rat liver. *Journal of Pharmaceutical Sciences* **1997,** *86* (8), 958-966.

20.   Torto, N.; Laurell, T.; Gorton, L.; Marko-Varga, G., Recent trends in the application of microdialysis in bioprocesses. *Anal. Chim. Acta* **1999,** *379* (Copyright (C) 2012 American Chemical Society (ACS). All Rights Reserved.), 281-305.

21.   Kehr, J., A survey on quantitative microdialysis: theoretical models and practical implications. *J Neurosci Methods* **1993,** *48* (3), 251-61.

22.   Espinal Cabrera, R. F. Development of a microfluidic device coupled to microdialysis sampling for the pre-concentration of cytokines. M.S., University of Arkansas, United States -- Arkansas, 2012.

23.   Li, Z.; Hughes, D.; Urban, J. P. G.; Cui, Z., Effect of pumping methods on transmembrane pressure, fluid balance and relative recovery in microdialysis. *Journal of Membrane Science* **2008,** *310* (1–2), 237-245.

24.   Polak, J. M., *Advances in tissue engineering*. Imperial College Press: 2008.

25.   Tsai, T.-H., *Applications of microdialysis in pharmaceutical science*. John Wiley & Sons: 2011.

26.   Ao, X. Microdialysis Sampling of Some Hydrophobic Drugs and Inflammatory Cytokines. Rensselaer Polytechnic Institute Troy, New York, 2005.

27.   Wang, Y. X.; Stenken, J. A., Affinity-based microdialysis sampling using heparin for in vitro collection of human cytokines. *Analytica Chimica Acta* **2009,** *651* (1), 105-111.

28.   Sakai, K., Determination of pore-size and pore-size distribution: 2. Dialysis membranes. *Journal of Membrane Science* **1994,** *96* (1-2), 91-130.

29.   Bungay, P. M.; Morrison, P. F.; Dedrick, R. L., Steady-state theory for quantitative microdialysis of solutes and water in vivo and in vitro. *Life Sciences* **1990,** *46* (2), 105-19.

30.   Plock, N.; Kloft, C., Microdialysis - theoretical background and recent implementation in applied life-sciences. *European Journal of Pharmaceutical Sciences* **2005,** *25* (1), 1-24.

31.   Benveniste, H.; Hansen, A. J.; Ottosen, N. S., Determination of brain interstitial concentrations by microdialysis. *J. Neurochem.* **1989,** *52* (6), 1741-50.

32.   Sykova, E.; Nicholson, C., Diffusion in brain extracellular space. *Physiol. Rev.* **2008,** *88* (4), 1277-1340.

33.   de Lange, E. C. M., Recovery and Calibration Techniques:Toward Quantitative Microdialysis. In *Microdialysis in Drug Development*, Müller, M., Ed. Springer: New York, 2013; pp 13-33.

34.   Stenken, J. A., Methods and issues in microdialysis calibration. *Anal. Chim. Acta* **1999,** *379* (3), 337-357.

35. Chu, J.; Hjort K Fau - Larsson, A.; Larsson A Fau - Dahlin, A. P.; Dahlin, A. P., Impact of static pressure on transmembrane fluid exchange in high molecular weight cut off microdialysis. (1572-8781 (Electronic)).

36. Czosnyka, M.; Pickard, J. D., Monitoring and interpretation of intracranial pressure. *Journal of Neurology, Neurosurgery & Psychiatry* **2004,** *75* (6), 813-821.

37. Yu, L.; Kim, B. J.; Meng, E., Chronically Implanted Pressure Sensors: Challenges and State of the Field. *Sensors (Basel, Switzerland)* **2014,** *14* (11), 20620-20644.

38. Choi, S.; Lee, M. G.; Park, J.-K., Microfluidic parallel circuit for measurement of hydraulic resistance. *Biomicrofluidics* **2010,** *4* (3).

39. Hershey, N. D.; Kennedy, R. T., In vivo calibration of microdialysis using infusion of stable-isotope labeled neurotransmitters. *ACS Chem Neurosci* **2013,** *4* (5), 729-36.

40. Snyder, K. L.; Nathan, C. E.; Yee, A.; Stenken, J. A., Diffusion and calibration properties of microdialysis sampling membranes in biological media. *Analyst* **2001,** *126* (8), 1261-1268.

41. Quintanilla, V. A. Y., *Rejection of Emerging Organic Contaminants by Nanofiltration and Reverse Osmosis Membranes: Effects of Fouling, Modelling and Water Reuse*. CRC Press: 2010.

42. www.basinc.com/library/TechNotes/BASi_TN_1013.pdf.

43. www.lifetechnologies.com/us/en/home/life-science/protein-biology/protein-biology-learning-center/protein-biology-resource-library/pierce-protein-methods/dialysis-methods-protein-research.html.

44. Fournier, R. L., *Basic transport phenomena in biomedical engineering*. CRC Press: 2011.

45. Schutte, R. J.; Oshodi, S. A.; Reichert, W. M., In Vitro Characterization of Microdialysis Sampling of Macromolecules. *Analytical Chemistry* **2004,** *76* (20), 6058-6063.

46. Li, Z.; Cui, Z., Application of microdialysis in tissue engineering monitoring. *Progress in Natural Science* **2008,** *18* (5), 503-511.

47. www.microdialysis.com/us/basic-research/faq-basic-research.

48. Nicholson, C.; Phillips, J. M., Ion diffusion modified by tortuosity and volume fraction in the extracellular microenvironment of the rat cerebellum. *The Journal of Physiology* **1981,** *321*, 225-257.

49. Hrabe, J.; Hrabětová, S.; Segeth, K., A Model of Effective Diffusion and Tortuosity in the Extracellular Space of the Brain. *Biophysical Journal* **2004,** *87* (3), 1606-1617.

50. Jacobson, I.; Sandberg, M.; Hamberger, A., Mass transfer in brain dialysis devices—a new method for the estimation of extracellular amino acids concentration. *Journal of Neuroscience Methods* **1985,** *15* (3), 263-268.

51. Westerink, B.; Justice Jr, J., Microdialysis compared with other in vivo release models. *Microdialysis in the neurosciences, techniques in the behavioral and neural sciences* **1991,** *7*, 23-46.

52. Duo, J.; Stenken, J. A., In vitro and in vivo affinity microdialysis sampling of cytokines using heparin-immobilized microspheres. *Analytical and Bioanalytical Chemistry* **2011,** *399* (2), 783-793.

53.   Duo, J.; Fletcher, H.; Stenken, J. A., Natural and synthetic affinity agents as microdialysis sampling mass transport enhancers: Current progress and future perspectives. *Biosensors & Bioelectronics* **2006,** *22* (3), 449-457.

54.   Duo, J.; Espinal, R.; Stenken, J. A. Comparison of heparin-immobilized vs. antibody-immobilized microspheres for the capture and detection of cytokines during microdialysis sampling *IEEExplore Digital Library* [Online], 2009, p. 112-115.

55.   Fletcher, H. J.; Stenken, J. A., An in vitro comparison of microdialysis relative recovery of Met- and Leu-enkephalin using cyclodextrins and antibodies as affinity agents. *Analytica Chimica Acta* **2008,** *620* (1–2), 170-175.

56.   Gutierrez, A.; Anderstam, B.; Alvestrand, A., Amino acid concentration in the interstitium of human skeletal muscle: a microdialysis study. *European Journal of Clinical Investigation* **1999,** *29* (11), 947-952.

57.   Korf, J.; Huinink, K. D.; Posthuma-Trumpie, G. A., Ultraslow microdialysis and microfiltration for in-line, on-line and off-line monitoring. *Trends in Biotechnology* **2010,** *28* (3), 150-158.

58.   Lerma, J.; Herranz, A. S.; Herreras, O.; Abraira, V.; Martin del Rio, R., In vivo determination of extracellular concentration of amino acids in the rat hippocampus. A method based on brain dialysis and computerized analysis. *Brain Res* **1986,** *384* (1), 145-55.

59.   Sternberg, F.; Meyerhoff, C.; Mennel, F. J.; Hoss, U.; Mayer, H.; Bischof, F.; Pfeiffer, E. F., Calibration problems of subcutaneous glucosensors when applied \"in-situ\" in man. *Hormone and Metabolic Research* **1994,** *26* (11), 523-5.

60.   Sternberg, F.; Meyerhoff, C.; Mennel, F. J.; Bischof, F.; Pfeiffer, E. F., Subcutaneous glucose concentration in humans: real estimation and continuous monitoring. *Diabetes Care* **1995,** *18* (9), 1266-1269.

61.   Bungay, P. M.; Wang, T.; Yang, H.; Elmquist, W. F., Utilizing transmembrane convection to enhance solute sampling and delivery by microdialysis: Theory and in vitro validation. *Journal of membrane science* **2010,** *348* (1), 131-149.

62.   Chu, J.; Hjort, K.; Larsson, A.; Dahlin, A. P., Impact of static pressure on transmembrane fluid exchange in high molecular weight cut off microdialysis. *Biomedical microdevices* **2014,** *16* (2), 301-310.

63.   Chu, J.; Hjort, K.; Larsson, A.; Dahlin, A. P. In *Consequence of static pressure on transmembrane exchanges during in vitro microdialysis sampling of proteins*, Monitoring Molecules in Neuroscience: 14th International Conference, September 16–20, London, UK, 2012.

64.   Hillered, L.; Dahlin, A. P.; Clausen, F.; Chu, J.; Bergquist, J.; Hjort, K.; Enblad, P.; Lewén, A., Cerebral Microdialysis for Protein Biomarker Monitoring in the Neurointensive Care Setting – A Technical Approach. *Frontiers in Neurology* **2014,** *5* (245).

65.   Array type microdialysis probe. Google Patents: 2013.

66.   Strouch, M. B.; Jackson, E. K.; Mi, Z.; Metes, N. A.; Carey, G. B., Extracellular Cyclic AMP—Adenosine Pathway in Isolated Adipocytes and Adipose Tissue. *Obesity Research* **2005,** *13* (6), 974-981.

67.   Yuen, P. K.; DeRosa, M. E., Flexible microfluidic devices with three-dimensional interconnected microporous walls for gas and liquid applications. *Lab on a Chip* **2011,** *11* (19), 3249-3255.

68.   www.ddw-online.com/enabling-technologies/p149617-pharmaceutical-&-biomedical-research-likely-to-use-$1-billion-worth-of-microfluidics-devices-by-2016-summer-12.html.

69.   de Jong, J.; Lammertink, R. G. H.; Wessling, M., Membranes and microfluidics: a review. *Lab on a Chip* **2006,** *6* (9), 1125-1139.

70.   Tüdős, A. J.; Besselink, G. A.; Schasfoort, R. B., Trends in miniaturized total analysis systems for point-of-care testing in clinical chemistry. *Lab on a Chip* **2001,** *1* (2), 83-95.

71.   Hsieh, Y.-C.; Zahn, J. D., Glucose recovery in a microfluidic microdialysis biochip. *Sensors and Actuators B: Chemical* **2005,** *107* (2), 649-656.

72.   Kricka, L. J., Miniaturization of analytical systems. *Clinical Chemistry* **1998,** *44* (9), 2008-2014.

73.   Subrebost, G. Silicon-based microdialysis chip with integrated fraction collection and biofouling control. The Robotics Institute Carnegie Mellon University, 2005.

74.   Lee, W. H.; Ngernsutivorakul, T.; Mabrouk, O. S.; Wong, J. M. T.; Dugan, C. E.; Pappas, S. S.; Yoon, H. J.; Kennedy, R. T., Microfabrication and in Vivo Performance of a Microdialysis Probe with Embedded Membrane. *Analytical Chemistry* **2016,** *88* (2), 1230-1237.

75.   Kim, C.; Ryu, C.; Kim, B. W.; Sim, S. J.; Chae, H.; Yoon, H. C.; Yang, S. S., Microfluidic dialysis device fabrication for protein solution enrichment and its enrichment enhancement by plasma surface treatment of a membrane. *Journal of The Korean Physical Society* **2007,** *51* (3), 993.

2 Chapter 2. Proof of principle recycling flow approach using 100 μM methyl orange solution
2.1 Background and Significance

This chapter describes the work that was performed to demonstrate that a recycling flow approach could be used to improve relative recovery of small molecules during microdialysis sampling experiments. Methyl orange, a small molecule of 330 Da was used as the analyte. A solution of 100 μM methyl orange in high performance liquid chromatography (HPLC) grade water was used. The availability and cost of methyl orange made it an ideal analyte for this work. The recycling flow experiments described in this chapter laid the foundation of the microdialysis probes in series approach. A detailed description of the microdialysis probes in series approach is covered in chapter 3. Experiments were conducted to evaluate the number of microdialysis probes in series necessary to achieve ~100% relative recovery. The experiments were performed under quiescent and stirred conditions. The main purpose was to study the influence of flow rate and number of cycles on relative recovery.

2.2 Experimental section

A solution of 100 μM methyl orange (Sigma-Aldrich, St. Louis, MO) in HPLC grade water was used as the target analyte. A 0.6 mL plastic reservoir was used to place the microdialysis probe. The microdialysis probe used was a CMA/20 microdialysis probe having a 10-mm polyethersulfone (PES) membrane of 100 kDa molecular weight cutoff (MWO) (Harvard Apparatus, Holliston, MA), see Figure 2.1. A MAB-20 microdialysis pump was used to recycle the dialysate through the probe (Microbiotech, Stockholm, Sweden), see Figure 2.2. HPLC grade water was used as perfusion fluid. One cycle was defined as one dialysate or sample collection. This was equivalent to collections conducted during regular microdialysis sampling. The first dialysate collected was used as perfusion fluid for the second collection, the second dialysate collected was used as perfusion fluid for the third collection, and so on, see Figure 2.3. The experiments were performed under quiescent and stirred conditions see Figure 2.2 and Figure 2.4. The bulk of the experiments were performed under quiescent conditions. The flow rates used for the recycling flow microdialysis experiments under quiescent condition were 0.8, 1.0, 2.5, and 5.0 μL/min. A flow rate of 2.5 μL/min was used for the recycling experiments performed under stirred (on a stir plate at 800 rpm) condition and a maximum of 5 cycles, see Figure 2.5.
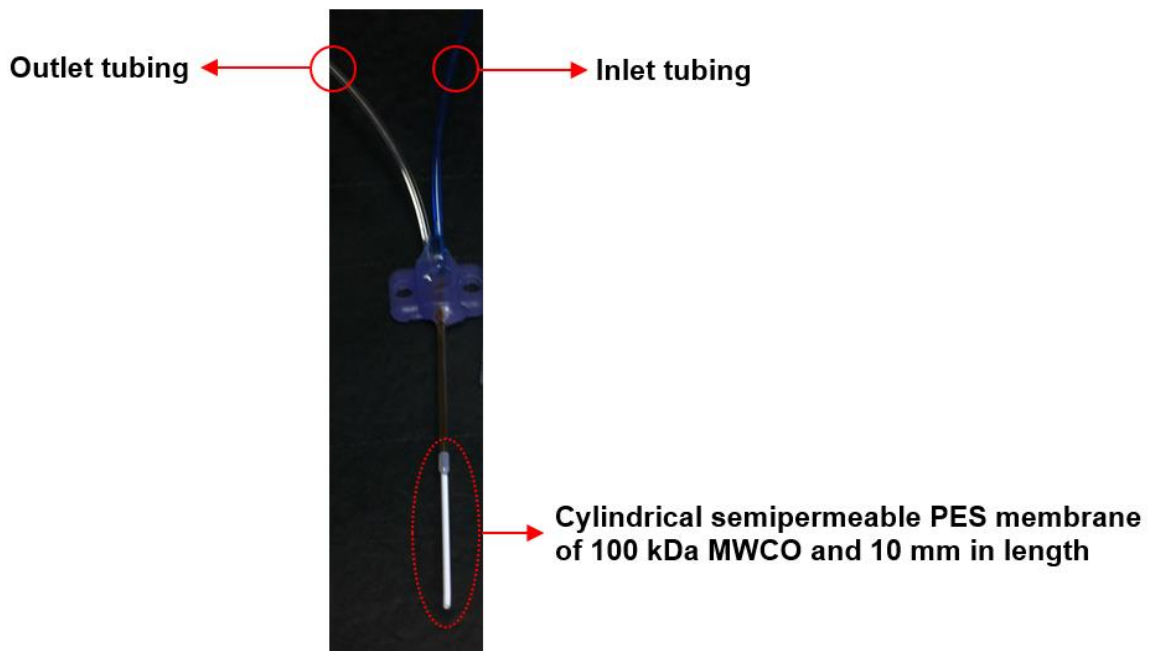
Figure 2.1. CMA/20 microdialysis probe of 100 kDa and PES membrane of 10 mm in length used for the experiments.
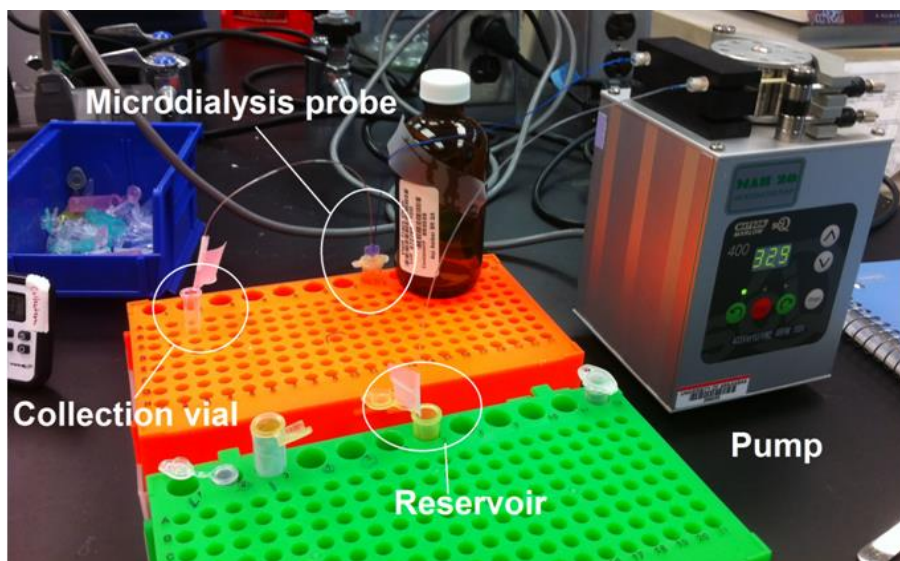
Figure 2.2. Recycle flow set up used for microdialysis experiments conducted under quiescent condition using MAB-20 pump.
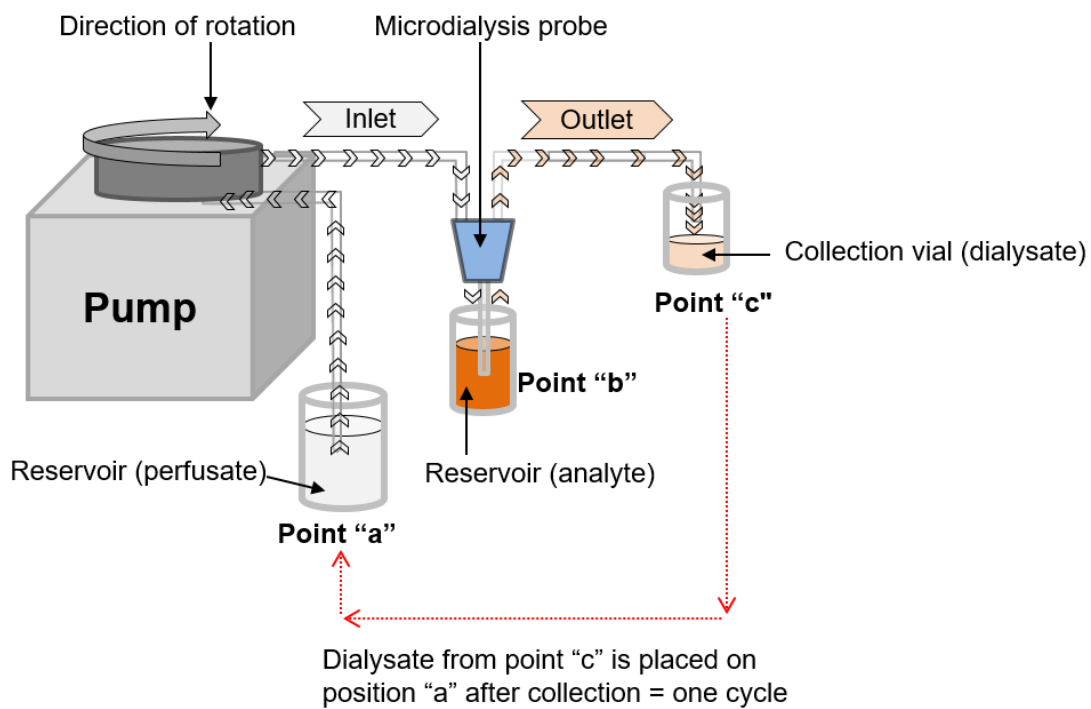
Figure 2.3. Set up used to recycling flow experiments. Point a) HPLC grade water reservoir (perfusate). Point b) 100 µM methyl orange solution or analyte. Point c) Collection vial (dialysate).
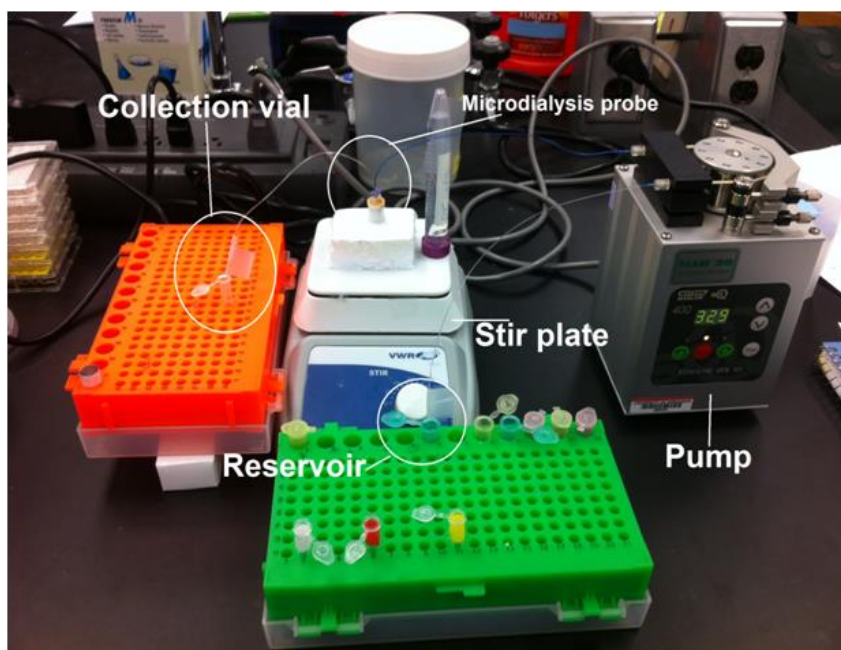
Figure 2.4. Recycle flow set up used for microdialysis experiments conducted under stirred condition using MAB-20 pump.
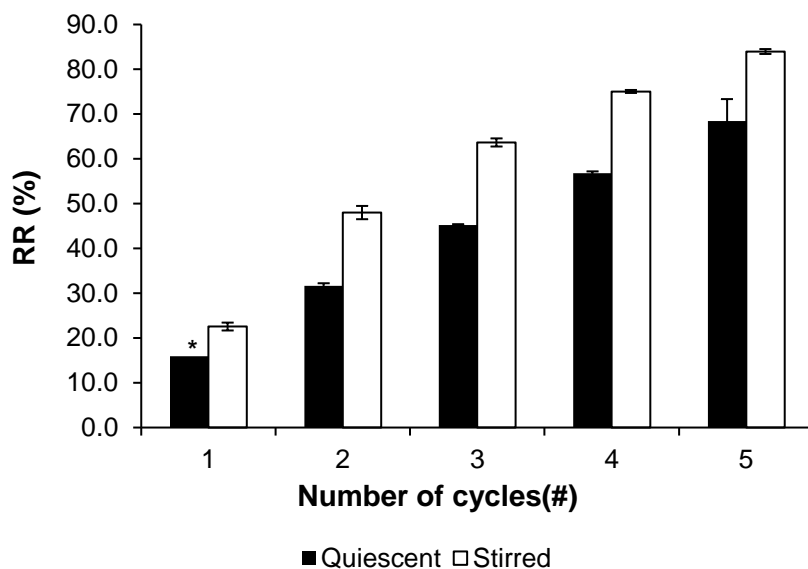
Figure 2.5. Comparison of relative recovery (RR) of 100 µM methyl orange under quiescent and stirred conditions during microdialysis recycling flow experiments using a 100 kDa CMA/20 microdialysis probe having a 10 mm PES membrane in length, 5 cycles. HPLC water was used as perfusion fluid at 2.5 µL/min. n = 3, *n = 2, and average ± standard deviation

The maximum number of cycles used for the collections of methyl orange under quiescent condition was four for 0.8, 1.0, and 5.0 µL/min, and five and ten cycles for 2.5 µL/min, see Figure 2.5, Figure 2.6, and Figure 2.7. The absorbance of each dialysate was measured at a wavelength of 466 nm using a TecanSpectraFluor plate (96 wells) reader (Tecan Group Ltd., Männedorf, Switzerland) and was compared vs. a calibration curve. At least 50 µL of dialysate was required for measurement with the plate reader. Three aliquots were taken from each dialysate and each one was diluted to 100 µL in HPLC grade water.

2.3 Results and discussion

A logarithmic relationship between flow rate and the number of cycles was found for the recycling flow experiments, see Figure 2.6 and Figure 2.7. This finding is in line with what has been previously reported in the literature by Lerma et al.[1] The highest relative recoveries for methyl orange using recycling flow were obtained at 0.8 µL/min and 4 cycles (100.3%) and 2.5 µL/min and 9 cycles (98.1% ± 2.7%), see Figure 2.7. These results show the tradeoff between flow rate and number of cycles.
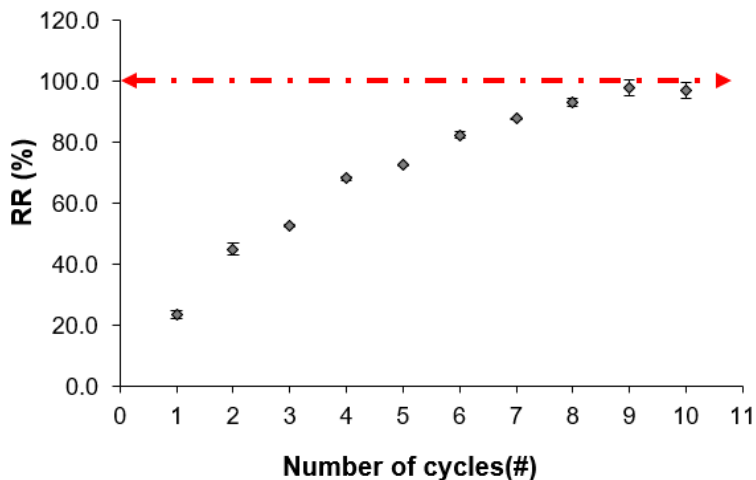
Figure 2.6. Relative recovery (RR) of 100 µM methyl orange under quiescent conditions collected during microdialysis recycling flow experiments at 2.5 µL/min, 10 cycles. HPLC water was used as perfusion fluid. n = 3 and average ± standard deviation. The red line shows the 100% RR region.

◆ At 0.8 µL/min   ● At 1.0 µL/min   ▲ At 2.5 µL/min   ◆ At 5.0 µL/min
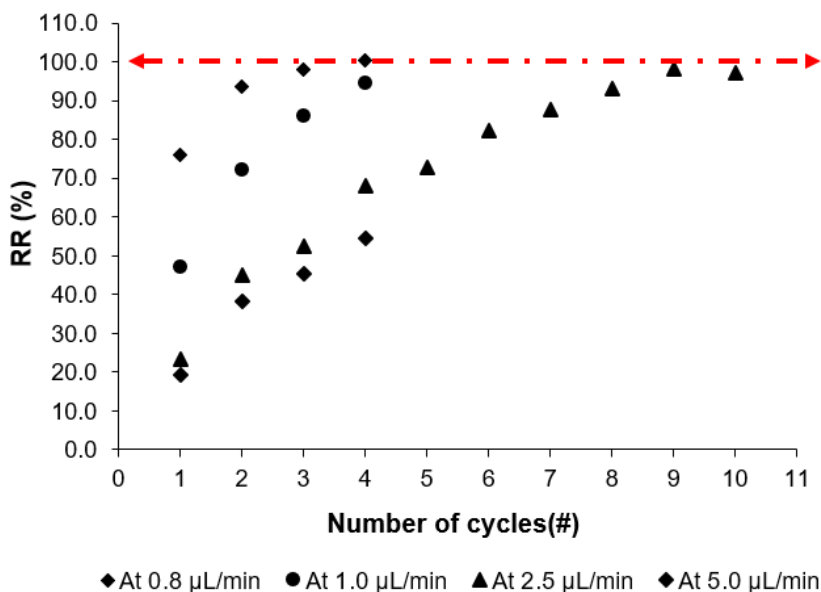
Figure 2.7. Relative recovery (RR) of 100 µM methyl orange using recycling flow method under quiescent condition. HPLC water was used as perfusate at different flow rates.

This was expected for a diffusion-based technique such as microdialysis. The residence time or the time analyte stays in contact with the perfusion fluid across the membrane/sample interface, increases at lower flow rates. Lower flow rates allow more time for methyl orange to diffuse through the microdialysis membrane and be carried by the perfusion fluid. Therefore, fewer cycles are needed as compared to higher flow rates. Higher flow rates require more cycles to increase the residence time. For the experiments conducted under stirred condition the relative recovery of methyl orange as a function of the flow rate was higher (83.9% ± 0.6%) compared to the quiescent experiments (68.5% ± 4.9%), see Figure 2.5. This is due to the fact that the mass transport resistance of the quiescent medium external to the microdialysis probe (R_q) approaches zero in well-stirred solutions reducing its influence on the relative recovery (see Equation 1.2 in chapter 1). The problem with collecting 50 µL was that it significantly increased the amount of time necessary to conduct an experiment due to the experimental set up chosen. As can be seen on Table 2.1 ~8 hours and 20 minutes were needed to conduct one set of experiments for one flow rate. This was necessary to conduct the five-cycle's experiments. The rinse time was determined by measuring the time that the perfusion fluid took from the reservoir to the collection vial (from point "a" to point "c"), see Figure 2.3. The set up was chosen in order to have more control over each individual cycle. To reduce time, sample volume, and cost, a different approach was developed. The flow rates used for the microdialysis in series approach experiments, chapter 3, were based on the results obtained on this chapter. The new approach consisted of several microdialysis probes in series.

Table 2.1. Sequence used for the collection of 100 µM methyl orange at 2.5 µL/min.

Cycle #	Calculated collection volume (µL)	Collection time (min)
1	450	180
2	350	140
3	250	100
4	150	60
5	50	20

Notes: The calculated collection volume was calculated by multiplying the flow rate times the collection time.

2.4   References

1.   Lerma, J.; Herranz, A. S.; Herreras, O.; Abraira, V.; Martin del Rio, R., In vivo determination of extracellular concentration of amino acids in the rat hippocampus. A method based on brain dialysis and computerized analysis. *Brain Res* **1986,** *384* (1), 145-55.

2.   www.harvardapparatus.com/cma-20-elite-probes.html.

3.   http://www.microdialysis.se/us/products/probes/cma-20.

4.   http://en.wikipedia.org/wiki/File:Polysulfone_repeating_unit.png.

3   Chapter 3. In vitro collection of methyl orange and fluorescein isothiocyanate-dextrans (FITCs) using microdialysis probes in series

3.1   Introduction

A new microdialysis sampling method was developed to reduce the amount of time, sample volume, and cost required to perform the recycling flow experiments (Table 2.1). The new approach consisted of two microdialysis probes in series, see Figure 3.1 and Figure 3.2. The number of microdialysis probes connected in series was extended to four probes, see Figure 3.3. Four microdialysis probes was the maximum number probes in series that was tested for this work. The method was called microdialysis probes in series due to the fact that microdialysis sampling probes were connected in series. To evaluate the probes in series method two set ups were used. The reservoir where the microdialysis probes in series were placed went through different iterations. This was done to minimize the volume of analyte needed for the experiments. In this chapter, the was to demonstrate *in vitro* microdialysis probes in series approach for a series of compounds with a wide-range of molecular weight (methyl orange, FITC-4, FITC-10, FITC-20, and FITC-40). This work serves as a proof of principle for next generation microdialysis probe. The latter will be addressed in chapter 5 in detail.
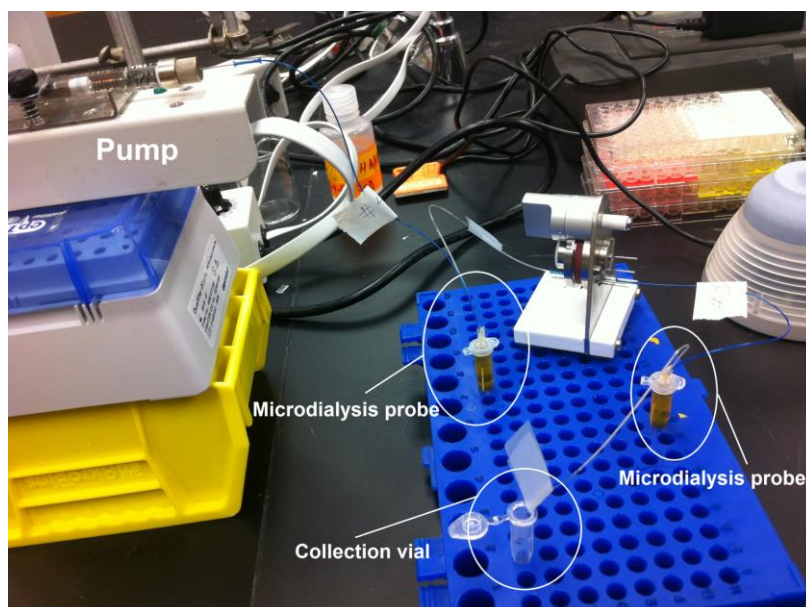
Figure 3.1. Microdialysis probes in series method having each probe in separate vials (two probes), 0.6 mL plastic vials.
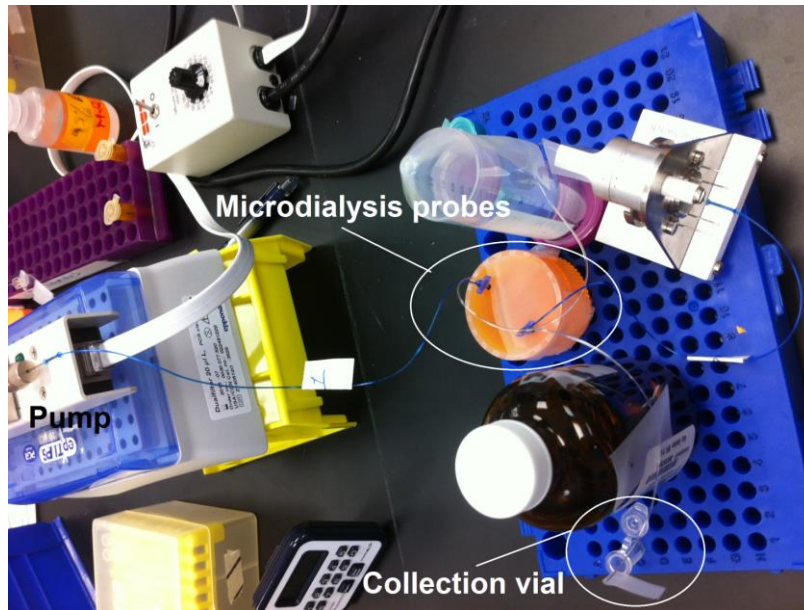
Figure 3.2. Microdialysis probes in series method having the probes in the same vial (two probes), 20.0 mL house-made reservoir.
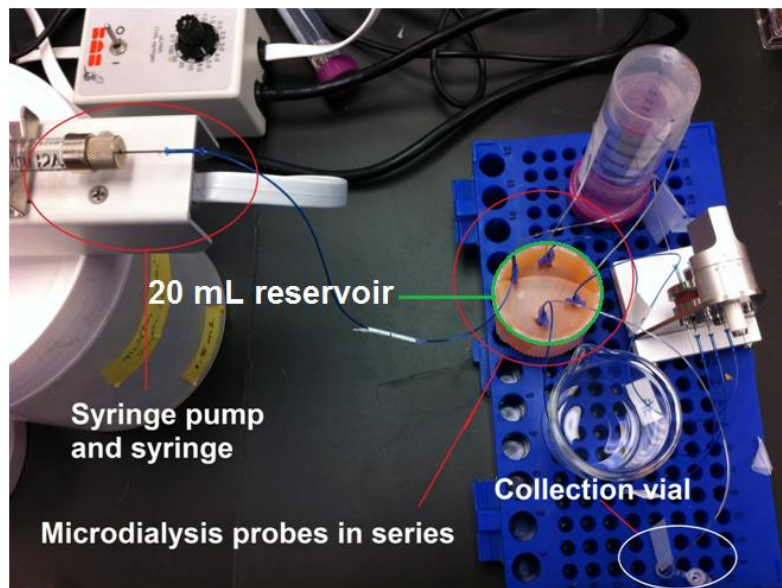
Figure 3.3. Microdialysis probes in series method having the probes in the same vial (four probes).

3.2 Experimental section

3.2.1 Proof of principle and initial settings

The microdialysis probes in series approach went through a series of iterations as mentioned before, see Table 3.1. This was done to reach the optimal settings of the method for future experiments using proteins. The first set of iterations consisted of two and four microdialysis probes in series, see Figure 3.1, Figure 3.2, and Figure 3.3. These probes were either placed in separate reservoirs or in the same reservoir. A CMA 110 liquid switch from Harvard Apparatus, Holliston, MA was used as tubing holder to facilitate the connections between probes, see Figure 3.4. The MAB-20 pump previously used for the recycling flow experiments, chapter 2, was replaced by a BASi syringe pump system (West Lafayette, IN). Microdialysis probes (CMA/20) of 100 kDa molecular weight cutoff (MWCO) and 10 mm polyethersulfone (PES) membrane were from Harvard Apparatus (Holliston, MA). The absorbance of each dialysate was measured at a wavelength of 466 nm using a TecanSpectraFluor plate (96 wells) reader (Tecan Group Ltd., Männedorf, Switzerland) to determine their concentration using an appropriate calibration curve.

Table 3.1. Iterations performed to the microdialysis in series approach.

Iteration #	Settings	Perfusion fluid	Instrument	Reservoir
1	Two probes in separate vials. Two and four probes in same reservoir.	HPLC water	TecanSpectraFluor plate reader requiring sample volume of ≥ 50 μL. Samples were diluted.	0.6 mL vials for probes placed separate and 20.0 mL house-made container for probes placed together using Parafilm M® and a plastic lid.
2	Same	Same	NanoDrop 2000 requiring sample volume of 2 μL. Samples were not diluted	Same
3	Same	4% dextran-70 or 0.1% BSA in 10 mM PBS pH 7.4	Same	0.6 mL vials for probes placed separate and 5.0 mL house-made plastic vial for probes place together.
4	Same	4% dextran-70 in 10 mM PBS pH 7.4	Same	0.6 mL vials for probes placed separate and ~2.5 mL house-made plastic vial wrapped with aluminum foil for probes place together
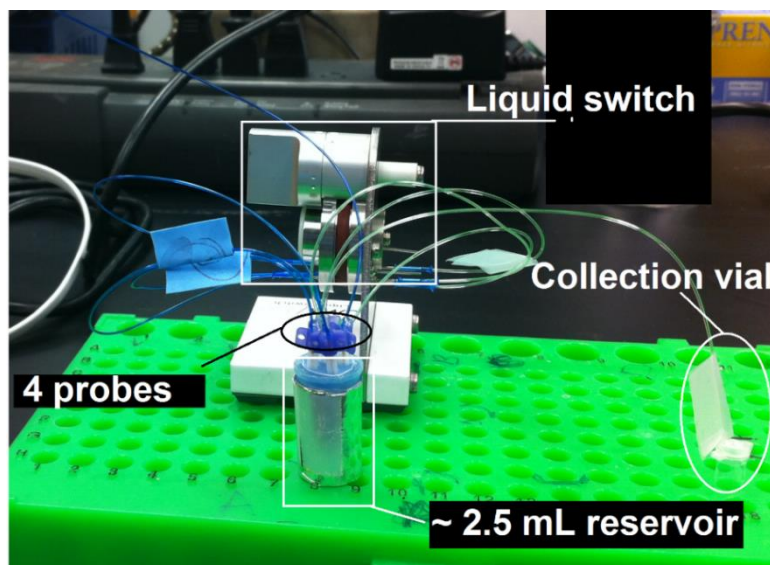
Figure 3.4. Four microdialysis probes in series in the house-made ~2.5 mL reservoir showing aluminum paper for light protection.

At least 50 μL of dialysate was required in order to measure the concentration of methyl orange samples using the plate reader. Three aliquots were taken from each dialysate and each one dilute to 100 μL in HPLC grade water.

For this set of iterations, a solution of 100 μM methyl orange in HPLC grade water was used as the analyte. A house-made reservoir was built to hold the microdialysis probes in the same container. The reservoir was made out of a plastic lid and Parafilm M®, see Figure 3.2 and Figure 3.3. The volume of the reservoir was 20.0 mL. The reservoirs used for the microdialysis probes placed in separate reservoirs were clear plastic microvials of 0.6 mL. Collections of two independent microdialysis sampling experiments, regular microdialysis, were added. This was done to compare the relative recovery of two probes in series in separate and same reservoir versus adding the relative recoveries of two probes from separate microdialysis experiments. The flow rate used for these experiments was 2.5 μL/min. For the next iteration a NanoDrop 2000 UV-Vis spectrophotometer from Thermo Scientific (Wilmington, DE) was used to measure the absorbance of the dialysates. The advantage of using the NanoDrop is that it only requires 2 μL of sample volume, reducing significantly the sample size and collection time. From this point forward, all experiments were conducted using the NanoDrop unless otherwise stated.

For these experiments 100 μM methyl orange solution was used as the analyte and HPLC water as the perfusion fluid. The flow rates used were 1.0, 1.5, 2.0, 2.5, 3.0, and 4.0 μL/min. The 20.0 mL plastic reservoir was used.

After several experiments performed using HPLC water as the perfusion fluid, the chemical composition of the perfusion was changed to match the composition of the extracellular fluid. The chemical or ionic composition of the extracellular fluid is: Sodium 0.142 mol, potassium 0.005 mol, calcium 0.002 mol, magnesium 0.001mol, chloride 0.105 mol, bicarbonate 0.024 mol, and phosphate 0.0007 mol.[1, 2] This is commonly used to maintain appropriate osmotic pressure and ionic composition. Also, it is used to minimize the level of disturbance of biology in living systems during microdialysis sampling collections performed *in vivo*. The perfusion fluid used for the *in vitro* experiments was a solution of 10 mM phosphate buffered saline (PBS) pH = 7.4 having either 4% (w/v) dextran-70 or 0.1% (w/v) bovine serum albumin (BSA) from Sigma-Aldrich, St. Louis, MO. It is good to point out that for this dissertation *in vivo* experiments were not conducted. The PBS used for this dissertation was composed of 10 mM disodium phosphate, 1.8 mM monopotassium phosphate, 2.7 mM potassium chloride, and 137 mM sodium chloride. Calcium chloride dihydrate and magnesium chloride hexahydrate are supplemented in some applications such as *in vivo* experiments.[3] The objective of adding dextran-70 and BSA was to evaluate how these osmotic agents would influence the relative recovery of methyl orange.[4, 5]

The flow rates used were 1.0, 2.5, and 5.0 μL/min. HPLC water was used as control. Previously, Parafilm M® was used to hold the microdialysis probes connected in series for the 20.0 mL plastic reservoir. The problem with using this is that it is very fragile and tends to give away. A new 5 mL reservoir able to hold four microdialysis probes firmly was made for these experiments. One of the aims of this iteration was made to reduce the volume of the reservoir from 20.0 mL to 5.0 mL.

The last iteration was made to the microdialysis in probes in series approach. This was done to further reduce the volume of the reservoir from 5 mL to ~2.5 mL. Aluminum foil was used to minimize the interaction of light and the analyte in the reservoir of ~2.5 mL, see Figure 3.4. All experiments done using this reservoir used aluminum foil unless otherwise stated. By reducing the volume of analyte in the reservoir, more expensive compounds could be used to further evaluate the microdialysis probes in series method.

The idea was to eventually use the method to collect proteins such as cytokines. It is good to point out that proteins were not used for this dissertation.

3.2.2   Four microdialysis probes in series

For this last iteration, four microdialysis probes in series, a set of experiments were conducted. Solutions of 100 µM methyl orange, FITC-4, FITC-10, FITC-20, and FITC-40 were prepared in 10 mM phosphate buffered saline (PBS) pH = 7.4. The perfusion fluid used for the experiments was 10 mM (PBS) pH = 7.4 having 4% dextran-70 as osmotic agent commonly used in microdialysis experiments to reduce fluid loss and "counterbalance the transmembrane hydrostatic driving pressure".[4] All the chemicals used were purchased from Sigma-Aldrich (St. Louis, MO) unless otherwise stated. BASi syringe pumps and gastight 1.0 mL syringes were used (Bioanalytical Systems Inc., West Lafayette, IN). Microdialysis probes (CMA/20) of 100 kDa molecular weight cutoff (MWCO) and 10 mm polyethersulfone (PES) membrane were used. The idea behind these experiments was to obtain detailed information about the relationship between recovery, number of probes in series (i.e., 1, 2, 3, and 4), flow rate, and molecular weight. Probes were connected to each other in series without altering the standard tubing lines (200 mm length and 0.12 mm internal diameter inlet and outlet lines) that comes with the CMA/20 dialysis probes. For the number of probes in series the collection through one or a single microdialysis probe was used a control. This was chosen because one microdialysis probe is commonly used during microdialysis sampling experiments.
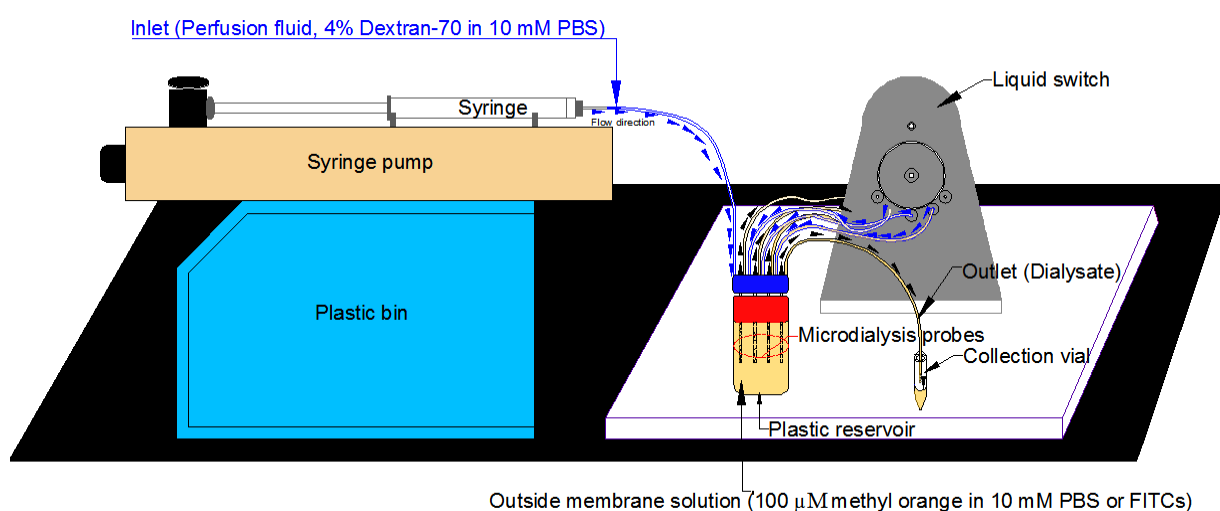
Figure 3.5. Schematic representation of microdialysis probes in series approach.

The same experiments were conducted having two, three, and four microdialysis probes in series. Figure 3.5 shows a schematic representation of the new four microdialysis probes in series approach. Flow rates of 0.8, 1.0, and 1.5 µL/min were used.

A simple and straightforward procedure was developed: a) Perfuse perfusion fluid (PBS) for ~15 min or until dialysate absorbance was within 5% relative standard deviation (RSD), measurements were performed in triplicate unless otherwise stated, b) measure the absorbance of the outside solutions or solutions place in the in-house made plastic container before changing to a new flow rate, and c) after changing flow rates flush the system for the same amount of time and criteria than "a" to avoid cross contamination from one flow rate to another.

3.3 Results and discussion

3.3.1 Proof of principle and initial settings

Figure 3.6 shows the relative recoveries of 100 µM methyl orange collected using two microdialysis probes either in series or individually. According to these preliminary results the relative recovery of methyl orange was higher (46.0% ± 1.7%, n=3) when microdialysis probes were connected in series and placed in the same reservoir than when they were placed in separate reservoirs (36.1%, n=2). This could be due to fluid loss having a greater impact or diluting the methyl orange in a smaller reservoir (0.6 mL) than in the larger reservoir (20.0 mL) used to place the two probes together.

As comparison, relative recovery of methyl orange was determined using two microdialysis probes. To explain, the relative recoveries were added together, and the total was used to compare it to the two probes in series. These two microdialysis probes were not connected in series, but regular microdialysis sampling experiments were performed on both. The relative recoveries of these microdialysis probes were 26.0% ± 1.3%, n=3 and 22.2% ± 1.1%, n=3 respectively. The total relative recovery of these probes was 48.2% ± 1.7%, n=3. The fluid loss and transmembrane pressure of two probes in series is significantly different than having two separate microdialysis probes. Fluid loss will be address in more detail later in the chapter. When four microdialysis probes were connected in series a relative recovery of 100.8% ± 2.4%, n=3 was obtained for methyl orange at a perfusion fluid flow rate of 1.0 µL/min.

The outside solution was under quiescent condition and HPLC water was used as perfusion fluid without any osmotic agents. Compared to the recycling flow method relative recoveries obtained under similar conditions, the four microdialysis probes in series relative recoveries were higher, see Figure 3.7. For example, the methyl orange relative recovery using four probes in series at a perfusion rate of 2.5 µL/min was 83.9% ± 1.3%, n=3 and the methyl orange relative recovery using recycling flow (four cycles) at the same rate was 75.0% ± 0.3%, n=3. These results are a good indication of the benefits of adding microdialysis sampling probes in series for small molecules. Nevertheless, the opposite effect was found for large molecules such as FITC-40. For larger molecules the fluid loss is the critical factor influencing relative recovery. This will be addressed in the four probes in series discussion, section 3.3.2.

Several perfusion fluids of different chemical compositions were tested using a reservoir of 5 mL to hold the microdialysis probes in series more firmly. The results are shown on Figure 3.8. The perfusion fluid that yielded the highest relative recovery of methyl orange was 4% dextran-70 in 10 mM PBS. For instance, the relative recovery of methyl orange using this perfusion fluid at 2.5 µL/min was 94.0% versus the control, HPLC water, 80.1%. These results are in agreement with what is found in the literature on regular microdialysis sampling, even though the transmembrane pressure in the microdialysis in series approach is higher.[6, 7]
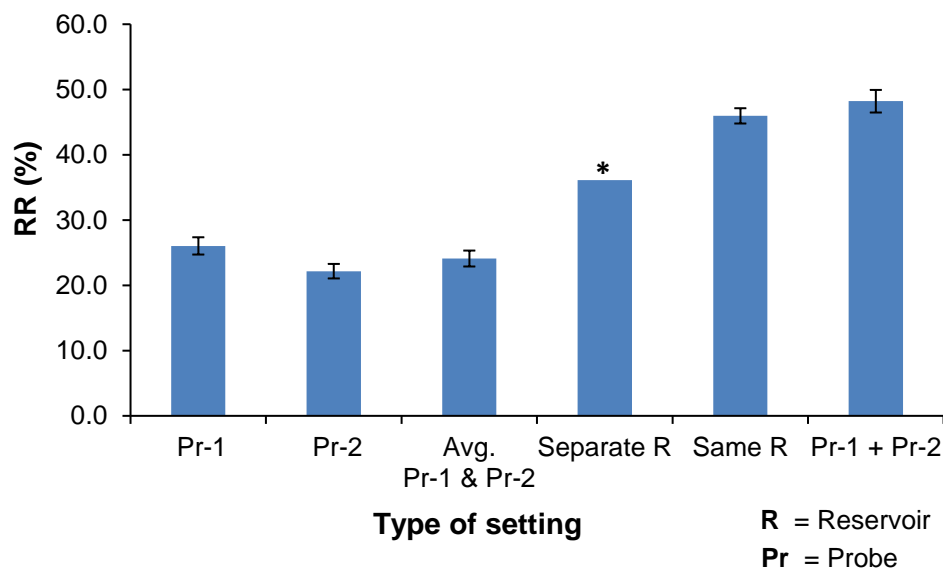
Figure 3.6. Relative recovery (RR) of 100 µM methyl orange in HPLC water using two microdialysis probes in series in the 20.0 mL reservoir under different settings at 2.5 µL/min. (Control = Avg. Pr-1 & Pr-2). n = 3, *n = 2, and average ± standard deviation.
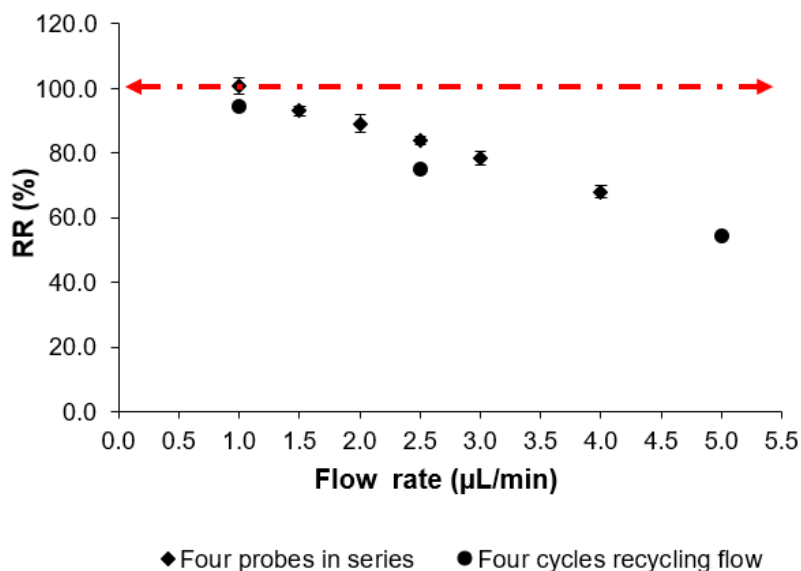
Figure 3.7. Comparison of relative recovery (RR) of 100 µM methyl orange using microdialysis recycling flow and four probes in series method at different flow rates. Four cycles and four probes in series were used during the experiments (20 mL reservoir for probes in series). n = 3 and average ± standard deviation.

According to Li et al., "To minimize fluid loss from the probe due to osmotic effect, the osmolarity of the perfusate is often adjusted to balance the physiological osmolarity by adding osmotic agents, e.g. dextran-70 or a protein such as bovine serum albumin (BSA)."[6] Regulating the transmembrane pressure or fluid loss across microdialysis probe membranes is vitally important during microdialysis sampling experiments, especially during *in vivo* experiments.

3.3.2 Four microdialysis probes in series

Figures 3.9, 3.10, and 3.11 show the relative recoveries of FITCs and methyl orange collected using one, two, three, and four probes at different flow rates (0.8, 1.0, and 1.5 µL/min), respectively. These results show that the relative recovery significantly improves as the number of probes in series increases. For instance, if the collections of methyl orange at 0.8 µL/min for one probe or control (regular microdialysis) (66.7 ± 4.6 %, n=3) and four probes (99.7 ± 1.0 %, n=3) are compared, you can see the significant improvement on the recovery (~33%). However, when we compared the recoveries of two probes versus three probes, and three probes versus four, the improvement was not as significant (~4%), see Figure 3.9.
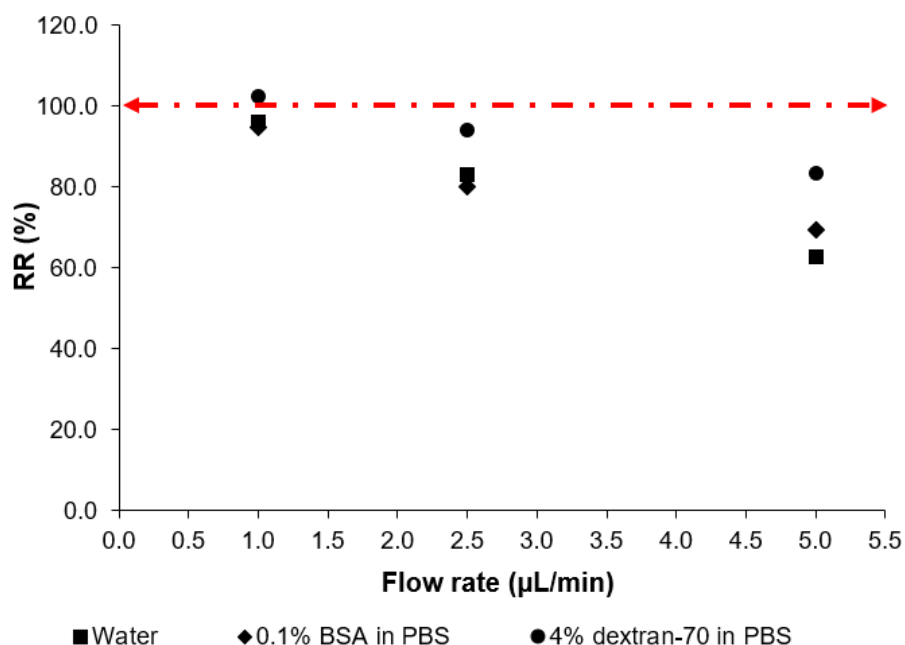
Figure 3.8. Relative recovery (RR) of 100 µM methyl orange under different perfusion fluid chemical compositions and flow rates using 5.0 mL reservoir and four probes in series method.

This could be explained by the size and diffusion properties of methyl orange (330 Da, and a high mass transfer coefficient, *kA,* of ~0.9 µL/min). For one probe the surface area of the system is at its minimum, but the concentration gradient is higher. As the number of probes increases the surface area becomes larger (greater residence time) increasing recovery, but decreasing concentration gradient. Since the probes are in series, the dialysate of one probe becomes the perfusate of the probe attached to it. As a result, the concentration gradient decreases due to the presence of a non-zero analyte concentration inside the probe (membrane) relative to the outside. That is why after two probes in series there is a steady increase in recovery rather than a sharp one. Another factor that could play a role in this behavior is osmotic pressure or fluid loss. For example, the fluid losses measured during microdialysis probes in series approach experiments using 100 µM methyl orange as the analyte were as follows: 1) One probe or control +8.40% (gained fluid), 2) two probes in series -1.30%, 3) three probes in series -11.40%, and 4) four probes in series -28.40%. The fluid losses were quantified by measuring the amount of dialysate collected over a set period of time and relating this to the pumping flow rate. For instance, collections conducted at a pumping flow rate of 5.0 µL/min for 2 min would yield a dialysate volume of 10.0 µL, if not fluid loss or gain was present.

Thus, if fluid loss was present and the dialysate measured volume was 7.0 μL, it would yield a fluid loss of -30% for FITC-4, see Figure 3.9, the change in recovery from one probe to four probes at 0.8 μL/min was ~32% (34.1% vs. 66.3%) and after two probes in series the difference was ~11%.

Overall the change in relative recovery from one probe to four probes was follows: a) Methyl orange ~33%, b) FITC-4 ~32%, c) FITC-10 ~17%, d) FITC-20 ~4%, and e) FITC-40 ~2%. It is good to point out that even though the change in recovery for methyl orange and FITC-4 were similar, their relative recoveries were different for one probe and four probes. These results show how molecular weight not only affects recovery, but also the diffusion behavior of molecules across a membrane. For larger molecules the increase in relative recovery as the surface area increases is linear as compared to smaller molecules logarithmic, see Figures 3.9, 3.10, and 3.11. This is because as the concentration of molecules increase (for a fixed period of time), for larger molecules, inside the microdialysis probe membrane, the movement of them decreases. In other words, there are more molecules colliding into each other to move from outside the membrane of the probe to the inside, reducing the relative recovery. This is known as concentration polarization.
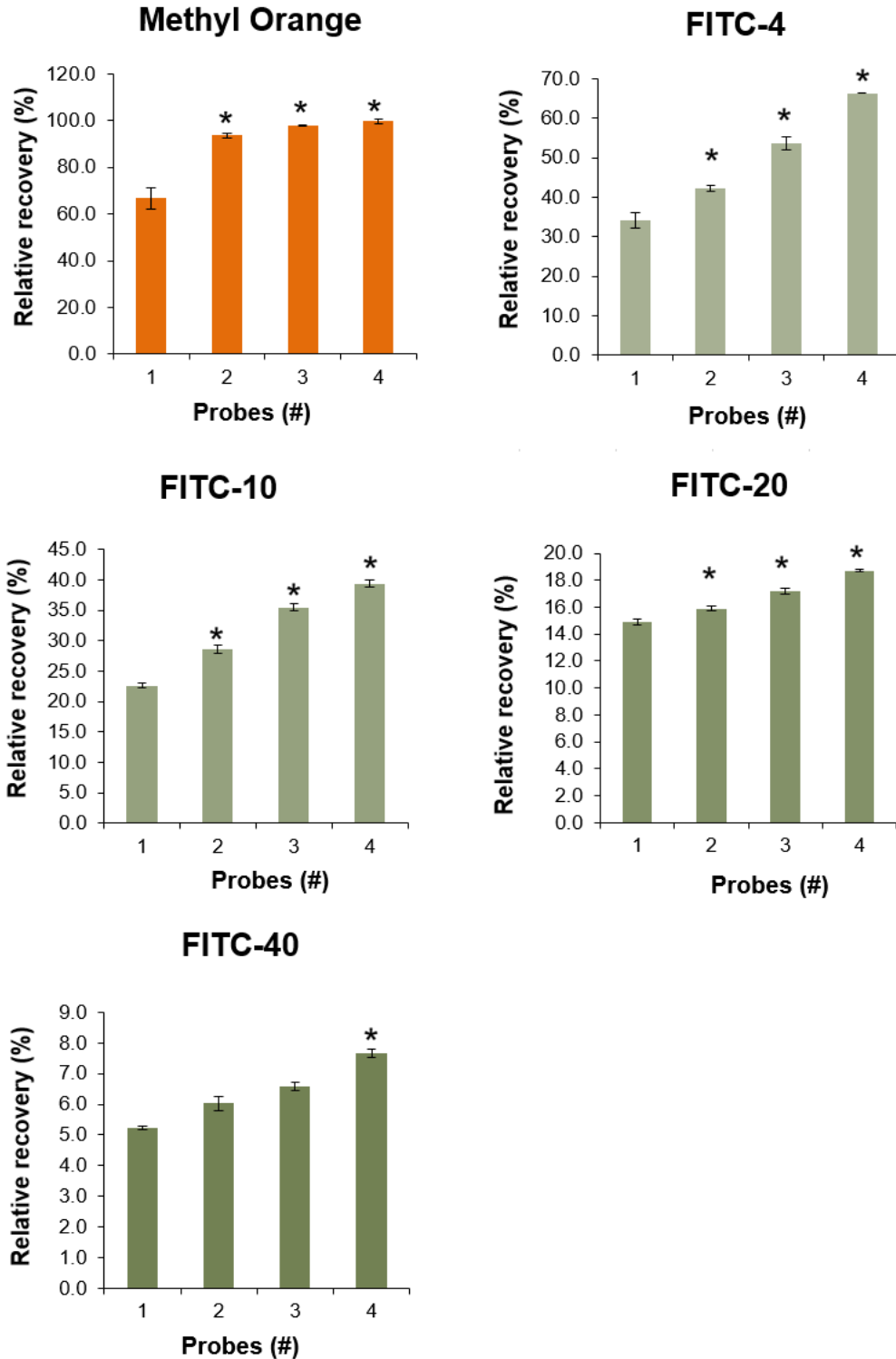
Figure 3.9. Relative recoveries (RR) of 100 μM methyl orange, FITC-4, FITC-10, FITC-20, and FITC-40 at 0.8 μL/min flow rate using probes in series. One probe on the above graph represents the control or regular microdialysis and two, three, and four probes represent probes in series respectively. (*) Denotes a one-way ANOVA ($p < 0.05$) showed a statistically significant difference among control and probes RR. n = 3 and average ± standard deviation.
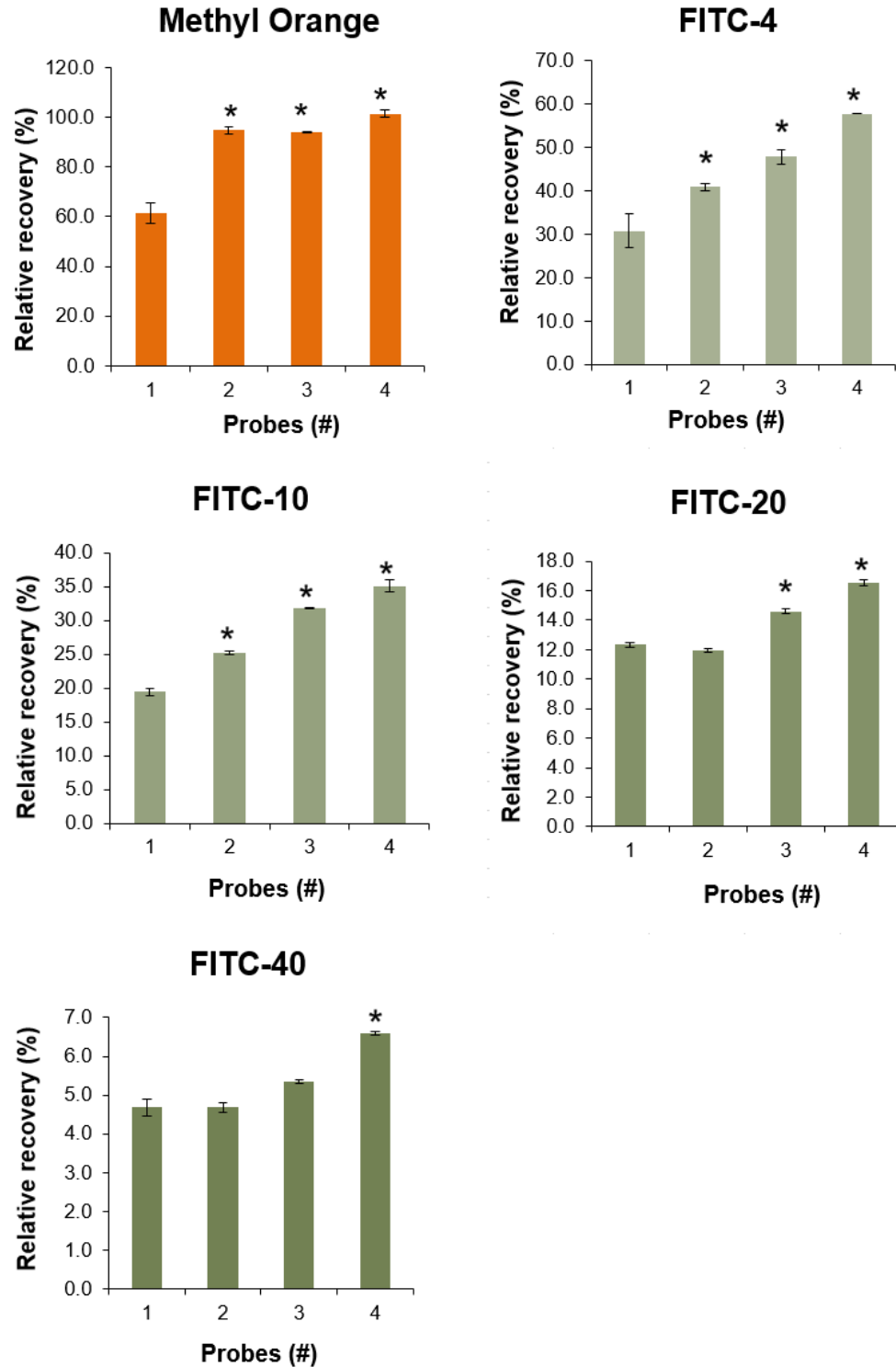
Figure 3.10. Relative recoveries (RR) of 100 µM methyl orange, FITC-4, FITC-10, FITC-20, and FITC-40 at 1.0 µL/min flow rate using probes in series. One probe on the above graph represents the control or regular microdialysis and two, three, and four probes represent probes in series respectively. (*) Denotes a one-way ANOVA ($p<0.05$) showed a statistically significant difference among control and probes RR. n = 3 and average ± standard deviation
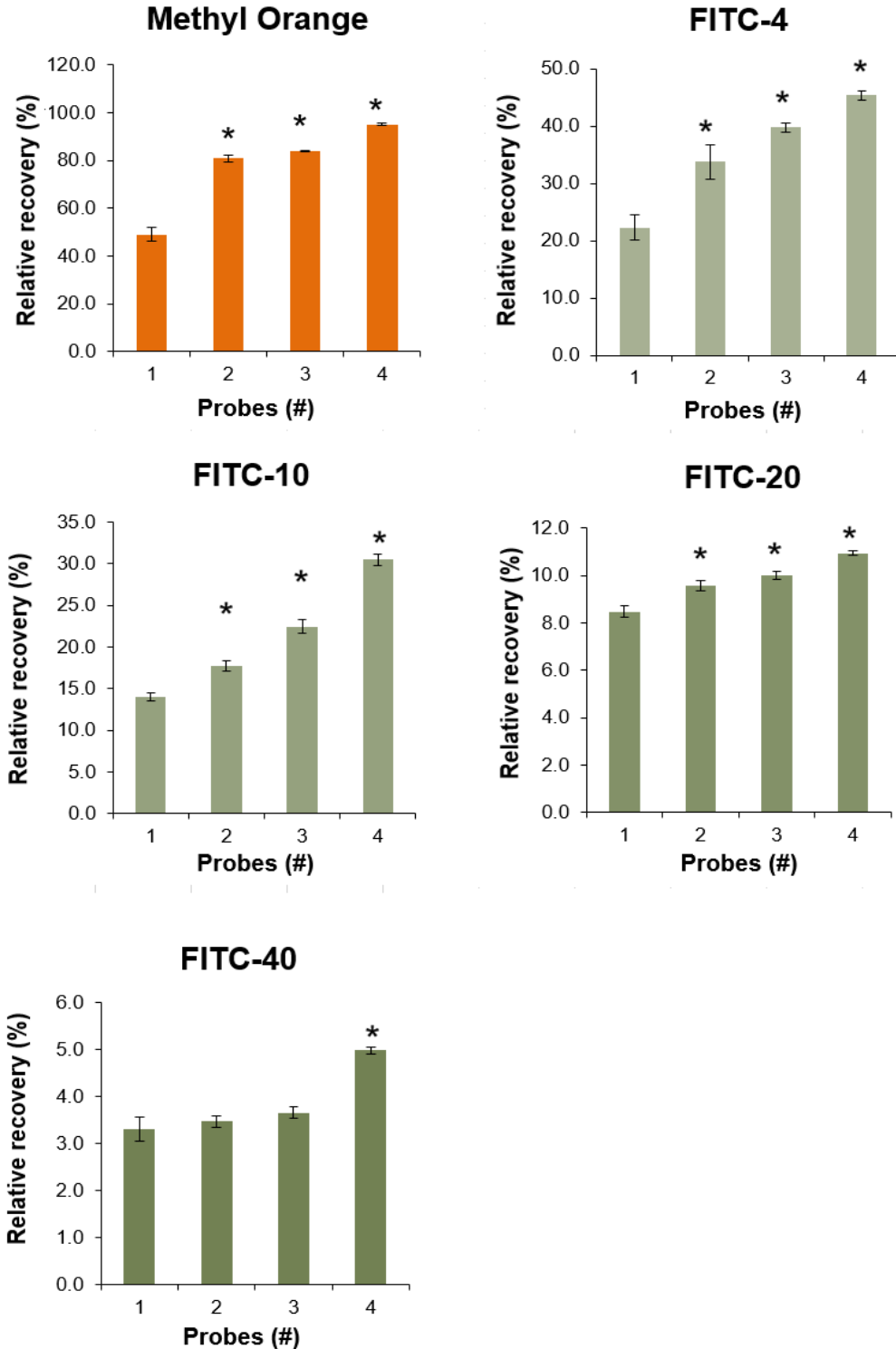
Figure 3.11. Relative recoveries (RR) of 100 µM methyl orange, FITC-4, FITC-10, FITC-20, and FITC-40 at 1.5 µL/min flow rate using several probes in series. One probe on the above graph represents the control or regular microdialysis and two, three, and four probes represent probes in series respectively. (*) Denotes a one-way ANOVA ($p<0.05$) showed a statistically significant difference among control and probes RR. n = 3 and average ± standard deviation

Another factor that could be playing a role on how the relative recovery of larger molecules increases as a function of adding microdialysis sampling probes in series (increasing surface area) is the mass transfer coefficient (k). Mass transfer coefficient is a rate constant for molecules moving from the boundary to the bulk per area.[8]This is commonly used in engineering to analyze diffusion processes. When k is large, a faster mass transfer is taking place. On the other hand, when k is small the mass transfer is slower.[8] There is an inverse exponential relationship between molecular weight and k for the CMA/20 microdialysis probe used, see Figure 3.12. These values were determined experimentally in order to estimate how many probes were needed to achieve nearly 100% recovery using this system. The latter will be addressed in detail in chapter 4. To sum up, increasing the number of probes in series (up to 4 for methyl orange) or surface area significantly improves relative recovery and it is limited by the pore size or MWCO of the microdialysis probe.

To determine if a greatly reduced convective force would increase the relative recovery for increased probes, we set up a recycled microdialysis sampling system with a peristaltic pump. As previously mentioned in section 3.3.1, for small molecules (330 Da) such as methyl orange the relative recovery during microdialysis probes in series experiments were higher than recycling flow method, see Figure 3.7. However, the opposite was true for large molecules (FITC-40, 40 kDa), see Figure 3.13. This could be due to the mass transfer differences between methyl orange (kA~0.9 µL/min) and FITC-40 (k~0.05 µL/min). The relative recovery of FITC-40 using the recycling flow method for four cycles was almost two times higher than the relative recovery of FITC-40 during four probes in series experiments. During recycling flow experiments the fluid loss is minimal, since the same fluid is recirculated in one microdialysis probes. Methyl orange is approximately eighteen times faster than FITC-40. This allows methyl orange to overcome the opposition to move from outside the microdialysis probes membrane to the inner part caused by fluid loss.

$$y = 1.4351e^{-0.665x}$$
$$R^2 = 0.9632$$
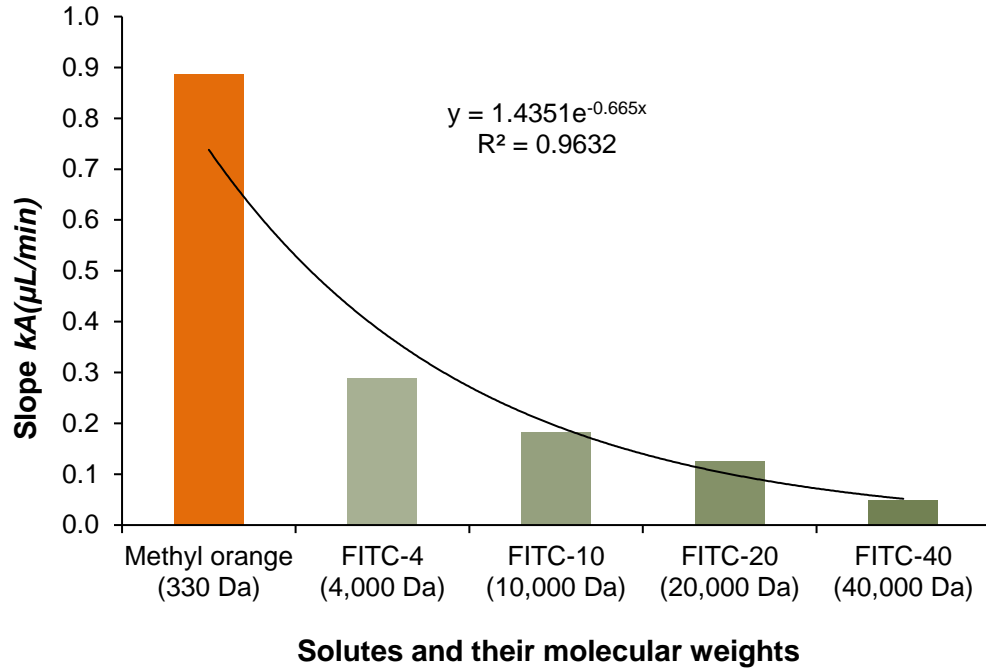
Figure 3.12. Relationship between molecular weight (MW) and mass transfer coefficient (kA) for a CMA/20 microdialysis probe. Each bar represents one solute and one set of experiments.
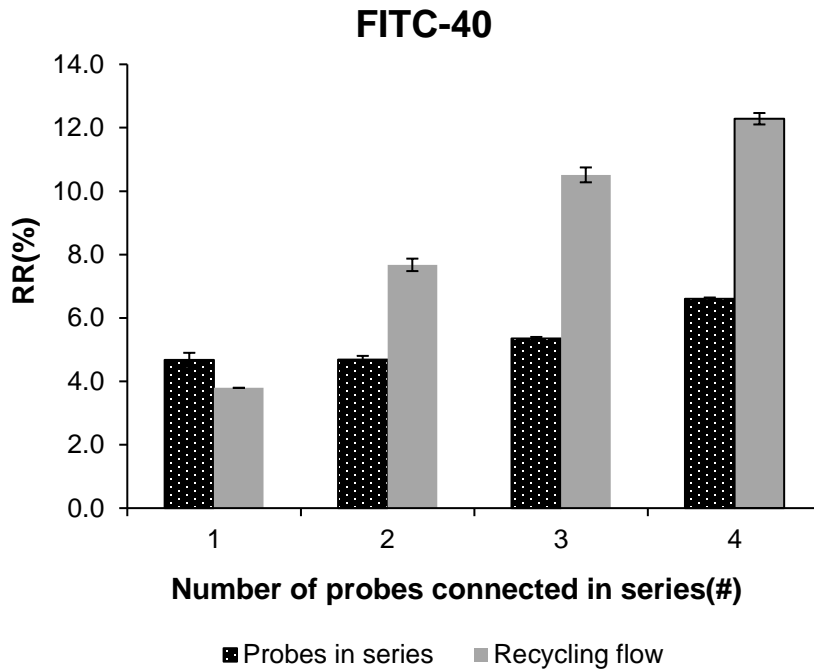
Figure 3.13. Comparison of the relative recovery (RR) of 100 μM FITC-40 using the recycling flow and the probes in series method at 1.0 μl/min. The perfusion fluid was 4% dextran-70 in 10 mM PBS pH = 7.4. n = 3 and average ± standard deviation.

3.4 Conclusion

An *in vitro method* consisting of four microdialysis probes in series to determine the needed number of probes for the collected dialysate to reach near equilibrium with the solute concentration was devised. This method significantly improved the recovery of methyl orange, FITC-4, FITC-10, FITC-20, and FITC-40 without the need of using slow flow rates (< 0.5 μL/min). This work may serve as a basis for the development of a programmable microfluidic system for the collection of biomolecules.

Additionally, one could envision using this approach to get an estimate of *in vivo* concentrations and use it periodically within experimental runs to verify *in vivo* concentrations. To continuously run with multiple probes will certainly reduce temporal resolution, but again it could be used at the start and completion of an *in vivo* experiment to gain important information about biological concentrations, without using the cumbersome *in vivo* calibration methods for microdialysis sampling described in the literature.

3.5 References

1. http://chemistry.elmhurst.edu/vchembook/250fluidbal.html.

2. http://www.slideshare.net/mvraveendrambbs/body-fluid-and-electrolyte-balance.

3. http://cshprotocols.cshlp.org/content/2006/1/pdb.rec8247.

4. Zhou, Q. Y.; Gallo, J. M., In vivo microdialysis for PK and PD studies of anticancer drugs. *Aaps Journal* **2005,** *7* (3), E659-E667.

5. Tsai, T.-H., *Applications of microdialysis in pharmaceutical science.* John Wiley & Sons: 2011.

6. Polak, J. M., *Advances in tissue engineering.* Imperial College Press: 2008.

7. Stenken, J. A., Methods and issues in microdialysis calibration. *Anal. Chim. Acta* **1999,** *379* (3), 337-357.

8. Cussler, E. L., *Diffusion: mass transfer in fluid systems.* Cambridge university press: 2009.

4 Chapter 4. Recovery estimations of methyl orange, FITC-4, FITC-10, FITC-20, and FITC-40 using a modified version of Jacobson et al. linear regression method and Bungay's mathematical model for microdialysis sampling

4.1 Introduction

After demonstrating that the microdialysis sampling probes in series approach improves the relative recovery of methyl orange, FITC-4, FITC-10, FITC-20, and FITC-40, a mathematical method to estimate how many probes or microchannels are needed to achieve ~100% recovery was derived.

Jacobson et al. pointed out that the mass transfer coefficient (k) of any molecule can be determined experimentally during microdialysis sampling by measuring its recovery at different flow rates and plotting the results to find the slope (kA) using the following approach:[1] a) Since $kA(n) = \left(\frac{1}{R_d + R_m + R_q}\right)$, Equation 1.4, where A is surface area of the probe and n is the number of probes, b) Equation 1.2 (Bungay's equation[2]), $RR = 1 - \exp\left\{\frac{-1}{Q_d(R_d + R_m + R_q)}\right\}$, combining "a" and "b" to get c) Equation 1.5, $RR = 1 - \exp\left(\frac{-kA(n)}{Q_d}\right)$, and rearranging "c" we obtain d) $kA(n) = [-\ln(1 - EE)]Q_d$, **Equation 1.6**. This equation can be used if (1-RR) ≠ 0. By plotting –ln(1-RR) vs. Q_d^{-1} the values of kA or the slope regardless of the surface area were obtained, see Figure 4.1.
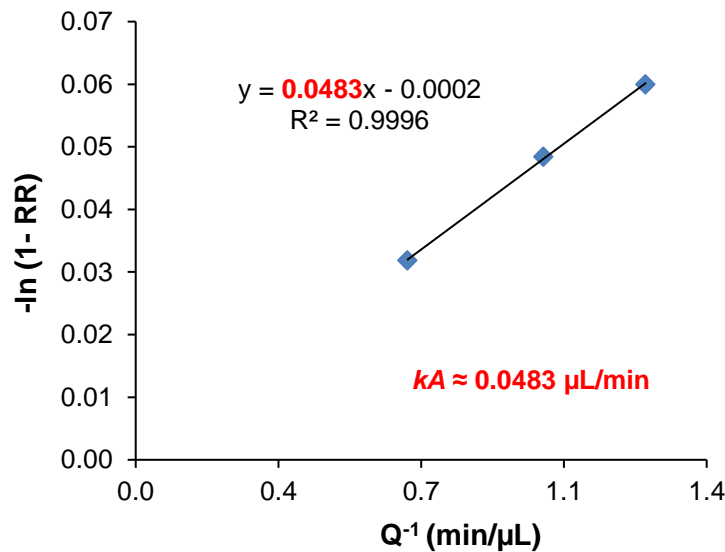
Figure 4.1. Estimation of kA for FITC-40 using Equation 1.6 and Jacobson's approach.[1]

The value of kA was determined for methyl orange, FITC-4, FITC-10, FITC-20, and FITC-40. This was done by calculating their relative recoveries using one microdialysis probe at different flow rates (0.8, 1.0, 1.5 µL/min) and plotting the results, see Figure 4.1. The mass transfer coefficient, kA, of each compound was determined experimentally using a CMA/20 microdialysis probe. Then kA was multiplied by n or the number of probes to estimate the recoveries using Equation 1.6. These estimations were compared to the experiments conducted on Chapter 3.

4.2 Results and discussion

The theoretical estimations agreed with the experiments for methyl orange, Figure 4.2, and FITC-4, Figure 4.3. For example, the deviation from experiments of methyl orange was -1% (underestimation) and +15% (overestimation) for FITC-4 using four probes in series at 0.8 µL/min. However, the theoretical estimations started deviating from experiments at a molecular weight of ~10,000 (FITC-10). The deviation from experiments using four probes in series at 0.8 µL/min for FITC-10 (Figure 4.4), FITC-20 (Figure 4.5), and FITC-40 (Figure 4.6) were +52%, +149%, and +179% respectively.
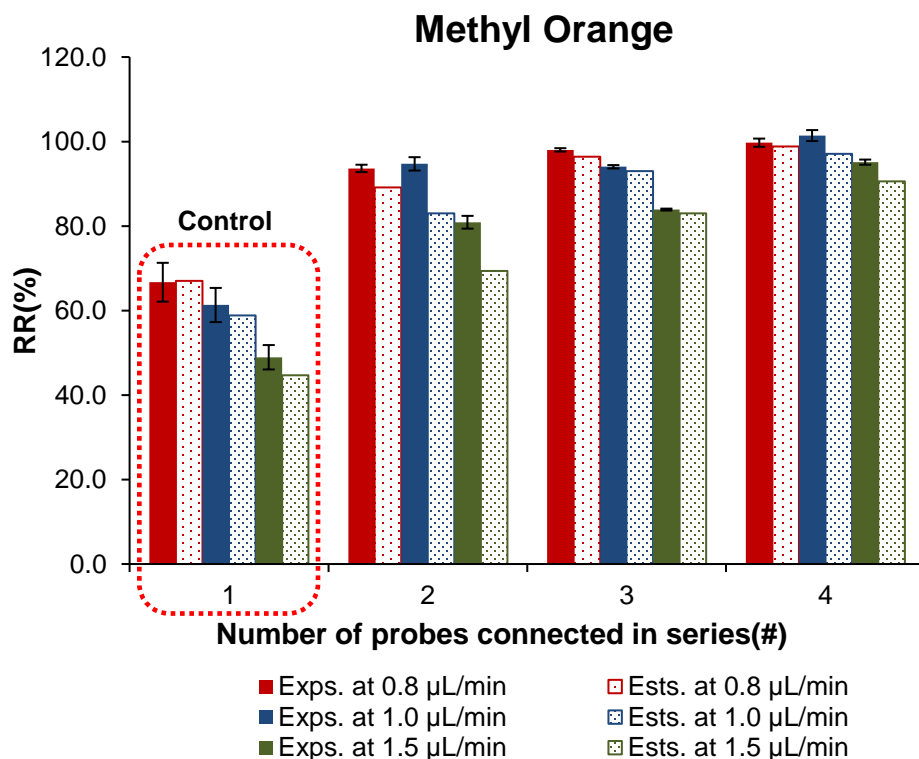
Figure 4.2. Comparison of experimental (Exps.) and estimated (Ests.) relative recoveries of 100 µM methyl orange at different flow rates. The perfusion fluid used was 4% dextran-70 in 10 mM PBS pH 7.4. n = 3 and average ± standard deviation
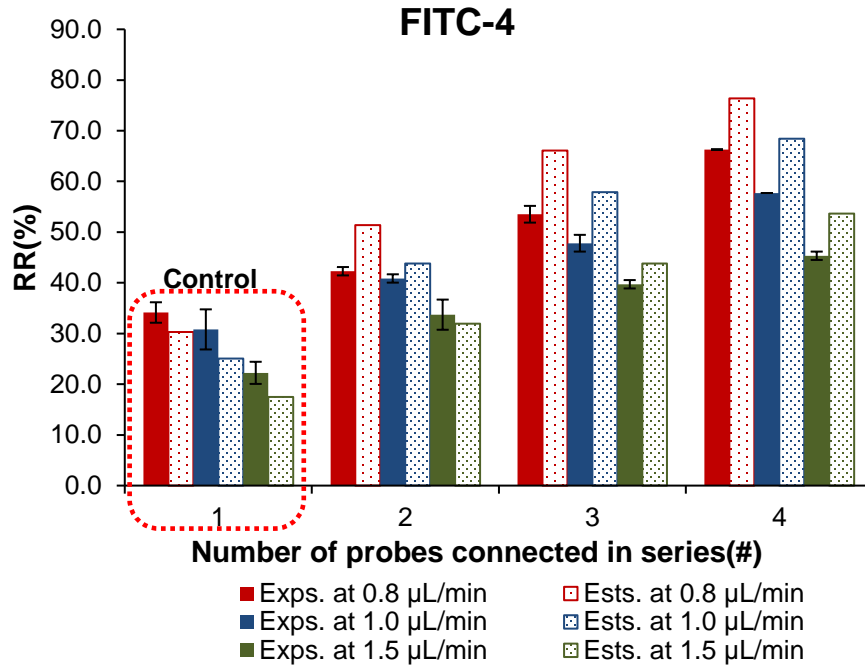
Figure 4.3. Comparison of experimental (Exps.) and estimated (Ests.) relative recoveries of 100 μM FITC-4 at different flow rates. The perfusion fluid used was 4% dextran-70 in 10 mM PBS pH 7.4. n = 3 and average ± standard deviation
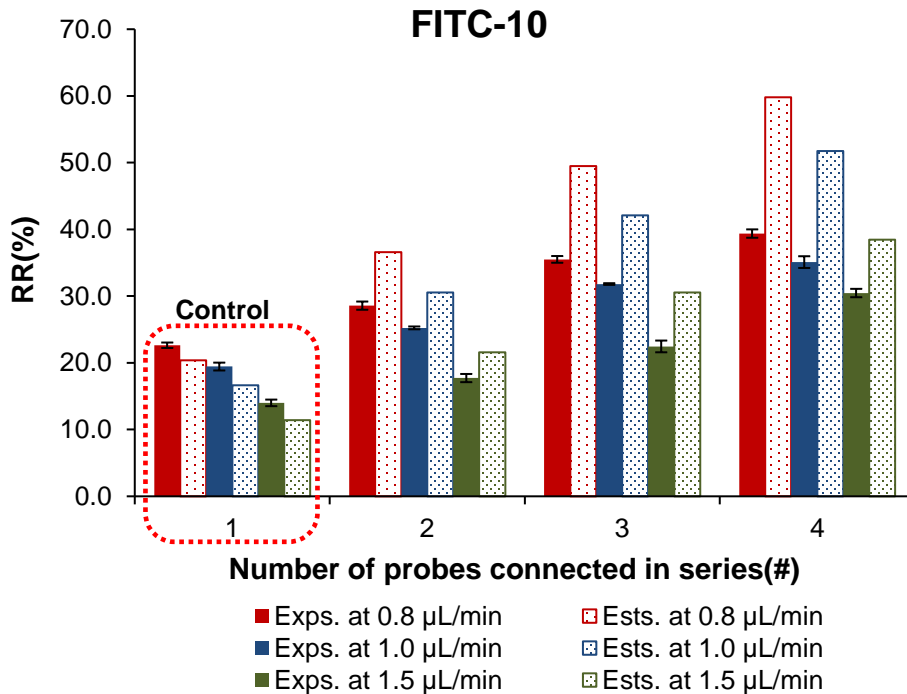
Figure 4.4. Comparison of experimental (Exps.) and estimated (Ests.) relative recoveries of 100 μM FITC-10 at different flow rates. The perfusion fluid used was 4% dextran-70 in 10 mM PBS pH 7.4. n = 3 and average ± standard deviation
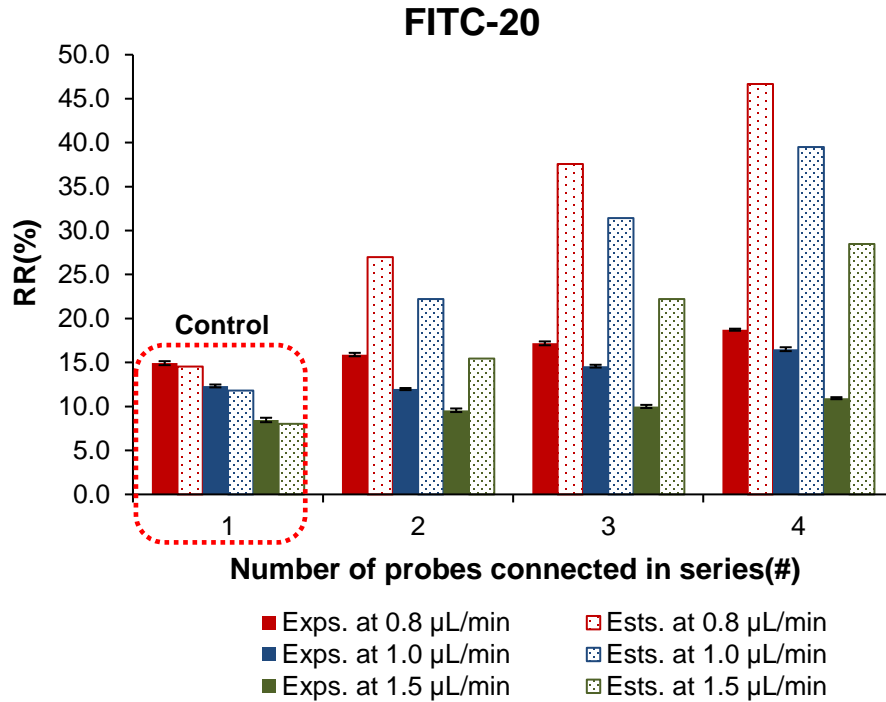
Figure 4.5. Comparison of experimental (Exps.) and estimated (Ests.) relative recoveries of 100 μM FITC-20 at different flow rates. The perfusion fluid used was 4% dextran-70 in 10 mM PBS pH 7.4.n = 3 and average ± standard deviation
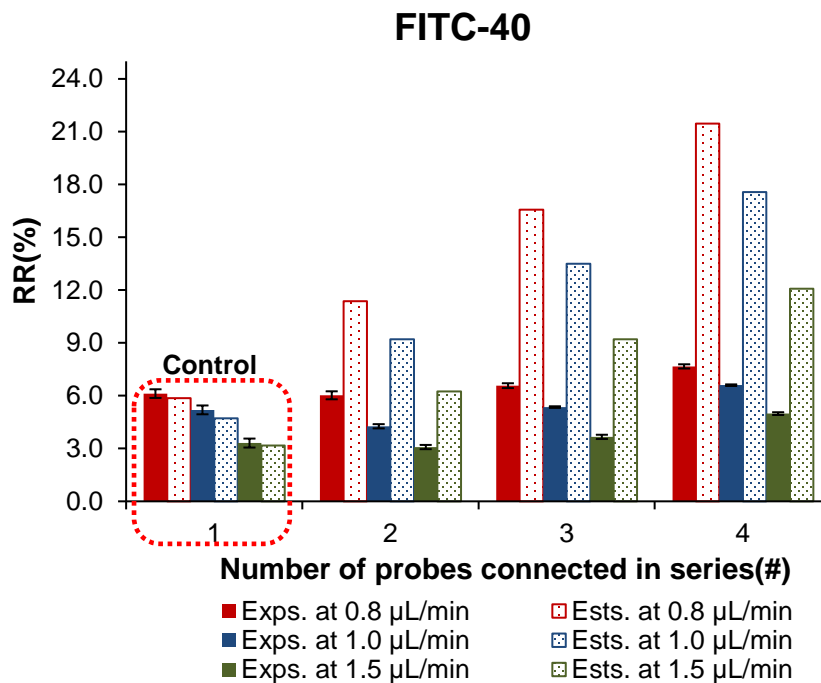
Figure 4.6. Comparison of experimental (Exps.) and estimated (Ests.) relative recoveries of 100 μM FITC-40 at different flow rates. The perfusion fluid used was 4% dextran-70 in 10 mM PBS pH 7.4. n = 3 and average ± standard deviation

As the molecular weight increases the deviation increases. One of the reasons for the deviation could be fluid loss. For instance, collections of methyl orange conducted at 5.0 µL/min using 4% dextran-70 as perfusion fluid yielded fluid losses of +8% (control), -1%, -11%, and -28% for zero (control or one probe), one, two, and three probes connected in series respectively, see Table 4.1. This means that the backpressure increases as the number of probes in series increases. More fluid was loss for the four probes (-28%) in series compared to one probe (+8%), two (-1%) and three probes (-11%).

Table 4.1. Fluid losses of 100 µM methyl orange after the addition of microdialysis probes in series.

Number of probes added in series	Fluid loss (%)
0*	+8.40*
1	-1.30
2	-11.40
3	-28.40

 *Control

The product kA (Figure 4.1) was determined for one probe and multiplied by the number of microdialysis probes (n) connected in series used for the experimental data. It was assumed that the system, in terms of hydraulic pressure, did not change from having one probe to two, three, and four probes in series. In other words, the product kA was the same for each system or probes connected in series ($kA_1 = kA_2 = kA_3 = kA_4$). The product kA_1 was the slope of the curve that was determined using one probe or control. After looking at the data and the system more closely a different approach to estimate the relative recoveries was used. The product kA was determined for each "system" individually (one probe = kA_1, two = kA_2, three = kA_3, and four probes = kA_4). Which means that the product was different for each setting used ($kA_1 \neq kA_2 \neq kA_3 \neq kA_4$). This was done to take into account the fluid loss of each system. For example, the product kA was determined for one probe and compared the estimated relative recovery versus the experimental relative recovery of one probe. After connecting another microdialysis probe in series, the product kA_2 was determined for that system. This was done for up to four probes (kA_4) connected in series. Each probe or probes in series was treated as an individual system. The estimations and experiments agreed considerably after using this approach, see Figure 4.7. It can be seen by comparing Figure 4.6 ($kA_1 = kA_2 = kA_3 = kA_4$) with Figure 4.7 ($kA_1 \neq kA_2 \neq kA_3 \neq kA_4$) a significant improvement on the agreement.

It is good to point out that for the microfluidic system (chapter 5) that was developed based on the microdialysis probes in series approach, the kA value would be determined for the entire system not individually as it was done with the microdialysis in series approach.
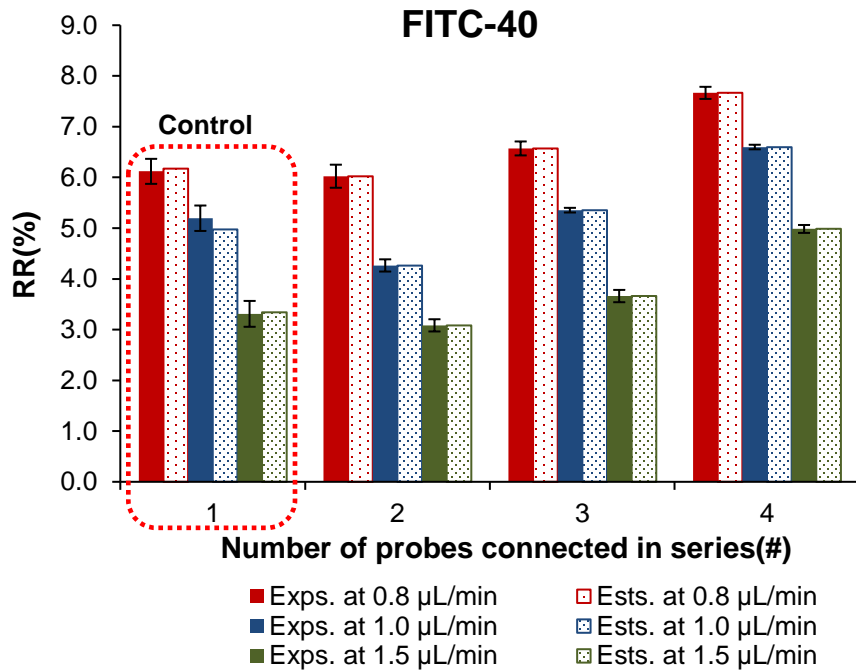
Figure 4.7. Comparison of experimental (Exps.) and estimated (Ests.) relative recoveries of 100 µM FITC-40 at different flow rates. The perfusion fluid used was 4% dextran-70 in 10 mM PBS pH 7.4. The estimations were done using kA for each system individually ($kA_1 \neq kA_2 \neq kA_3 \neq kA_4$). n = 3 and average ± standard deviation

4.2.1   Methyl orange

Using the kA value found in Table 4.2, the relative recovery (RR) for methyl orange was estimated to be 44.6%, 58.8%, and 67.0% at the 1.5, 1.0, and 0.8 µL/min flow rates, respectively, see Figure 4.2. The estimated RR for four probes was 91% or greater for all three perfusion fluid flow rates. The lower flow rates were estimated to achieve nearly 100% RR with four microdialysis probes in series. Compared to our experimental data (48.9%, 61.3% and 66.7%), this estimation is within (5%) of our experimental results indicating that the model described in Equation 1.6 could be used to estimate RR.

Table 4.2. Measured mass transfer (kA) values of 100 µM solutions of methyl orange, FITC-4, FITC-10, FITC-20, and FITC-40 using one CMA/20 microdialysis probe, slope of -ln(1-RR) vs. Q^{-1} at 0.8, 1.0, and 1.5 µL/min flow rates.

Solute used	kA (µL/min)	R^2
Methyl orange	0.8869	0.9995
FITC-4	0.2884	0.9783
FITC-10	0.1822	0.9972
FITC-20	0.1257	0.9996
FITC-40	0.0483	0.9996

Using the kA value, from the table above (Table 4.2), and Equation 1.6, the number of probes needed to reach 99% relative recovery (RR) for methyl orange was calculated using different perfusion fluid flow rates. These values are shown in Table 4.3 and show the expected flow rate dependence with needing only four probes at 0.8 µL/min and 8 probes at 1.5 µL/min to reach 99% relative recovery. Since lower flow rates have greater residence times, it would be expected that fewer probes are necessary to achieve 99% RR.

Table 4.3. Estimation of the number of probes needed (in series) to reach 99% relative recovery.

	Flow rate (µL/min)			
	0.8	1.0	1.5	
Solute used				
Methyl Orange	4	5	8	
FITC-4	12	15	22	Number of
FITC-10	19	24	35	probes
FITC-20	27	34	51	needed
FITC-40	70	87	131	

4.2.2 FITC-4

Using the mass transport coefficient, kA, found in Table 4.2, the estimations for FITC-4 RR through one microdialysis probe were 17.5%, 25.0%, and 30.3% at the 1.5, 1.0, and 0.8 µL/min flow rates. The estimated RR for four probes was of 54% or greater. Compared to the experimental data (22.2%, 30.8% and 34.1%), these estimations are in general agreement with our experimental results indicating that Equation 1.6 can be used to estimate RR for FITC-4. For FITC-4, the number of estimated microdialysis probes in series needed to reach 99% RR using the kA value in Table 4.2 was found to be 12 at 0.8 µL/min and 22 at 1.5 µL/min (Table 4.3).

4.2.3　FITC-10

The experimental data significantly deviated from the calculated relative recovery (RR) estimations for FITC-10. Unlike methyl orange and FITC-4, the estimates of RR started significantly deviating from experiments for 3 (49.5% vs. 35.5% at 0.8 µL/min) and 4 (59.8% vs. 39.4% at 0.8 µL/min) probes connected in series. The reason for this deviation could be that for larger molecules fluid loss has a greater influence on RR than for smaller molecules. In other words, the combination of outward convection combined with diffusion toward the dialysis membrane lumen may significantly affect the recovery of larger molecular weight solutes. The model used in Equation 1.6 assumes that fluid loss does not change with the number of probe added in series.

4.2.4　FITC-20

For FITC-20, the estimated relative recovery deviated from experimental observations for 2 (27.0% vs. 15.9% at 0.8 µL/min), 3 (37.6% vs. 17.2% at 0.8 µL/min), and 4 (46.6% vs. 18.7% at 0.8 µL/min) probes in series. Again, it is likely the convective force is greater than the diffusive force for collection of this larger molecular weight solute.

4.2.5　FITC-40

As with FITC-20, the RR% estimations for FITC-40 deviated from experimental observations for 2 (11.4% vs. 6.0% at 0.8 µL/min), 3 (16.6% vs. 6.6% at 0.8 µL/min), and 4 (21.5% vs. 7.7% at 0.8 µL/min) probes in series. The likely cause is the convection out of the dialysis probes at the higher probe numbers.

4.3　Conclusions

A model to predict the number of microdialysis probes connected in series necessary to achieve ~ 99% relative recovery was developed. This model was used to estimate the number of probes connected in series at different flow rates to achieve near equilibrium between the outer part of the microdialysis probe membrane and the inner part. This work served as a basis for the development of a microfluidic system for the collection of biomolecules. This is going to be cover in more detail in chapter 5. Additionally, one could envision using this approach to get an estimate of *in vivo* concentrations and use it periodically within experimental runs to verify *in vivo* concentrations.

To continuously run with multiple probes will certainly reduce temporal resolution, but again it could be used at the start and completion of an *in vivo* experiment to gain important information about biological concentrations, without using the cumbersome *in vivo* calibration methods for microdialysis sampling described in the literature.

4.4 References

1. Jacobson, I.; Sandberg, M.; Hamberger, A., Mass transfer in brain dialysis devices—a new method for the estimation of extracellular amino acids concentration. *Journal of Neuroscience Methods* **1985,** *15* (3), 263-268.

2. Bungay, P. M.; Morrison, P. F.; Dedrick, R. L., Steady-state theory for quantitative microdialysis of solutes and water in vivo and in vitro. *Life Sciences* **1990,** *46* (2), 105-19.

5   Chapter 5.   Miniaturization of microdialysis probes in series method: Design, microfabrication, and testing of microfluidic device

5.1   Introduction

After demostrating in chapter 3 that the microdialysis probes in series method improves the relative recovery of different chemical compounds (methyl orange, FITC-4, FITC-10, FITC-20, and FITC-40), the next step was to miniaturize the concept of extending the fluid path length into a microfluidic device. The general idea was to make a prototype on polydimethylsiloxane (PDMS) similar in shape as a commercially avaible microdialysis probe, see Figure 5.1. As previously stated in this dissertation there is a growing interest in miniaturizing microdialysis sampling technique into microfluidic systems.[1, 2, 3] However, this in most cases can be challenging. One of the main problems is the difficulty of incorparating pumping, valving, and detection systems into microfluidic devices due to their large volume to flow rate ratio between their components.[1] Section 1.2.1.1 covered this topic in more detail. Several steps were taken to miniaturize the microdialysis probes in series method into a microfluidic device. First, AutoCAD® computer-aided design and drafting software was used to design the microfluidic device and the photoplot. The dimensions of the design were chosen based on different factors: a) Cost of the photoplot (the smaller, ~10 µm, the features the more expensive the photoplot), b) previous experience working with microchannels of similar size, c) length of microdialysis probe membrane (4 mm), and d) basic fluid dynamic principles.
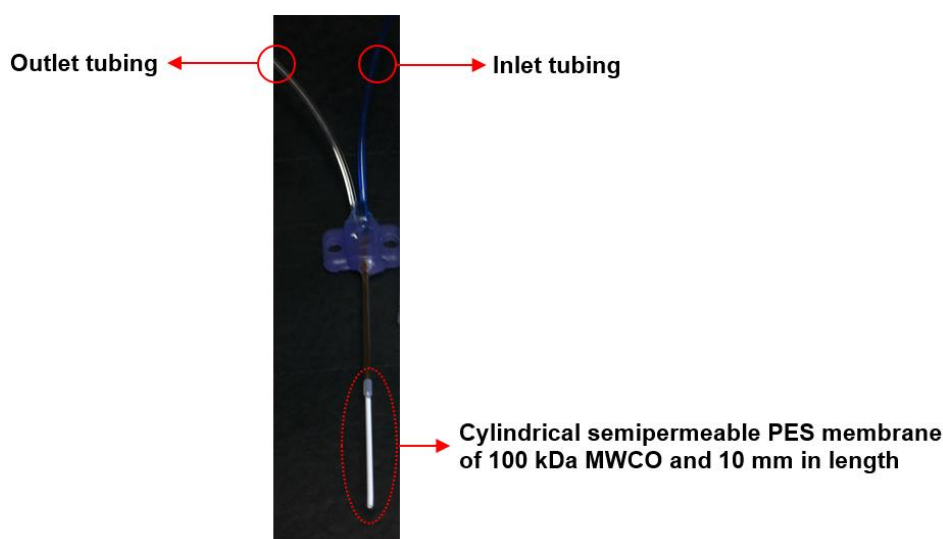
Figure 5.1. Commercially aviable CMA 20 microdialysis probe.

The microfluidic device developed for this dissertation had the following dimensions: 1) Overall length of 44.0 mm (1.7"), 2) overall height of ~100 µm, 3) nine microchannels with different widths to reduce backpressure, one of 40 µm (inlet), six of 50 µm (collection area), and two of 100 µm (outlet) respectively, and 4) the length and width of the collection area were 4.4 mm and 2.0 mm. Finally, standard microfabrication techniques were used.

5.2   Experimental section

5.2.1   Photoplot

Figure 5.2 shows a 2D drawing of the microfluidic device. A negative photoplot was ordered in-house from the University of Arkansas High Density Electronics Center (HiDEC). According to Varteresian, "A *photoplot* is nothing more than a high quality transparency, or view graph."[4] This means that some areas of the photoplot would allow ultraviolet (UV) light to pass through it and other would not. The areas expose or that allow UV to pass through it would be polymerized during the photolithography process. It is good to point out that if a negative photoplot is used, a similar photoresist must be used as well.
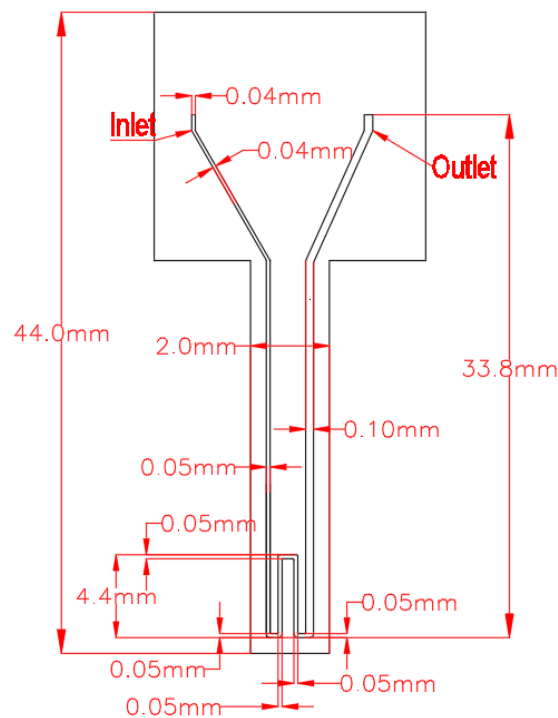
Figure 5.2. 2D drawing of the microfluidic device. This drawing is not to scale to facilitate the visualization of the microchannels.

The drawing used to order the photoplot was designed for a 4" in diameter silicon wafer. Five replicas could be made at the same time using this photoplot. After receiving the negative photoplot a SU-8 master mold was fabricated.

5.2.2   Microfabrication of PDMS replicas

A master mold was fabricated using a similar procedure (Figure 5.3) previously used by the author of this dissertation.[5] Standard photosensitive polymers, SU-8 50 and SU-8 3050, from MicroChem Corp., Westborough, MA were used to make the master mold. Both SU-8 50 and SU-8 3050 were used due to their in-house availability and the height of the channels (~100 μm). These two polymers can be used interchangeably. The SU-8 50 was purchased from MicroChem and the SU-8 3050 was available at HiDEC. The main difference between SU-8 50 and SU-8 3050 is the thickness that can be achieved during spin coating. SU-8 50 thickness ranges from ~40 μm to ~120 μm, whereas SU-8 3050 thickness ranges from ~45 μm to ~102 μm according to their data sheets.[6] Both photoresist resins can achieve the thickness range chosen for this work. To accomplish the desire thickness or overall height of the microchannels the MicroChem data sheet for SU-8 3000 permanent epoxy negative photoresist was followed.[6] A long pass optical filter (PL-360-LP) from Omega Optical, Inc, Battleboro, VT was used to eliminate UV radiation below 350 nm as recommend by the SU-8 3000 data sheet.[6] This optical filter was placed on top of the negative photoplot during the exposure step of the master mold. It was found that when the optical filter was not used during the master mold fabrication some SU-8 residues were observed after the development step (under development). This was due to the incomplete photopolymerization of the SU-8 during the exposure step. The permanent epoxy negative photoresist, SU-8, undergoes a phase change during photopolymerization. Due to the fact that a partially polymerized SU-8 is not soluble in the MicroChem's SU-8 developer solvent and a non-polymerized SU-8 is can be used as an indicator of incomplete photopolymerization. The SU-8 required more energy to complete the chemical reaction and change from liquid to solid after photopolymerization. It is good to note that the exposure time was increased by 40% as recommended by MicroChem data sheet for SU-8 3000.[6] The latter in terms increased the amount of energy applied to the SU-8 during photopolymerization (UV exposure). Figure 5.4 shows the SU-8 master mold after microfabrication. The master mold was inspected under a regular light microscope for quality purposes.

After the inspection, PDMS replicas were made using the master mold and following the procedure shown on Figure 5.3. To close the open channels on the replicas, PDMS lids were made using a silicon wafer. These lids were basically flat pieces of PDMS with and without indentations, see Figure 5.5.

Spincoat silicon wafer with ~5 mL **SU-8 photoresist** at 1200rpm for 40s

Polymerized SU-8

- Prebake 5 min on a hotplate
- Place a negative film glossy side up

- Expose the wafer to the UV lamp
- Postbake 5 min on hotplate
- Develop the wafer in propylene glycol

- To mix base: curing agent (10:1 w/w).
- Place in oven at 75 C° for 1 hr.
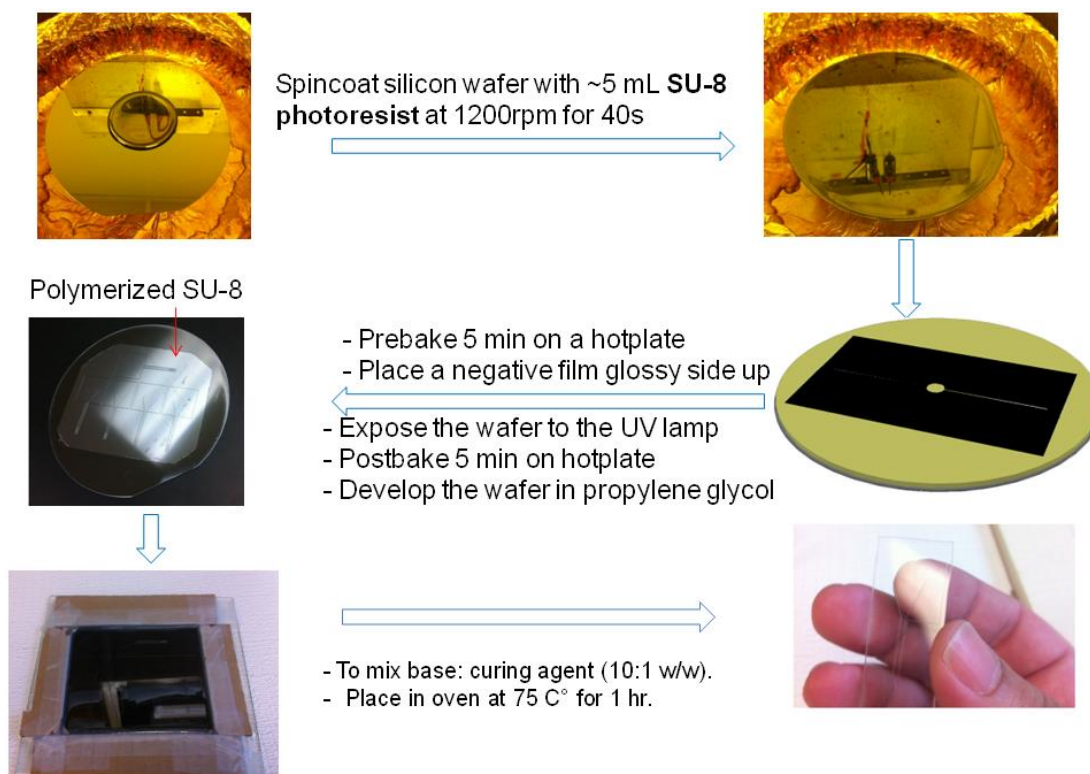
Figure 5.3. Standard microfabrication process used to make the PDMS replicas.[5] MicroChem's SU-8 developer was used instead of propylene glycol.[6]

Glass slides were used as lids for some of the preliminary devices. The advantage of using glass slides during microfabrication is that they reversibly stick to PDMS. Van der Waals forces at the surface of glass and PDMS form a weak reversible bond between them. It is only necessary, in most cases, to bring both surfaces together to achieve the reversible bond. This allowed the PDMS replicas to be tested using flow rates of up to 5.0 μL/min without any surface modification, see Figure 5.6. The PDMS was made using the standard Sylgard® 184 Silicone Elastomer Kit from Dow Corning Corporation, Midland, MI. The kit contains a base and curing agent that are typically mixed to a 10:1 ratio by weight. The ratio used for all the PDMS microchannels and lids fabricated was 10:1. The inlet and outlet of all the PDMS replicas were made using a round punch of 0.71 mm cutting edge diameter purchased from Technical Innovations, Inc., Angleton, TX.[5] In some instances a round punch of 3.02 mm (Figure 5.7) cutting edge diameter was used.

This was done when the inlet or outlet broke during the punching process (Figure 5.24, "C" or device on the right side).

Figure 5.4. SU-8 master mold in a wafer transport box after microfabrication. Up to five PDMS replicas at a time can be made using this mold.
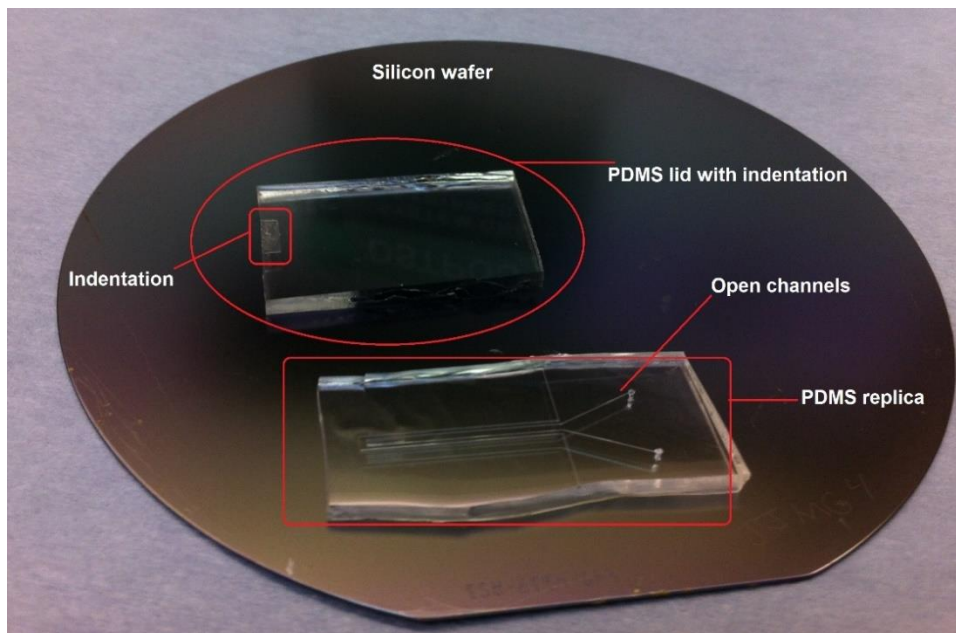
Figure 5.5. Uncut PDMS replica and lid with indentation on silicon wafer before plasma treatment.
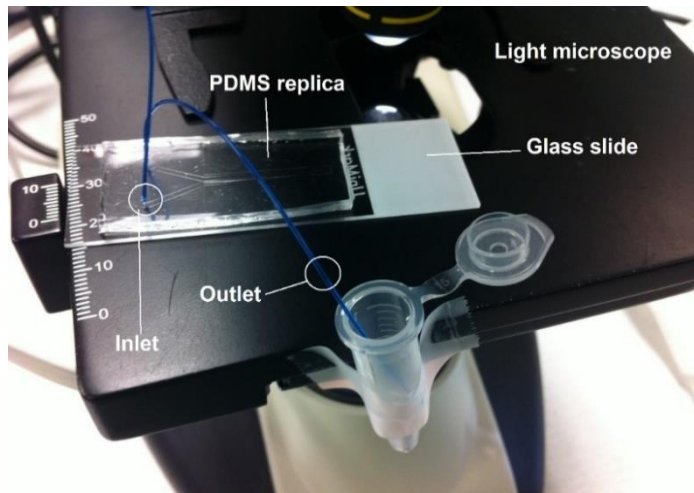
Figure 5.6. Testing of an uncut PDMS replica under a light microscope using a glass slide as a lid. The glass slide and PDMS replica were weakly bonded by Van der Waals forces.
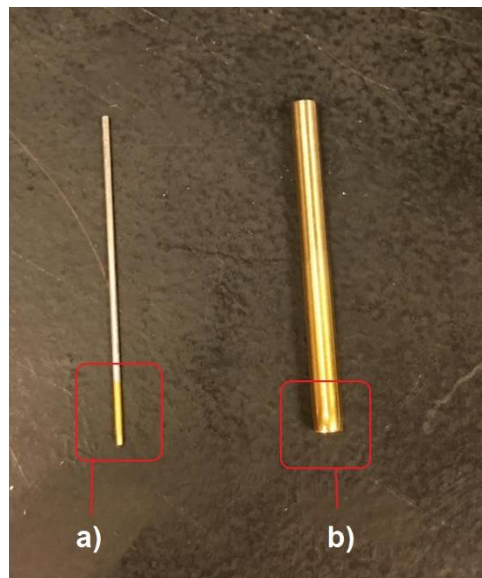
Figure 5.7. Round punches used to make the inlet and outlet of the PDMS microfluidic devices. The highlighted areas show their cutting edges. The round punch of 0.71 mm cutting edge diameter is shown on a) and the punch of 3.02 mm is shown on b).

Each PDMS replica (open channels) was tested under a light microscope using a glass slide as a lid and either 10 mM PBS pH 7.4 or HPLC water at a flow rate of 5.0 µL/min unless otherwise stated, see Figure 5.6. This was done before proceeding to bind the PES filters and PDMS/glass lids to the PDMS replicas. Testing the PDMS replicas saved time and money and made sure that none of the microchannels within the device were clogged.

5.2.3   Microfabrication of microfluidic devices

To reach the final working microfluidic device, five assembly iterations were performed. Figure 5.8 shows all the assembly approaches that were used. Each of the assembly's procedures and how they lead to the next procedure will be addressed in detail later in this section. The membrane chemical composition, polyethersulfone (PES), was chosen based on the CMA/20 microdialysis probes used in this dissertation (Chapters 2 and 3) since they have a PES membrane. As proof of principle Whatman™ Puradisc PES syringe filters of 25 mm in diameter and pore size of either 0.2 µm or 0.45 µm were used from Sigma-Aldrich, St. Louis, MO. The problem with using these syringe filters was that in order to retrieve the membrane from the plastic case it has to be broken. Figure 5.9 shows the PES syringe filter before and after retrieving the PES filter. Some of the grooves on the plastic case of the PES syringe filters were present on the PES filter after retrieving them, see Figures 5.18 and 5.19. However, the PES filters were very useful to test the effectiveness of the bonding method described by Aran et al. shown on Figure 5.10.[7] Following this method, the PES filters (membranes) were treated for 1 min at a pressure of 600 mTorr and 100 W of power in an Automated Plasma Cleaning System (APE 110), see Figure 5.11. After both sides of the membranes were treated, they were placed in a 5/95 (v:v) APTES:H_2O solution of 3-amino propyltriethoxysilane (APTES) at 80°C for 20 min. This solution was made using 99% (in water) v/v APTES stock solution purchased from Sigma-Aldrich, St. Louis, MO. The PDMS replicas and their lids (Figure 5.12) were treated in the APE 110 using the same parameters, but for a shorter period of time (20 s). It was found that when silicon wafers were used (Figure 5.11 vs. Figure 5.12) after the plasma treatment, the PDMS replicas and lids weakly attached to the wafers. This caused some problems, since they had to be physically removed from the wafers leading to breakage in some instances. Regular office Scotch™ tape was used to fix this problem. The silicon wafer was covered with the tape to prevent PDMS from binding to the wafer. After the 20 min in the 5% (in water) v/v APTES solution the membranes were let dry and were brought together to the PDMS replicas and lids. They were incubated for at least 24 hours having either a weight of ~6 pounds (Fisher Scientific Catalog 2008/09) on top or pressed using a c-clamp of 3" (Figure 5.13) to ensure a stronger bond.[7] When the c-clamp was used care was taken to make sure the microfluidic device was not bent or broken (glass lid). This was accomplished by placing pieces of PDMS on both sides of the device and a plastic lid under the device. The pressure was focused on the union area, see Figure 5.13.
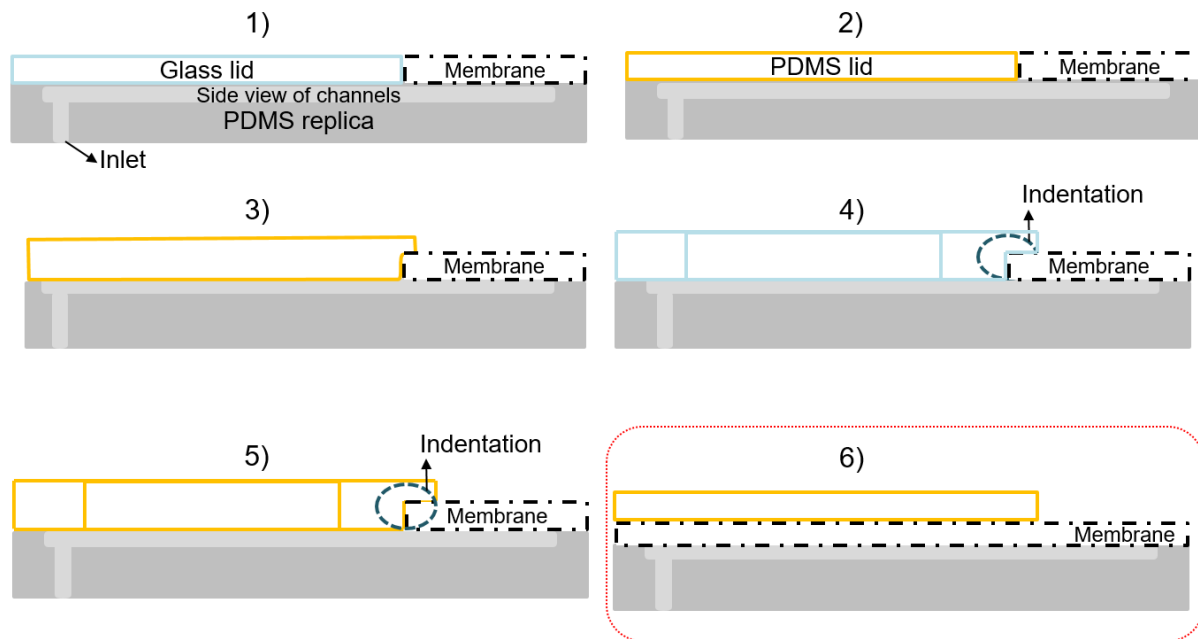
Figure 5.8. The five different assemblies (1-5) that were done before reaching to the final device (6): 1) Glass slide was used as lid and chemically bound on top of the PDMS replica next to the PES (filter) membrane (side by side), 2) same as 1), but PDMS was used as a lid, 3) PDMS lid was chemically bound to the PDMS replica and the membrane, but one of the etches of the lid was physically pushed on top of the etch of the membrane, 4) an indentation was made in the glass lid by drilling it and chemically bound on top of the PDMS replica and membrane, 5) same as 4), but the indentation was made on PDMS during curing, and 6) PES membrane was chemically bound the PDMS replica completely covering the replica and a PDMS was bound on top of the membrane leaving the collection area open.

PES Syringe filter before braking the plastic case

Outer part of PES syringe filter after retrieving the filter

Inner part of the PES syringe filter after retrieving the filter

Grooves

Grooves
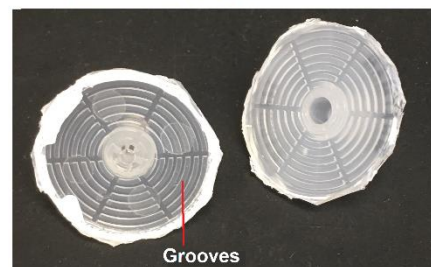
Figure 5.9. PES syringe filter before and after retrieving the PES filter.

a: (Left) Membrane coated with APTES.
(Right) PDMS surface after O₂ plasma treatment.

b: (Left) The functionalized membrane and activated PDMS microdevice are brought into contact.
(Right) A picture of the bonded laminate.

c: (Left) The second plasma treated PDMS layer.
(Right) The bonded laminate activated in O₂ plasma.

d: (Left) Schematic of the two compartment microdevice.
(Right) A picture of a sandwich structure.
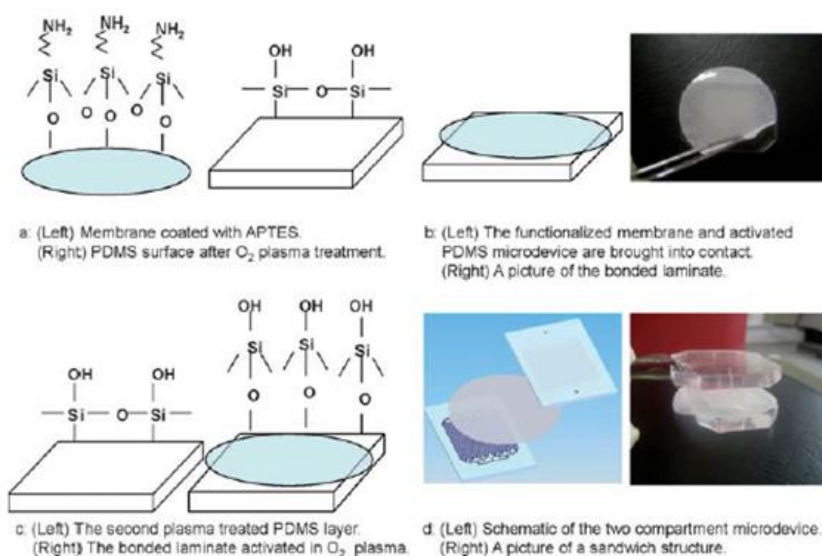
Fig. 1 Schematic of the bonding process between a porous membrane and a PDMS substrate. (a) (Left) The surface chemistry of a porous membrane functionalized by APTES and (right) the surface chemistry of PDMS after exposure to O₂ plasma. (b) (Left) The membrane is bonded to the first PDMS structure and (right) a picture of bonding a PCTE membrane to a PDMS layer during an experiment. (c) (Left) The second PDMS structure after exposure to O₂ plasma and (right) the surface chemistry of the bonded laminate. (d) (Left) Schematic of the two compartment microdevice including the two PDMS microchannels with a thin porous membrane sandwiched in between and (right) a picture of a sandwich structure of a two compartment device with a PCTE membrane and two PDMS layers.

Figure 5.10. Aran et al. bonding method used to bind the PES filter to the PDMS prototype.[7] Reproduced from reference 7 with Permission of The Royal Society of Chemistry (see appendices).

Figure 5.11. Oxygen plasma instrument used to chemically modify the surface of PDMS replicas and PES filters (left side). APE-110 - Automated Plasma Cleaning System (600 mTorr, 100 W).
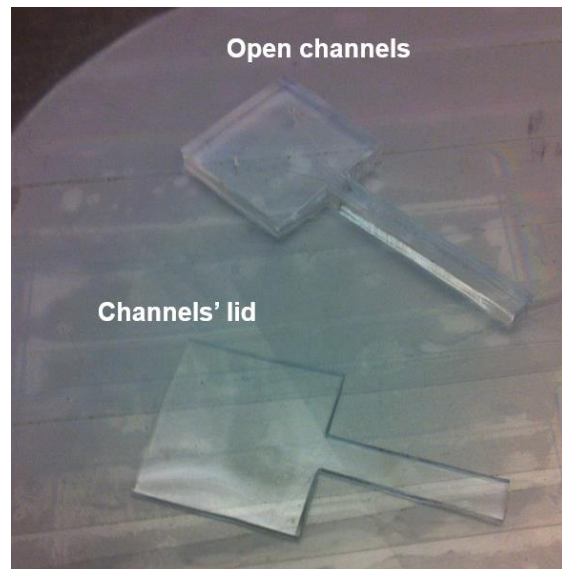
Figure 5.12. Cut PDMS replica and lid without indentation before plasma treatment on a tape covered silicon wafer.

The advantage of Aran et al's method was its simplicity and strength of the bond formed between the PDMS and the PES membrane. One of the drawbacks of this method is the 24 hours waiting time which is longer (48 hours) when glass is used. The devices were tested using either HPLC grade water or 10 mM PBS pH 7.4 at 5.0 µL/min unless otherwise stated. To evaluate the quality of the bonding between PDMS and PES membrane the devices were observed under a light microscope with and without a camera to see if any leaks were present during perfusion, see Figure 5.14. Before the first assembly was made a simple PDMS microfluidic device was fabricated to test the Aran et al's binding method. The device consisted of one straight channel of 100 µm in width and 100 µm in height, see Figure 5.15. The PES filter was used as a lid and bound on top of the channel. Two pieces of PDMS were chemically bound at both ends of the channel (inlet and outlet).

A simple pull test was conducted to evaluate the strength of the bond between the PES filter and the PDMS channel. The simple pull test consisted of pulling off the PES filter after the 24 hours incubation, see Figure 5.16. After successfully evaluating the binding method, the first assembly approach was made. For the assembly approaches from 1 to 5 the PES filter was placed on the collection area, see Figure 5.17.
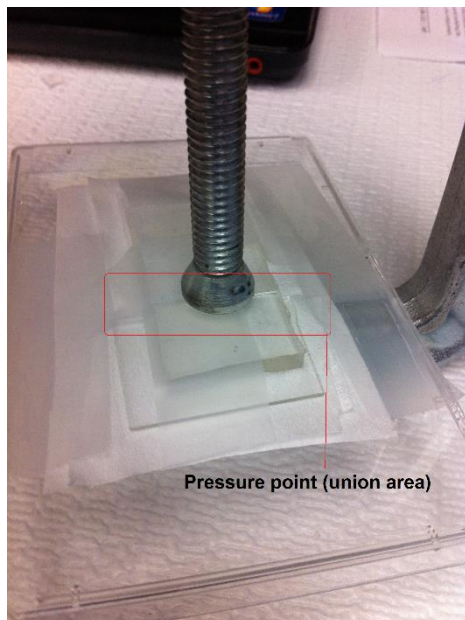
Figure 5.13. Setup used during the 24 or 48 hours incubation showing a microfluidic device pressed on the union area using a c-clamp of 3".

Figure 5.14. Setup used to inspect the microfluidic devices after microfabrication. The left side shows the perfusion fluid flowing in the channel having the PES membrane at the bottom. The microfluidic device shown in this picture corresponds to the simple microfluidic device of one channel made to test Aran et al's method (Figure 5.15).
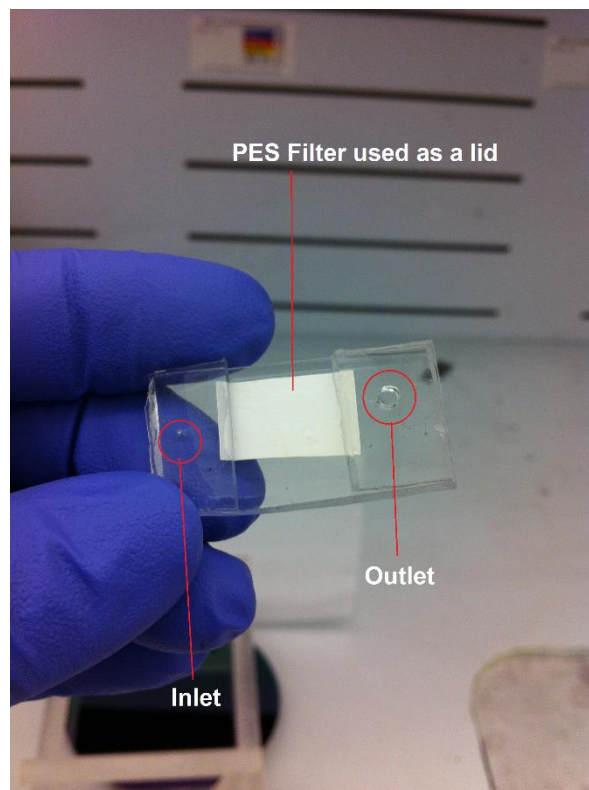
Figure 5.15. Microfluidic device fabricated to test Aran et al's binding method.
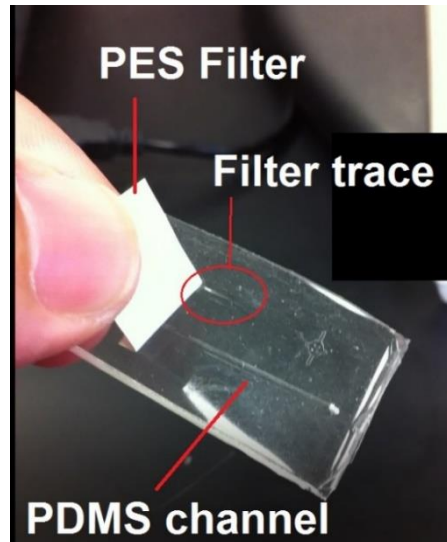
Figure 5.16. PDMS microfluidic device during simple pull test. Filter traces indicated the strength of the bond and the resistance to been pulled.
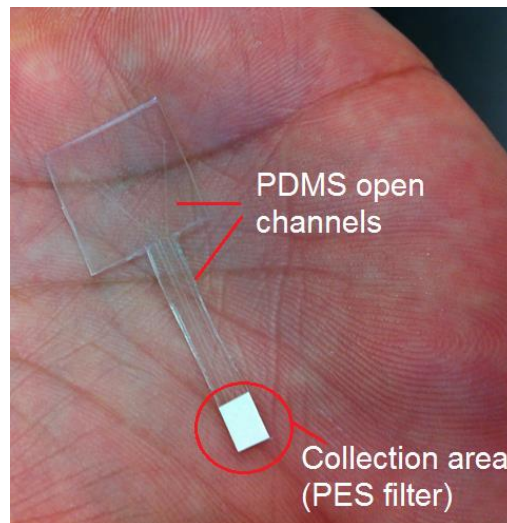
Figure 5.17. Cut PDMS replica with open channels and filter bound on collection area.

5.2.3.1 First assembly approach glass lid side by side

The first assembly approach used was made using a glass slide as lid and a syringe PES filter. As shown on Figure 5.8 1), the PES filter was first bound to the PDMS channels. After that the glass lid was chemically bound to the PDMS channels. The glass lid was positioned on top of the channels so that the edge of the lid and PES filter met. This was done to have the collection area covered with the PES filter only.

As mentioned before, the glass, PES filter, and PDMS were chemically bound using the Aran et al's procedure described on section 5.2.3. The microfluidic device was tested using HPLC water at a flow rate of 2.0 µL/min. The region between the PES filter and glass lid, "union region" (Figure 5.18 and 5.19), was where leakage occurred. To eliminate the leakage in the union region another assembly approach was made.

5.2.3.2 Second assembly approach PDMS lid side by side

The second assembly approach used was similar than the first approach, but PDMS was used as a lid. The idea of using PDMS was to have a more flexible material. Glass is more rigid than PDMS and that difference could cause microgaps, see Figure 5.20. Bhattacharya reported that when glass and PDMS are chemically bound a higher gap between the surfaces is formed.[8] On the other hand, the opposite was found when two PDMS surfaces were bound. Based on this finding, PDMS was used as a lid for this assembly. The same binding procedure as the first assembly (5.2.3.1) was used. After testing the device with HPLC water at 1.0 µL/min the same leakage was found as the first assembly. The device was leaking through the union area. A third assembly approach was conducted to eliminate the leakage in the union area.
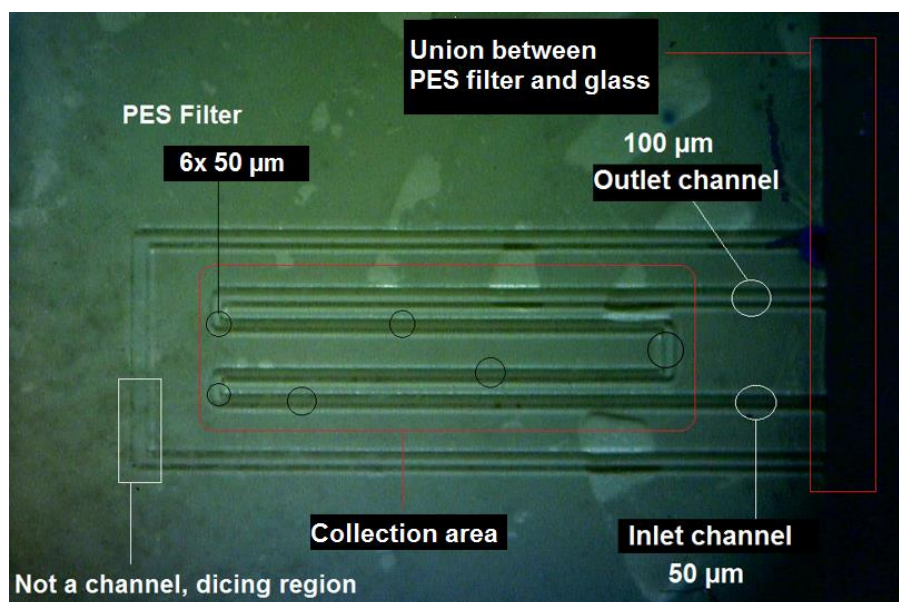
Figure 5.18. Microfluidic device during quality inspection under light microscope. This was the first assembly used (Figure 5.8 1)) during the development of the microfluidic system.
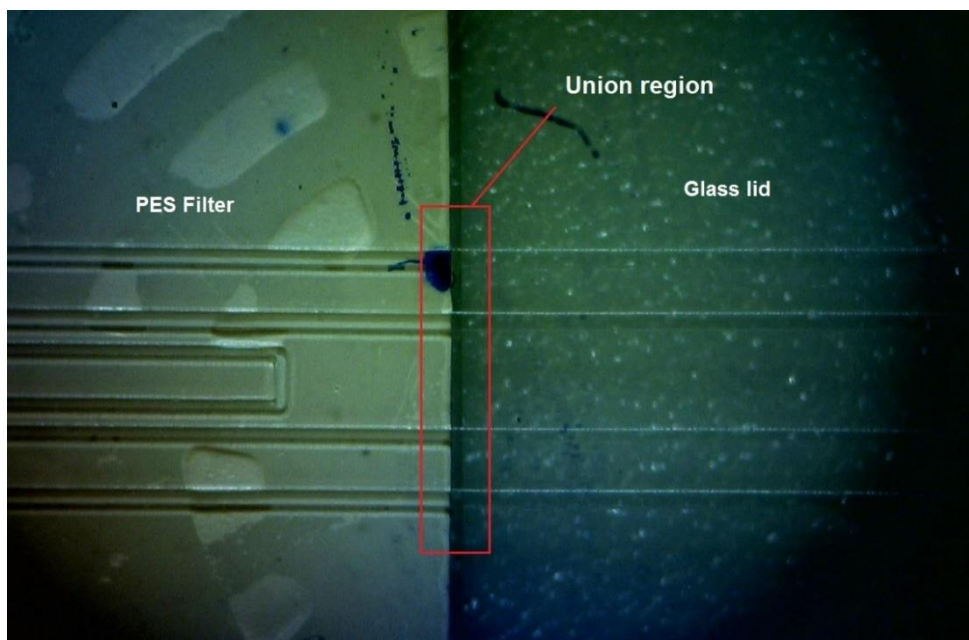
Figure 5.19. First assembly approach used during the development of the microfluidic device showing the union between the PES filter and the glass lid.
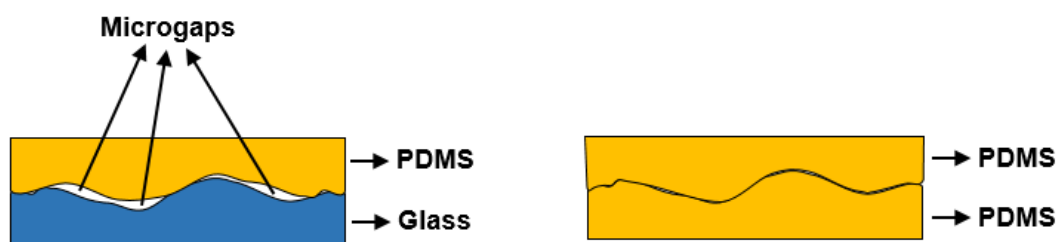
Figure 5.20. Diagram showing how microgaps could be formed when PDMS and glass are bound versus PDMS and PDMS according to Bhattacharya. Redrawn from reference [8].

5.2.3.3 Third assembly approach PDMS lid on top edge

This assembly approach consisted of the same components as second assembly (5.2.3.2), but the PDMS lid was bound at the edge of the PES filter. The idea was to apply a high pressure to a flexible PDMS lid positioned at the edge of the PES filter, see Figure 5.8 3), during binding incubation to increase the contact surface between the PES filter and PDMS lid. The PDMS curing time and temperature were reduced from 1 hr to 30 min and 75°C to 70°C respectively. These changes were made to have a more flexible PDMS. For this approach the c-clamp setup was used, see Figure 5.13. The device was leaking after perfusing it with HPLC water at 1.0 µL/min.

The leakage was found in the same union area. This assembly approach led to a fourth assembly with the same purpose of eliminating the leakage and be able to conduct collection experiments.

5.2.3.4 Fourth assembly approach glass indented

To solve the leakage problem, another assembly approach was performed. This approach consisted of using glass as a lid having an indentation of approximately 2 mm by 2 mm and depth of 60 µm (thickness of PES filter). The indentations were made on glass slides using a rotary diamond drill bit of 3/16". Water was used as lubricant to minimize friction. The diamond drill bit was mounted in a benchtop drill press. The pressure applied during drilling was controlled manually. A piece of PES filter was cut and used to verify the depth of the indentation.

When the indentation matched the thickness of the PES filter, the indented glass lid was used for the assembly. Figure 5.21 shows the microfluidic device before binding incubation. Two glass slides (without indentation) were used during incubation. One under the PDMS channels and the other on the PES filter next to the indented glass slide. This was done to ensure that the pressure was evenly applied during binding incubation. For this assembly, the c-clamp of 3" was used as well, see Figure 5.13. The device was leaking when it was tested after binding incubation under the same conditions as the third assembly. Since the manual drilling process added more variations to the assembly approach, another assembly approach was developed.
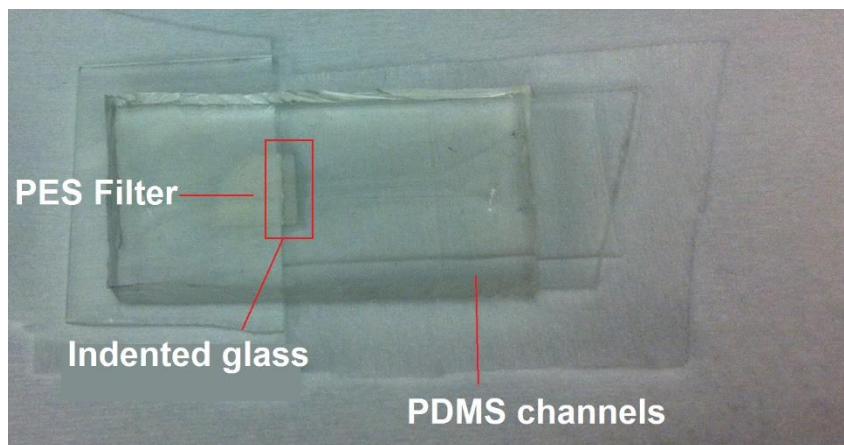

Figure 5.21. Microfluidic device made using fourth assembly before binding incubation using c-clamp.
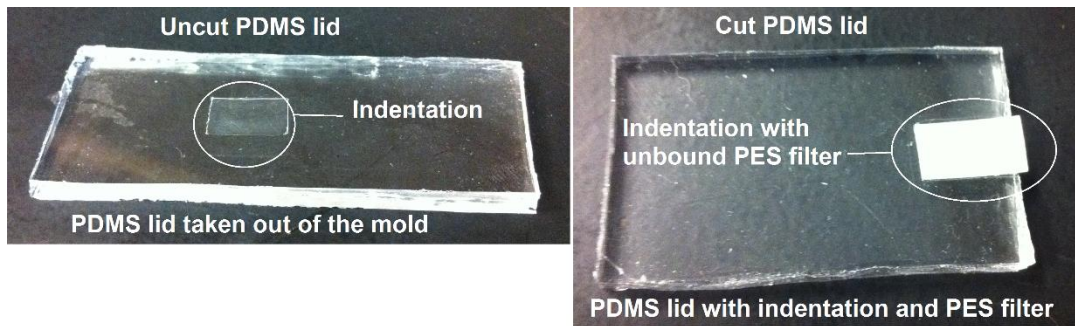
5.2.3.5 Fifth assembly approach PDMS indented

This new assembly approach was similar than the previous assembly (5.2.3.4), but the glass lid was replaced for PDMS, see Figure 5.8 5). For this approach the indentation on the PDMS lids were made by placing pieces of PES filter (larger than the collection area) on a 4" silicon wafer having cardboard taped around it. The PES filter pieces were cut larger than the collection area to make sure that the indented PDMS lids were wider. This was done to minimize leakage. To ensure the uniformity of the indentation, the PES filter pieces were glued using LOCTITE® super glue (gel control) to the wafer.

A thin layer of super glue was applied on the silicon wafer. To achieve a thin layer, a drop of the super glue was placed on the wafer and scraped using a metal blade. This ensured that a thin layer of super glue was used. After the super glue was applied on the wafer, three PES filters of 5 mm in height and 2 mm in width were placed on the wafer. This served as a mold for the PDMS lids with indentation. The Sylgard® 184 Silicone Elastomer Kit was used to make the PDMS lid replicas on the mold (see section 5.2.2). The mold with PDMS was incubated in an oven at 75 C° for 1 hour. After binding incubation, the three PDMS lids with indentation were cut, see Figures 5.22 and 23. Before binding each part (PDMS lid with indentation, PES filter, and PDMS channels), each device was assembled to make sure they fit well, see Figure 5.24. All three microfluidic devices (Figure 5.24) were tested using 100 µm methyl orange solution and 4% dextran-70 in 10 mM PBS pH 7.4 or HPLC water as perfusion fluid. The inlet of one of the devices (Figure 5.25 "C") was expanded using a punch of 3.02 mm cutting edge diameter. This was done to eliminate the leakage present in the inlet during perfusion. A plastic fitting was glued to the inlet using LOCTITE® super glue. To seal the other side of the inlet, a piece of PDMS was glued at the bottom of the plastic fitting, see Figure 5.25. The microfluidic device was leaking from the collection area (Figure 5.26) and was fixed with super glue. After fixing the leakage using super glue flow rate verification was conducted. The flow rate was verified using methyl orange and 4% dextran as perfusion fluid. This verification was done by collecting three samples from the outlet every 2 min at 2.0 µL/min and measuring their weight. A regular BASi syringe pump system (West Lafayette, IN) was used to push the perfusion fluid at 2.0 µL/min.
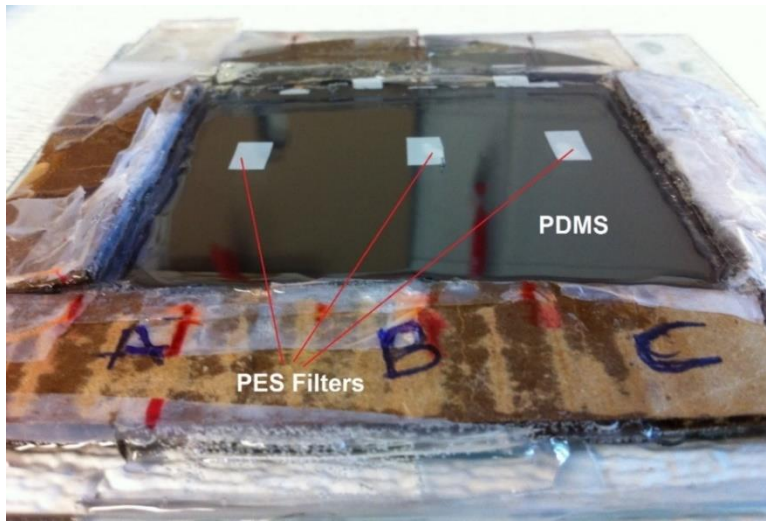
Figure 5.22. Indented PDMS lids inside the mold before been cut.

Figure 5.23. PDMS lid with indentation before (uncut) and after cutting.
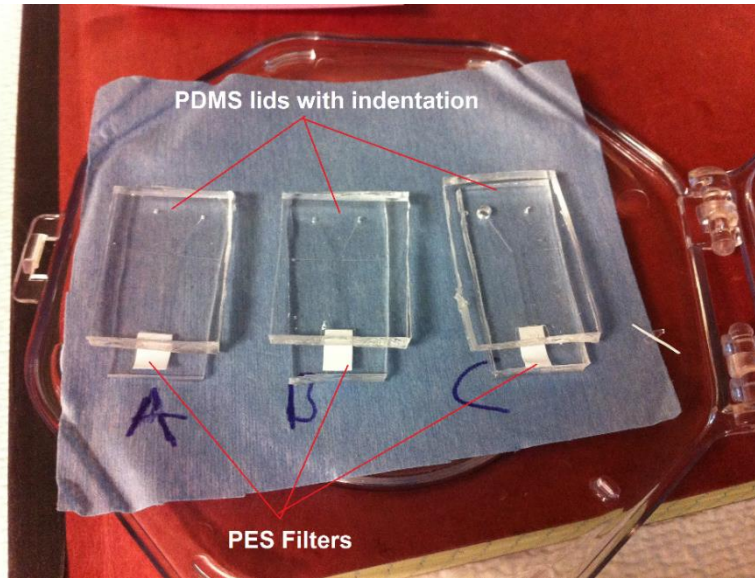
Figure 5.24. Uncut and unbound microfluidic devices for fifth assembly approach.
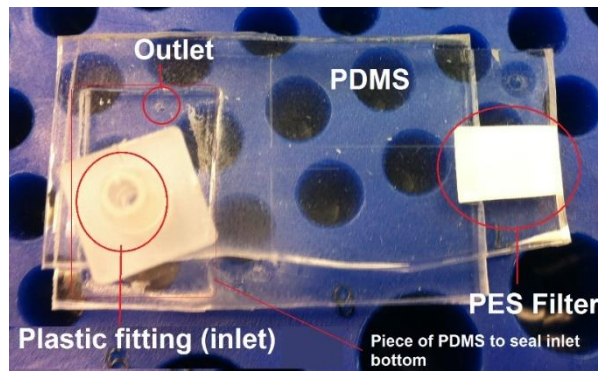
Figure 5.25. Microfluidic device made using fifth assembly having a plastic fitting in the inlet.

Figure 5.26. PDMS microfluidic device made using fifth assembly during leakage testing using 100 µM methyl orange solution. The red arrows indicate the leakage area where super glue was applied before testing.

For the gravimetric calculations, it was assumed that the density of the dialysate was 1.0 g/mL (the density of 100 µM in HPLC was previously determined, Chapter 3, to be 0.998 g/mL ± 0.004 g/mL). The calculated volume was 4.0 µL (collection time multiplied by flow rate). After collections, the measured flow rate or volume delivered overtime was 4.14 µL ± 0.19 µL. This result indicates a fluid gain of 3.5%. Since a larger fitting (Figure 5.25) was glued to the inlet, an in-house made tubing connection was used, see Figure 5.26 and 5.27. Two types of experiments were performed. The first experiment was performed by placing 7 mL of the methyl orange solution in a 20 mL beaker, a recovery experiment (Figure 5.27), and using 4% dextran as perfusion fluid pumped at a 2.0 µL/min rate. The second experiment was a delivery experiment in which the methyl orange solution was placed in the syringe of the BASi syringe pump system. The latter experimental setup can be seen on Figure 5.28. The flow rates used was this experiment 1.0 µL/min. No recovery or delivery was observed during these experiments. This was determined by measuring the absorbance of the dialysate using the NanoDrop 2000 UV-Vis spectrophotometer from Thermo Scientific (Wilmington, DE), data not shown here. Since super glue was used to fix the leakage from the membrane (Figure 5.26), this could have clogged the pores of the membrane. The super glue could have diffused into the pores clogging them. A microgap was found in the microfluidic devices explaining why the devices were leaking from the union area close to the membrane and collection area, see Figure 5.29.
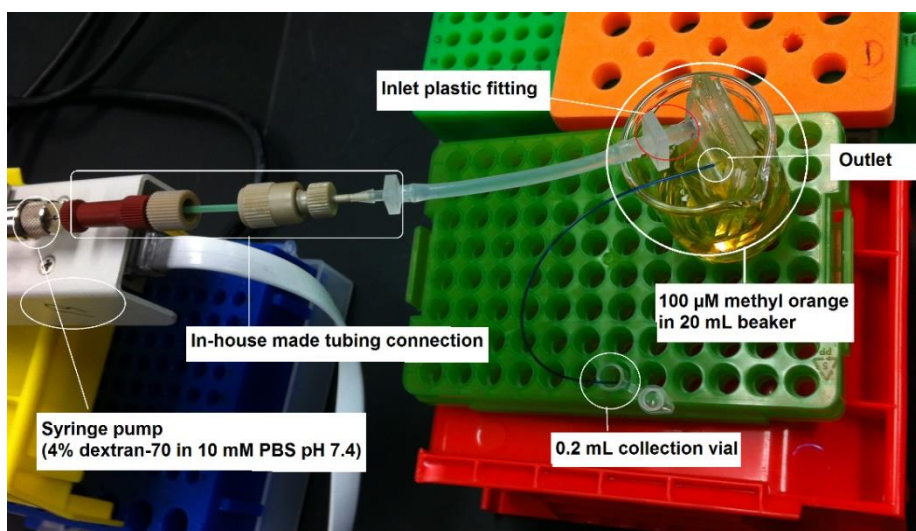
Figure 5.27. Collection of methyl orange experiment using microfluidic device made with fifth assembly approach.
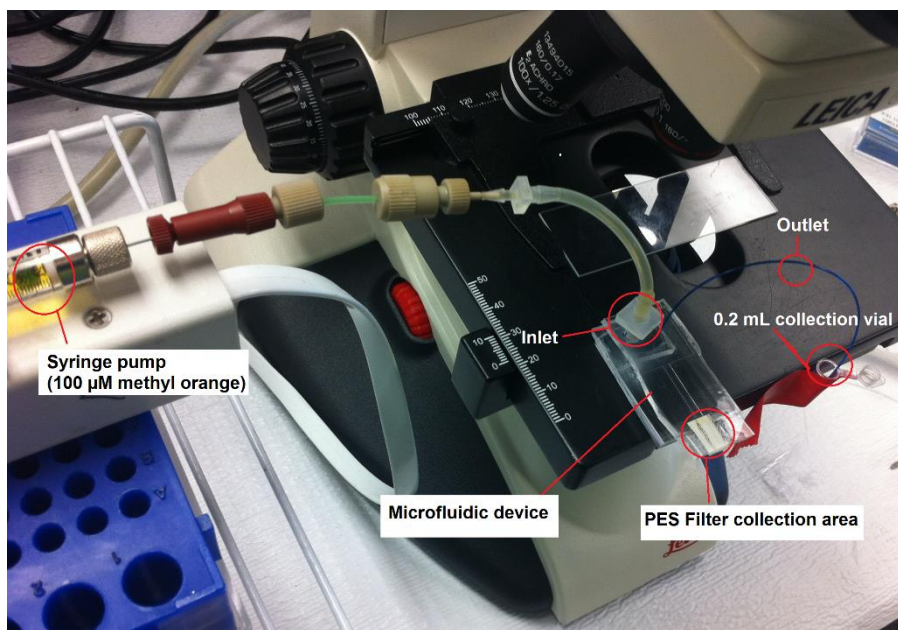
Figure 5.28. Setup used to test the microfluidic device made with the fifth assembly approach. Delivery experiments.

The other two devices (Figure 5.24 "A" and "B") were leaking as well after testing with HPLC water at 0.5 µL/min and 1.0 µL/min respectively. Figure 5.30 shows microfluidic device "B" during leakage testing. Unlike microfluidic device "C", the other two devices' inlet and outlet were made using a 0.71 mm round punch. This facilitated the tubing connections. The next logical step would have been to conduct this assembly approach under a microscope to make sure that microgaps were not present. However, one last assembly approach was developed to eliminate all the problems with the leakage. Before conducting this last assembly approach, the PES filter was tested to make sure that transport was occurring across the filter.
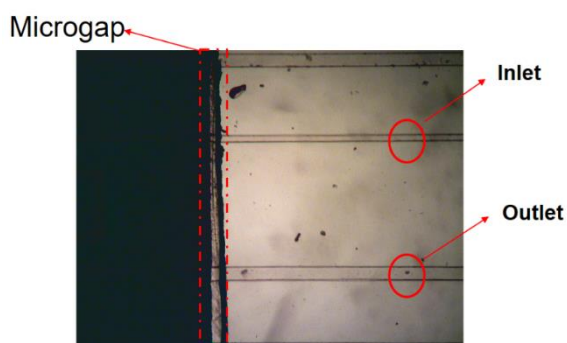
Figure 5.29. Microgap formed after assembly approach number 5 was used. This microgap was located at the union region between the PES filter and the PDMS lid.

95
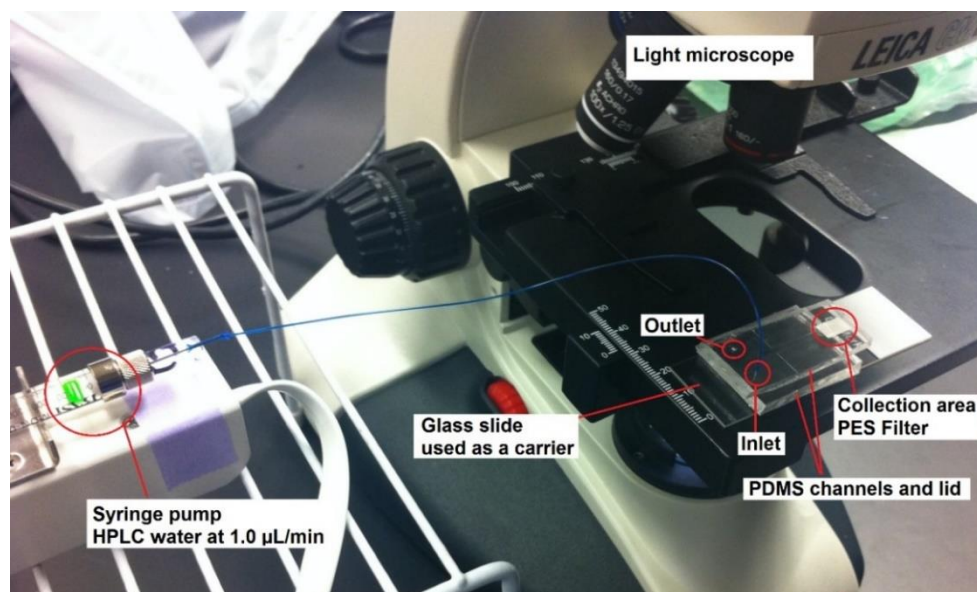
Figure 5.30. Microfluidic device made using assembly number 5 been tested using HLPC water under a light microscope.

5.2.3.5.1 Equilibrium dialysis

To evaluate whether or not analyte transport was occurring across the PES filter an equilibrium dialysis experiment was conducted. A micro-equilibrium dialyzer of 25 µL from Harvard Apparatus (Holliston, MA) was used, see Figure 5.31. In one chamber 25 µL of 10 mM PBS pH 7.4 were pipetted and in the other chamber 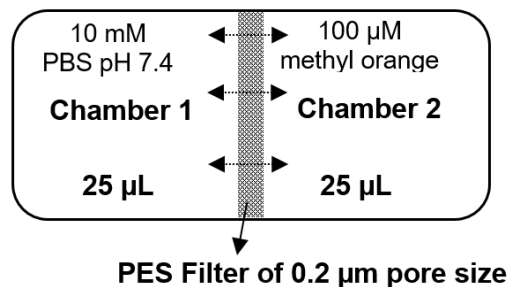the same volume of 100 µM methyl orange (diluted in the same buffer) was placed. The total volume used was 50 µL. A Whatman™ Puradisc PES syringe filter of 25 mm in diameter and pore size of 0.2 µm purchased from Sigma-Aldrich, St. Louis, MO was used. As previously mentioned the syringe filter was broken to retrieve the filter. After retrieving the filter, it was cut using a regular office scissors to the size of the chamber. The micro-equilibrium dialyzer was placed horizontally (as shown on Figure 5.31) on a bench for 1 hour and 22 minutes at room temperature. The concentration of methyl orange in each chamber was measured using an UV-Vis spectrophotometer (NanoDrop) after incubation. The results were reported as percent recovery. The measured concentrations of methyl orange were related to the initial concentration of methyl orange used (100 µM). It was found that a 49.7% of methyl orange was present in chamber 2 and a 41.4% in chamber 1. These results showed that transport across the PES filter occurred indicating that the PES filter was not the source of the problem with the microfluidic device.

```
┌──────────────────────────────────┐
│  10 mM      ◄┄┄►   100 µM         │
│  PBS pH 7.4        methyl orange  │
│                                   │
│  Chamber 1  ◄┄┄►   Chamber 2      │
│                                   │
│  25 µL      ◄┄┄►   25 µL          │
└──────────────────────────────────┘
```

PES Filter of 0.2 µm pore size

Figure 5.31. Schematic representation of the micro-equilibrium dialyzer used for the equilibrium dialysis experiment performed to test the PES filter transport.

### 5.2.3.6 Sixth assembly approach using UE50 membrane

The last assembly approach used to solve the leakage problem with the microfluidic system was conducted, see Figure 5.8 6). This assembly approach consisted of covering the PDMS replica with open channels using a PES membrane and used a flat PDMS as a lid. The collection area was only covered with the PES membrane to allow the transport of molecules across it. The idea was to eliminate the need for indentations or precision alignments during assembly. The sixth approach significantly simplified the microfabrication of the microfluidic device. To test this approach, TriSep UE50 flat-sheet polyethersulfone (PES) ultrafiltration membrane of 100 kDa (MWCO) from Sterlitech Corporation, Kent, WA was used. This flat-sheet membrane had two distinct roughness in each side. One side was called "shiny" and the other side "dull". The latter had a hair-like roughness, see Figure 5.32. According to Sterlitech, this difference is caused by their manufacturing process. They stated that the "shiny" side indicates tighter pores. This difference caused a problem during the microfluidic device assembly and will be addressed later in this section. The PDMS channels, PDMS lids, and PES membranes were attached chemically using the Aran et al's binding method (Figure 5.10 and 5.11). After the plasma and APTES treatments the "dull" side (Figure 5.32) of the PES membrane did not bind to the PDMS lid as the "shiny" side of the membrane. As soon as the "shiny" side of the membrane and PDMS channels were brought into contact a bond was formed. The same observation was reported by Aran et al ([7]). As previously mentioned, the "dull" side of the membrane caused a problem during the assembly process.
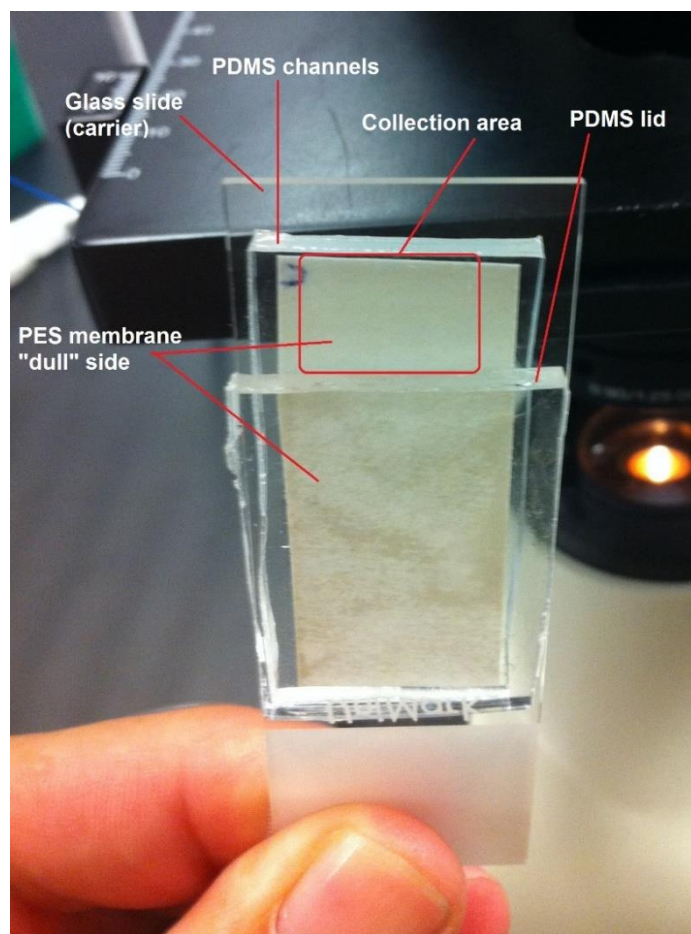
Figure 5.32. PDMS microfluidic device made using TriSep UE50 flat-sheet PES membrane. The roughness of the "dull" side can be seen in this picture. A glass slide was used to carry the device.

When the "dull" side and PDMS lid were brought into contact, they did not form a bond. This was visually observed as both parts did not attach or fell apart. To fix this problem, the surface of the "dull" side of the membrane and PDMS lid were treated using the APE 110 oxygen plasma at 600 mTorr and 100 W for 20 seconds. To increase the oxygen exposure to the surface and activate the surface. After one trial, the membrane and PDMS lid formed a bond and were incubated accordingly to ensure that a stronger bond was achieved. Figure 5.33 shows one of the four PDMS microfluidic devices made using the new membrane during leakage inspection. The microfluidic devices were inspected for leakage under a light microscope by pumping a solution of 10 mM PBS pH 7.4 at a 1.0 µL/min rate, see Figure 5.33. During this test the flow rate from the outlet of one of the microfluidic devices was measured gravimetrically. Two samples were collected every 5 minutes at the same pumping rate (1.0. µL/min).

It was assumed that the PBS density was 1.0 g/mL. Based on this assumption, the average (n = 2) amount of PBS delivered from the microfluidic device was 4.7 µL.
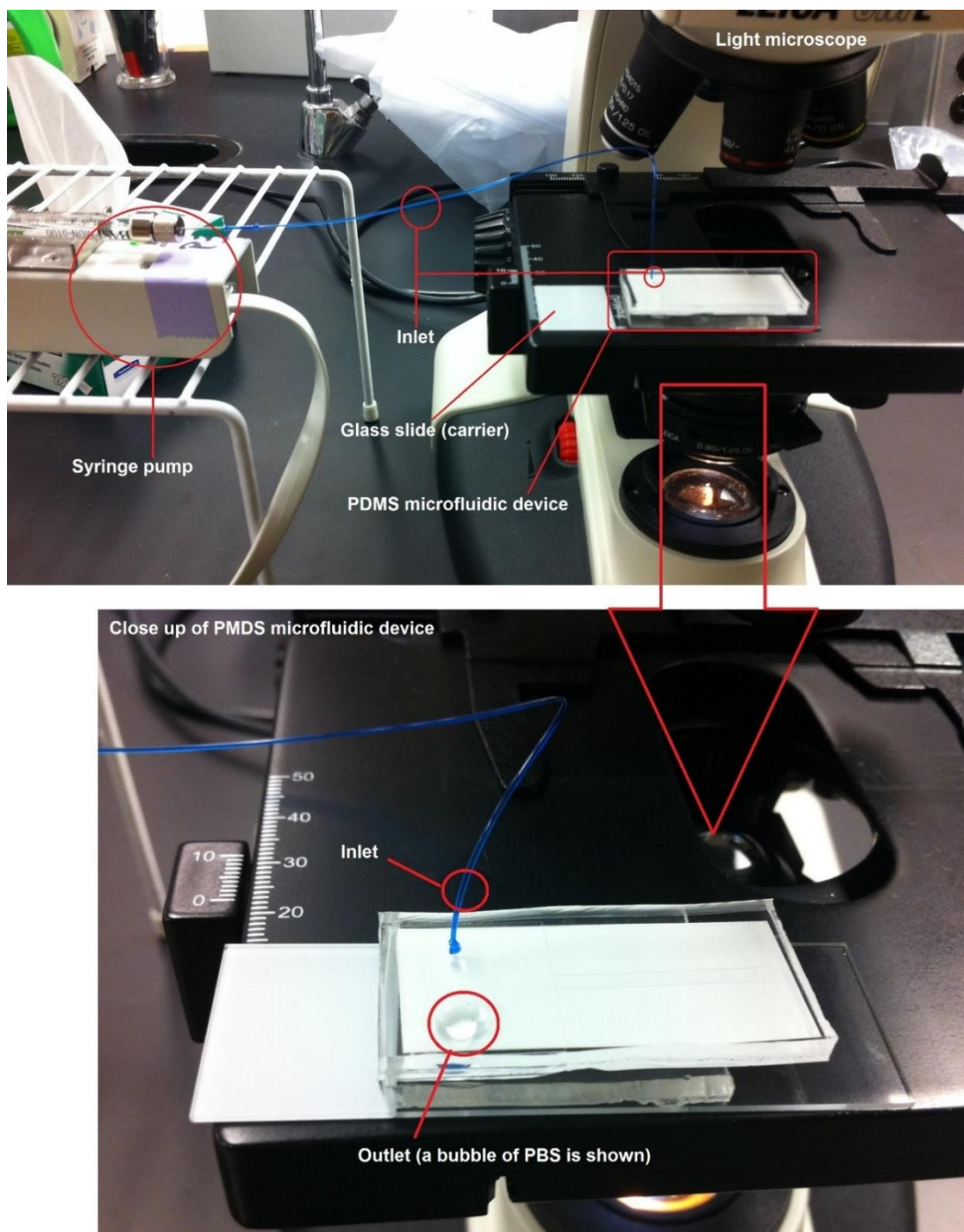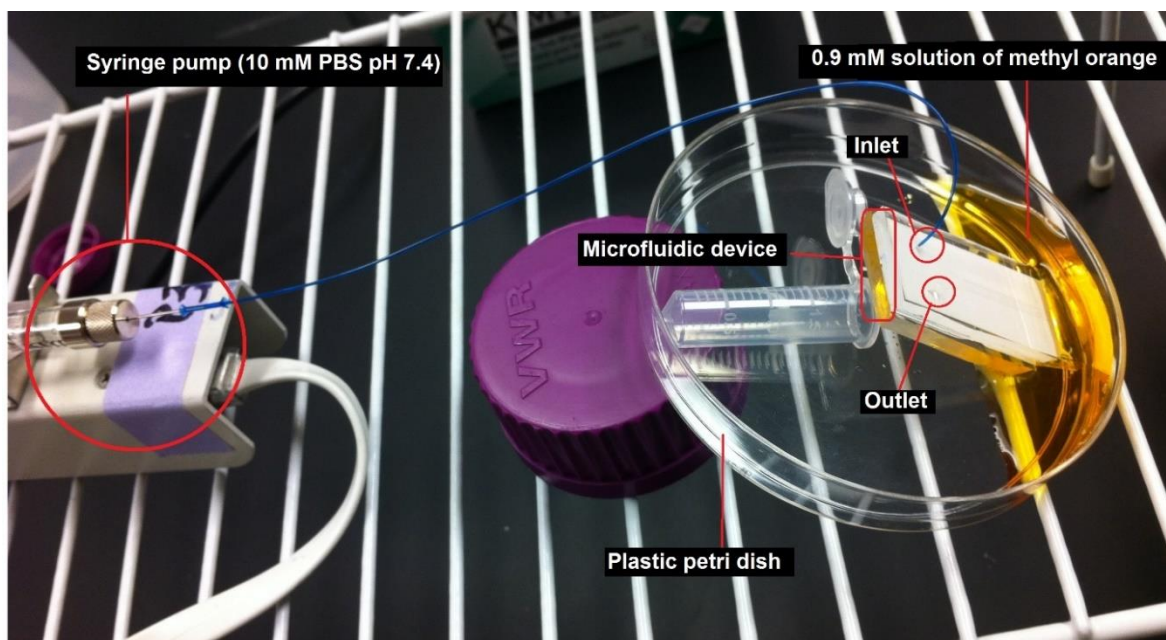

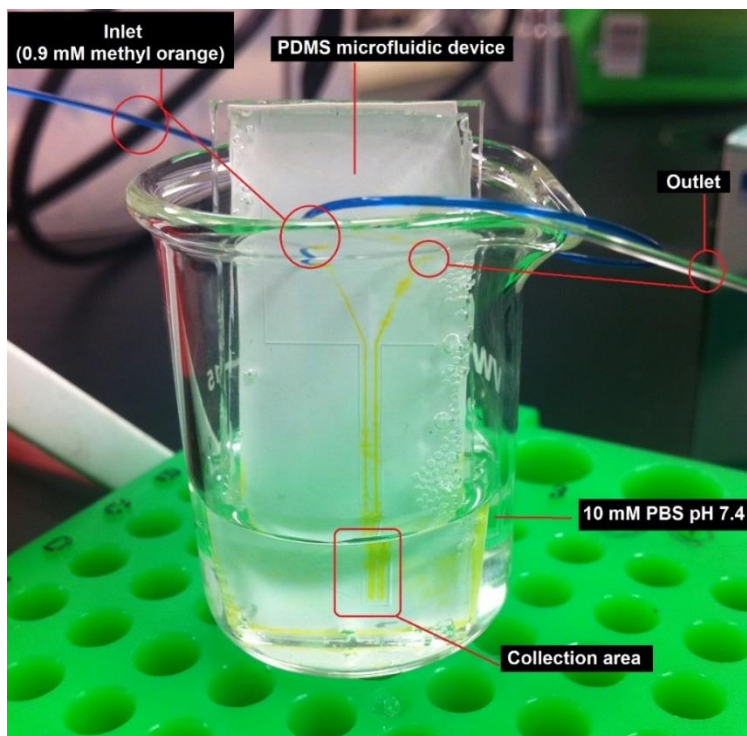**Figure 5.33.** PDMS microfluidic device (UE50) during leakage inspection under a light microscope.

Compared to the delivered theoretical volume of 5.0 µL, calculated using the collection time and pumping rate, the delivered measured volume (4.7 µL) was only 0.3 µL off. This indicated that only a small amount of fluid was loss across the membrane. After inspection, the devices were tested using 0.9 mM methyl orange in HPLC water as the analyte and PBS as perfusion fluid. Recovery and delivery experiments were performed on the devices. For the recovery experiments, the methyl orange was placed in either a 20 mL glass beaker (Figure 5.34) or a plastic petri dish (Figure 5.35). The methyl orange solution was placed in the syringe during the delivery experiments, see Figure 5.36. Of the four devices, two devices broke apart (Figure 5.37). After the 24 hours binding incubation, the PDMS lids came off. This indicated that a very weak bond was formed between the PES UE50 membranes ("dull" side) and PDMS lids. However, the other two microfluidic devices were successfully tested and not leakage were found.
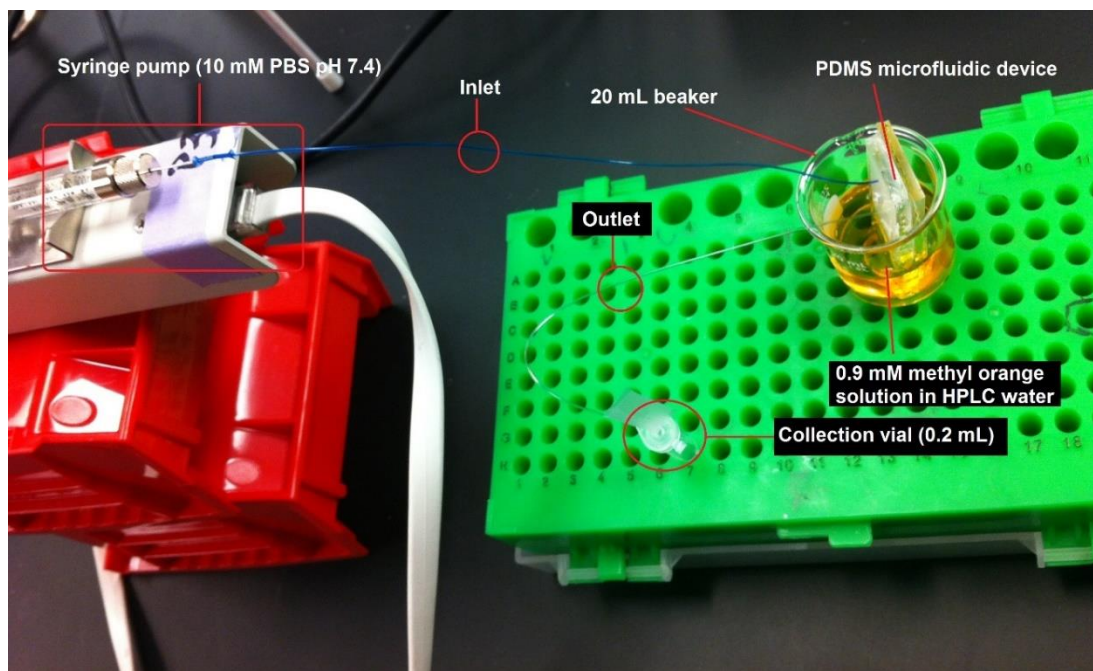
Figure 5.34. Experimental beaker set up used for recovery experiments performed on the PDMS microfluidic devices having UE50 PES membranes.
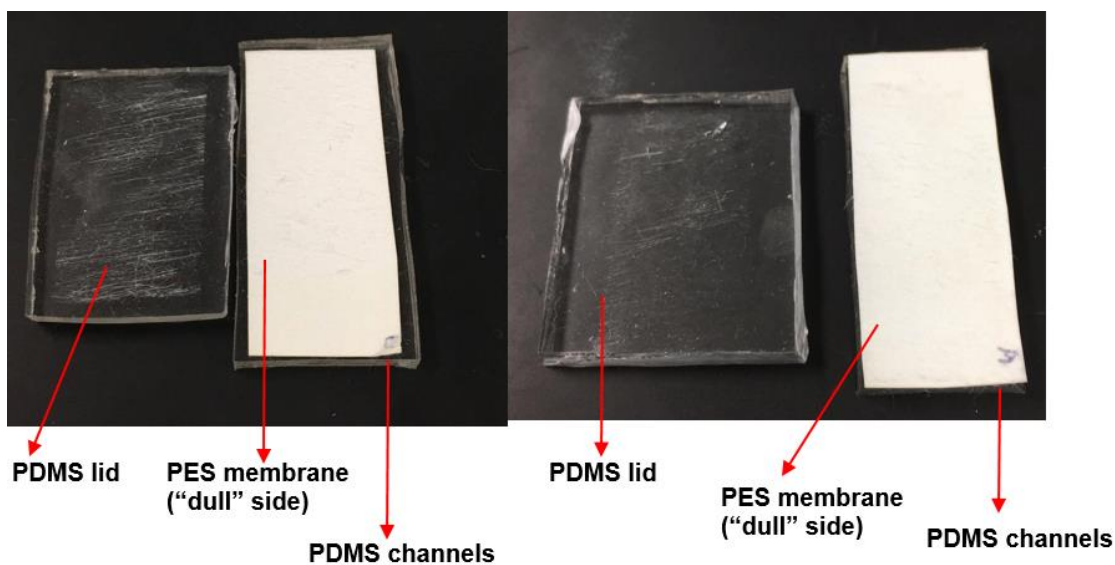
Figure 5.35. Recovery experiments performed using a plastic petri dish on the PDMS microfluidic devices (UE50 PES membranes).
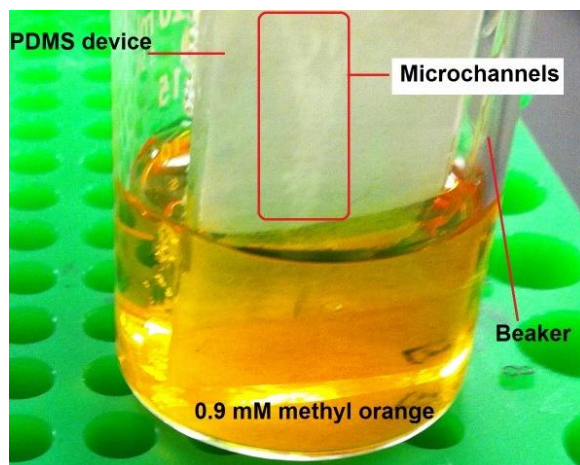

Figure 5.36. PDMS microfluidic device (UE50 PES membranes) during methyl orange delivery experiment. The orange marks indicated the methyl orange flow path inside the device.

Figure 5.37. PMDS microfluidic devices after binding incubation using UE50 PES membranes. The PDMS lids detached from the PES membranes.

These microfluidic devices were further tested as previously mentioned by either recovering methyl orange or delivering it in the device (Figures 5.34, 5.35, and 5.36). The recovery experiment conducted at 1.0 μL/min for 7 hours and 31 minutes, yielded dialysates not detectable by the NanoDrop 2000 UV-Vis spectrophotometer. Figure 5.38 shows physical appearance of the UE50 PES membrane after the recovery experiment was conducted. The fact that a lack of orange color was observed (see Figure 5.36 for color reference), could indicate that transport across the membrane was very poor or at an undetectable level (absorbance ≤ blank = PBS). After this result, the delivery experiment was conducted. The microfluidic device was placed in a beaker containing PBS and a methyl orange solution of 0.9 mM was delivered at a pumping rate of 5.0 μL/min into the device. A higher flow rate (1.0 μL/min vs. 5.0 μL/min) was chosen for the delivery experiment (Figure 5.36) to increase the amount of methyl orange delivery across the membrane. The same result as the recovery experiment was found. The dialysates measured spectrophotometrically were below the limit of detection. The orange marks shown on Figure 5.36 indicates that the methyl orange was flowing in the microfluidic channels and not leakage was present. One of the reasons why methyl orange was not detected during the delivery experiments, could be dilution. The amount of methyl orange delivered into the beaker could be negligible compared to the PBS in the beaker.

Figure 5.38. PDMS microfluidic device showing the wettability of the UE50 PES membrane during recovery experiments. This was one of the indications of poor transport across the membrane.

To elucidate whether the problem was the transport across the membrane or not, the UE50 PES membrane was tested using the equilibrium dialysis technique (see section 5.2.3.5.1 for details). This experiment was conducted by Dr. Sarah Phillips. According to Phillips, the equilibrium dialysis experiment was conducted using a solution of 200 µM FITC-10 diluted in ringer. She found that the recovery of FITC-10 after 13 hours and 30 minutes was ~6%. The equilibrium dialysis experiment of FITC-10 led to a new and final PES membrane. The sixth and final assembly approach was chosen as the more effective to make the microfluidic device, since not leakage was observed during testing or experiments. Nevertheless, the microfluidic devices made with the UE50 membranes did not work on either recovery or delivery mode. To solve both the membrane transport and membrane-PDMS binding problems, a new PES membrane was selected. The experiments conducted in the section were instrumental for the development of the microfluidic device. One important finding was how the roughness of the PES membrane surface affected the strength of the chemical bond formed between the membrane and PDMS. The next section will cover the results of changing the UE50 PES membrane.

5.2.3.6.1   Sixth assembly approach using PES019025 membrane

After six assembly iterations, the problem with the leakage found in the microfluidic devices was solved. The problem was solved by having a PES membrane covering the microfluidic channels of the device. This approach was simple and significantly reduced the need to have a precise assembly when only the collection area was covered in previous assemblies. However, for future further developments of the microdialysis-based microfluidic device engineered during this dissertation, the amount of PES membrane should be used reduce to minimize cost. Chapter 6 will cover the latter in more details.

5.2.3.6.1.1 Materials and methods

Flat polyethersulfone (PES) membrane filters of 90 mm in diameter and pore size of 0.1 µm were purchased from Sterlitech Corporation, Kent, WA. The thickness of the membrane was ~150 µm. This was determined using an in-house micrometer. This was within the Sterlitech thickness range for this type of membrane (110-150 µm) found on their website.[9] A solution of 5% (in water) v/v of 3-amino propyltriethoxysilane (APTES) was made using 99% v/v APTES stock solution purchased from Sigma-Aldrich, St. Louis, MO. The 5% v/v APTES solution was used to chemically modified the surface of the PES membrane during the Aran et al' binding method (Figure 5.10). This method was previously described in detail on section 5.2.3. The transport of 100 µM methyl in 10 mM PBS pH 7.4 solution across of the PES membrane was determined using equilibrium dialysis (see section 5.2.3.5.1) after plasma and APTES treatments. The solution of methyl orange was placed in one chamber (25 µL) and the PBS was placed (25 µL) in the other chamber. The micro-equilibrium dialyzer (Figure 5.31) with the solutions was incubated at room temperature for 2 hours.

The microchannels and lids were made using the standard Sylgard® 184 Silicone Elastomer Kit from Dow Corning Corporation, Midland, MI. The kit contains a base and curing agent that are typically mixed to a 10:1 ratio by weight. This kit was used to make the PDMS and the curing time and temperate used were 1 hr and 75 °C. The master mold was made using SU-8 3050 from MicroChem Corp., Westborough, MA. The same procured as described on section 5.2.2 was used. The PDMS microfluidic device was tested using a BASi syringe pump system (West Lafayette, IN) at pumping rates of 1.0, 2.0, and 5.0 µL/min.

The perfusion fluids used were 10 mM PBS pH 7.4 and 4% dextran-500 in 10 mM PBS pH 7.4. The amount of dialysate exiting the outlet of the microfluidic device over time was determined gravimetrically. This was performed to determine the fluid loss across the membrane. Push-pull experiments were conducted on the microfluidic device using a MAB-20 microdialysis pump from Microbiotech, Stockholm, Sweden. The following sequence was used for the push-pull experiments to find the optimal setting: a) 1.0-4.0 µL/min, b) 0.5-4.0 µL/min, c) 0.5-5.0 µL/min, d) 0.2-5.0 µL/min, e) 0.2-3.0 µL/min, f) 0.2-2.0 µL/min, and g) 0.2-1.0 µL/min. The last setting (0.2-1.0 µL/min) was performed on microdialysis probes having PES membranes of 100 kDa MWCO and length 10 mm (CMA/20) and 4 mm (CMA/12) respectively. These microdialysis probes were purchased from Harvard Apparatus, Holliston, MA. The analyte used was methyl orange. A solution of 0.9 mM methyl orange in HPLC water was used for the experiments. Push or regular microdialysis experiments were performed at 0.2 µL/min and 1.0 µL/min on the device. The latter flow rate was used for relative recovery experiments performed on a CMA/12 microdialysis probe. The perfusion fluid used for push and push-pull experiments was 4% dextran-500 in 10 mM PBS pH 7.4.

Theoretical estimations were made to evaluate the difference in fluid transport properties between the three systems (microfluidic device, CMA/12, CMA/20). The surface area of the membrane, linear velocity, pressure drop, and the resistance to flow were estimated for each system. The log mean surface area (S_m) was used to estimate the surface of the microdialysis probes.[10] For the microfluidic device, the pressure drop was estimated using an aspect ratio (a) of 0.5. Phosphate buffer saline was assumed to be the perfusion fluid. A pumping rate of 1.0 µL/min and temperature of 25 °C were also used for the estimations. These calculations were performed to further improve the performance of the microfluidic device in the future. Table 5.1 shows the equations used for the estimations. It was assumed, for the estimations, that the collection area of the device was a straight channel, see Figure 5.39. This was done to simplify the calculations.

Table 5.1. List of equations used to estimate the fluid transport properties of the three systems.

	Microdialysis probes	Microfluidic device
Surface area[10]	$S_m = 2\pi L_m \cdot \dfrac{(r_o - r_i)}{\ln\left[\dfrac{r_o}{r_i}\right]}$	Surface area = width * length
Linear Velocity[5]	$v = \dfrac{Q}{A(area)}$	$v = \dfrac{Q}{A(area)}$
*Pressure drop[10,11]	$\Delta p_a = \Re_a \cdot Q$	$\Delta P = f\dfrac{L}{D}\dfrac{\rho V_{avg}^2}{2}$
**Resistance to flow rate[5,10]	$\Re_a = \dfrac{8\eta \cdot L_m}{\pi r_i^4 \cdot \left(\dfrac{1 - \varsigma^4 + [1 - \varsigma^2]^2}{\ln[\varsigma]}\right)}$	$R_h = \dfrac{12\eta L}{1 - 0.63\left(\dfrac{h}{w}\right)}\dfrac{1}{h^3 w}$

*$f = \dfrac{24}{R_e}(1 - 1.3553a + 1.9464a^2 - 1.7012a^3 + 0.9564a^4 - 0.2357a^5)$ from reference 11.

** h = height and w = width from reference 5.
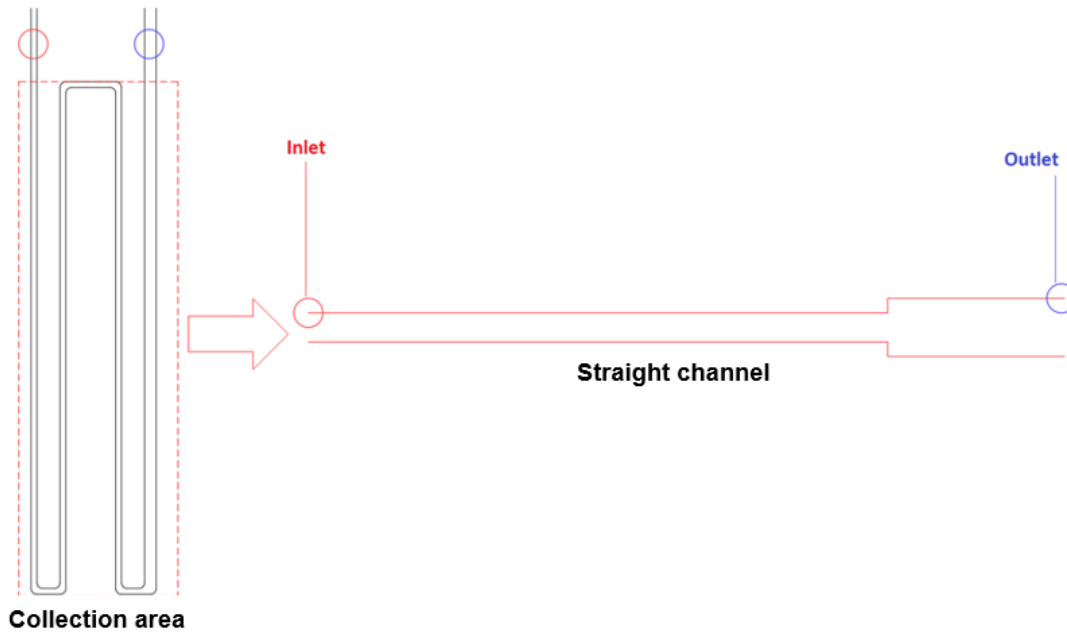
Figure 5.39. Schematic representation of microfluidic device collection area. For the estimations this area was assumed to be a straight channel to simplify the estimations.

5.2.3.6.1.2 Results and discussion

Analyte transport across the PES membrane was similar as the PES filters (section 5.2.3) first used to make the microfluidic devices. After the two hours incubation, the relative recovery was 44.74% ± 0.64% (n =3) from the chamber with methyl orange and 43.26% ± 2.22% (n = 3) from the chamber with PBS. The equilibrium dialysis results indicated that transport across the PES membrane was not an issue.

The fluid loss across the membrane of the PDMS microfluidic device was 36.10% ± 2.25% (n = 3) when a solution of 4% dextran-500 in 10 mM PBS pH 7.4 was pumped into the device at a rate of 5.0 μL/min for 2 min. On the other hand, a fluid gain of 4.10% ± 0.98% (n = 3) was observed when 10 mM PBS pH 7.4 was used. These results indicated that an increment in the internal pressure of the microfluidic device when 4% dextran-500 was used. This is due to the viscosity differences between the 4% dextran-500 solution (~1.18 mPa.s) and PBS (~0.89 mPa.s). A fluid gain is typically observed during regular microdialysis sampling experiments. The fluid gain for the CMA/12 microdialysis probe at 1.0 μL/min using 4% dextran-500 in PBS as perfusion fluid was 3.37% ± 0.06% (n = 3). The fluid loss across the membrane of the device increased with the pumping rate. The fluid loss across the membrane was measured at pumping rates of 2.0 μL/min and 1.0 μL/min using 4% dextran-500 as perfusion fluid. It was found that the fluid loss at 2.0 μL/min was 26.40% ± 3.80% (n = 3) and at 1.0 μL/min was 22.30% ± 2.40% (n = 3). At lower pumping rates the fluid loss across the membrane is reduced. This means that the hydraulic pressure generated by the syringe pump is smaller. When 4% dextran-500 was pumped at 5.0 μL/min into the device a bubble was observed at the collection area, see Figure 5.40. The bubble indicated that a higher internal pressure was generated at the pumping rate. The bubble was smaller when slower pumping rates were used (Figure 5.41) and no bubble was observed when PBS alone was used. The relative recovery of methyl orange at 0.2 μL/min was 8.41% ± 0.31% (n = 2) and at 1.0 μL/min was 1.64% ± 0.22% (n = 3). These results showed that the microfluidic device was able to collect methyl orange, but that the device needs to be optimized.

As a comparison, the relative recovery of methyl orange was determined using a CMA/12 microdialysis probe at a pumping rate of 1.0 μL/min. CMA/12 microdialysis probes have PES membranes of 4 mm length and the device has a collection area length of ~4.4 mm. The relative recovery was 30.60% ± 1.35% (n = 3). One of the reason why the device yielded a lower relative recovery than the microdialysis probe could be that the microfluidic device has a thicker membrane. Microdialysis probes have a membrane thickness of 50 μm, but that thickness includes the supporting layer. The active layer is of ~5 μm thick. In contrast, the thickness of the microfluidic device membrane is ~150 μm. The thickness of the microfluidic device significantly reduced the transport across the membrane. Push-pull experiments were performed to increase the transport across the membrane based on the latter results. The optimal setting for the microfluidic device during push-pull experiments of methyl orange was found to be 0.2 μL/min-1.0 μL/min.
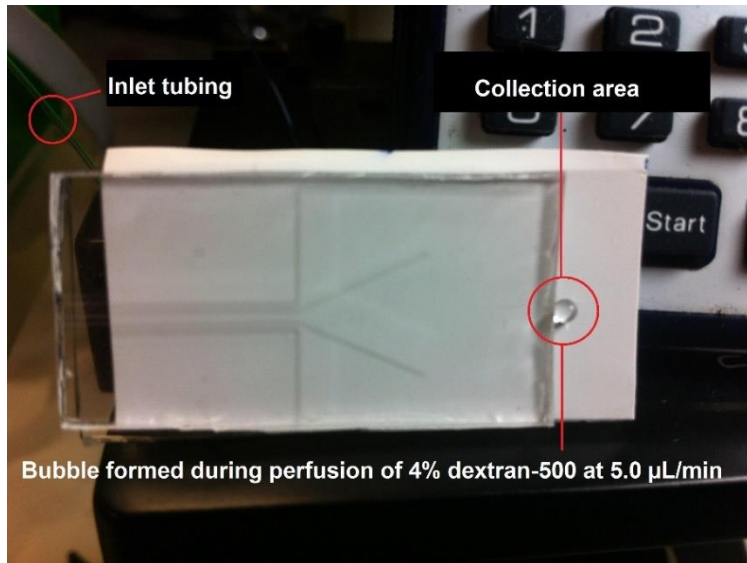
Figure 5.40. PMDS microfluidic device during flow verification testing using 4% dextran-500 in 10 mM PBS pH 7.4 as perfusion fluid pumped at 5.0 µL/min. A bubble was formed at the collection area during testing.
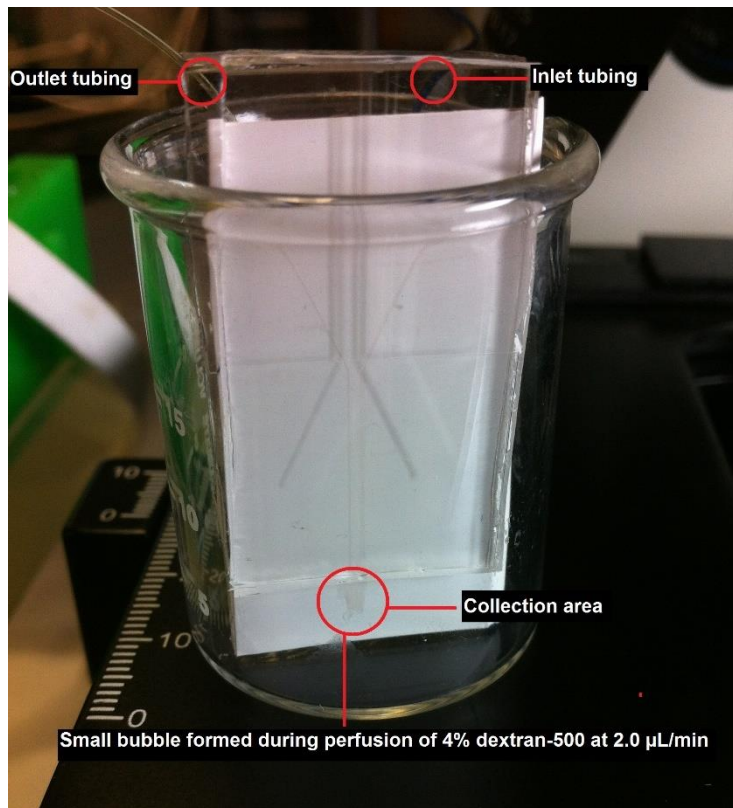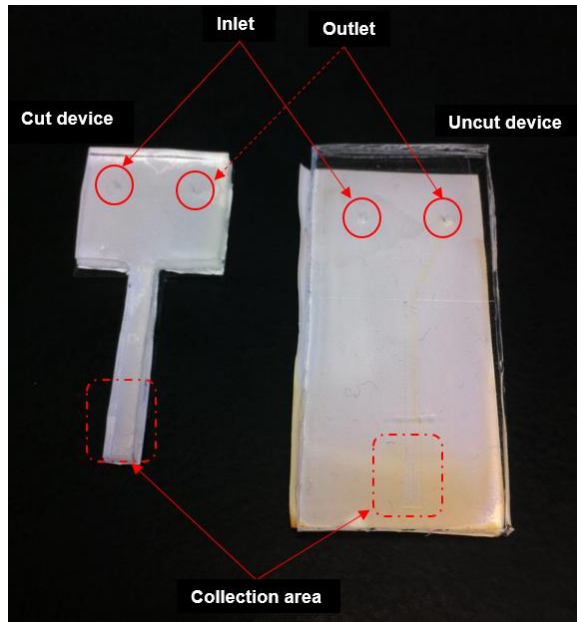

Figure 5.41. Microfluidic device during fluid verification testing at 2.0 µL/min using 4% dextran-500 as perfusion fluid. A small bubble was observed at the collection area during this experiment.

The relative recovery of methyl orange using this setting was 78.78% ± 2.46% (n = 3). The same setting was used on CMA/20 and CMA/12 microdialysis probes. The relative recovery of these probes was 89.38% ± 0.91% (n = 3) and 88.29 ± 2.88% (n = 3), respectively. The difference in relative recoveries of the microfluidic probes and the microfluidic device was significantly smaller during push-pull experiments than push experiments. Based on these results it can be stated that the thickness of the membrane is the main source for a lower relative recovery as compared to the microdialysis probes. Figure 5.42 shows the relative recoveries of the full sequence used for the push-pull experiments performed on the microfluidic device. The full sequence was compared to the push-pull recoveries of the CMA/20 and CMA/12 microdialysis probes. All the experiments were conducted on uncut microfluidic devices, see Figure 5.43. This was done to reduce time and minimize the possibility of breaking the device. Figure 5.44 shows the microdialysis probes in series approach before and after miniaturization into the PDMS microfluidic device.
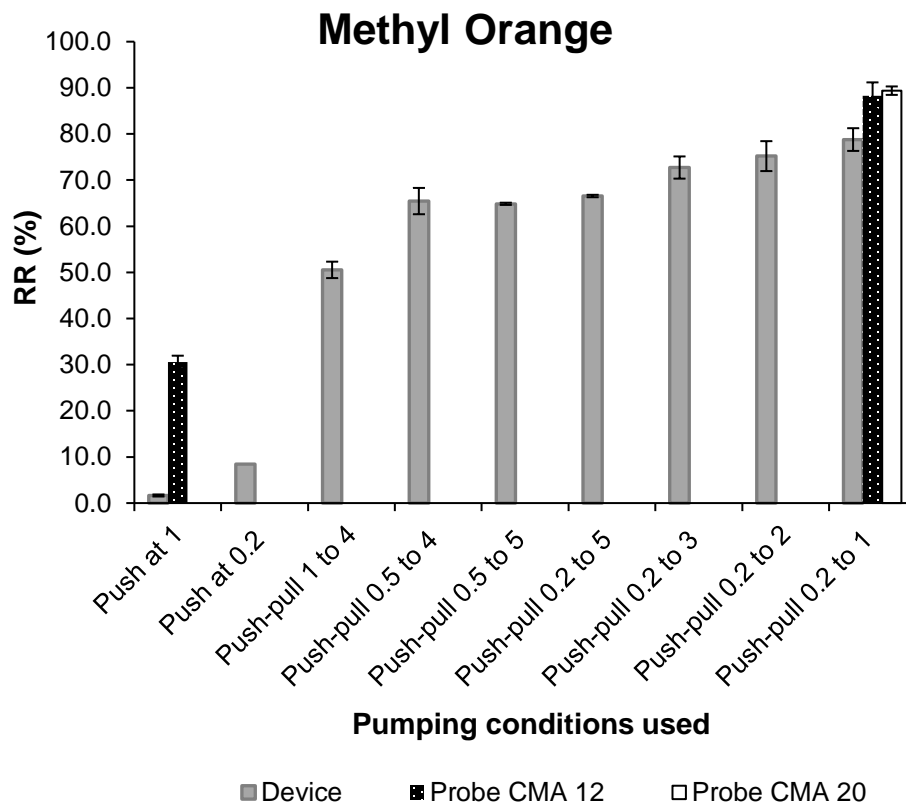

Figure 5.42. Comparison of relative recovery of methyl orange performed on the microfluidic device and microdialysis probes (CMA 20 and CMA 12) under different pumping conditions. Note that for push at 0.2 µL/min n = 2 and for the rest n = 3 and average ± standard deviation

Figure 5.43. Cut and uncut PDMS microfluidic devices. Uncut microfluidic devices were the only one used for testing.
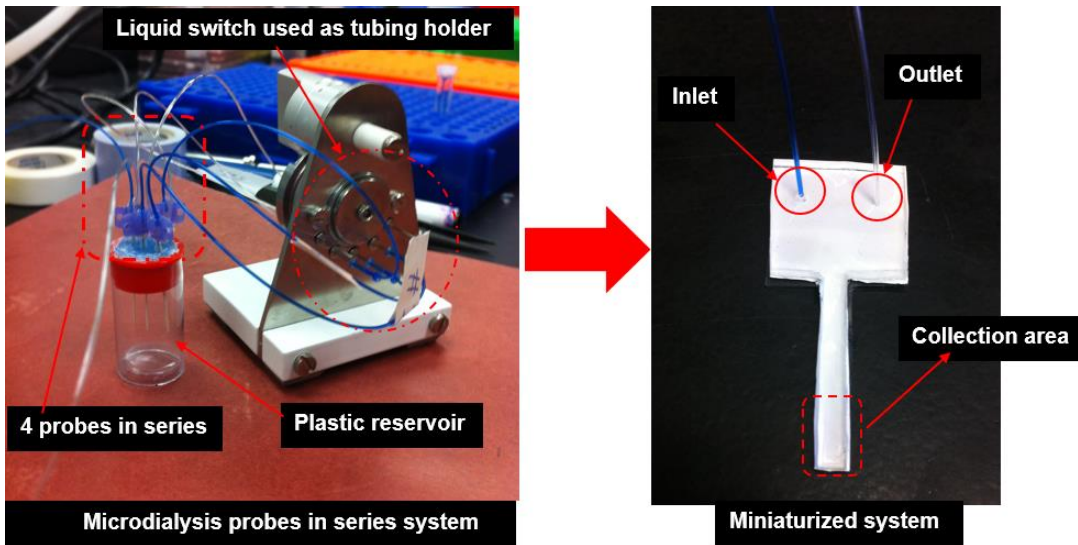
Figure 5.44. Microdialysis probes in series system, left, miniaturized into a PDMS microfluidic device, right.

The results of the estimations, performed to further elucidate the source of variation between the relative recovery of the device and the two microdiaysis probes, are shown on Table 5.2. These estimations indicated that the microfluidic device had a surface area three and seven times smaller than the CMA/12 and CMA/20 microdialysis probes, respectively. As previously stated, the surface area of the membrane is directly related to the relative recovery. This means that the device could be further improved by increasing the surface area of the membrane. The linear velocity and resistance to the flow for the microfluidic device were higher than the microdialysis probes. Consequently, the residence time of the device was shorter than the microdialysis probes, limiting the relative recovery of the device. Increasing the residence time of the collection area in the device could further improve the relative recovery.

Table 5.2. Surface area, linear velocity, pressure drop, and resistance to the flow estimations for the microfluidic device, CMA/12 and CMA/20 microdialysis probes. The results of the push-pull experiments were added as reference.

Type of system	Membrane length (mm)	Surface area (mm^2)	v (m/s)	$\Re_a$ or R_h (Pa.s/m^3)	Δp_a or ΔP (Pa)	Push-pull RR (%)
Microfluidic device	4.4	~2	5×10^{-3}	3×10^{12}	56	78.78 ± 2.46
CMA/12 probe	4.0	~6	8×10^{-4}	8×10^{10}	8×10^{10}	88.29 ± 2.88
CMA/20 probe	10.0	~14	9×10^{-4}	2×10^{11}	2×10^{11}	89.38 ± 0.91

5.2.3.6.1.3 Conclusions

After multiple iterations (7), a PMDS microfluidic device able to mimic current microdialysis sample probes was developed. The microfluidic device was able to collect 8.41% ± 0.31% (n = 2) and 1.64% ± 0.22% (n = 3) of methyl orange when push experiments were performed at 0.2 µL/min and 1.0 µL/min respectively. Compared to the relative recovery (30.60% ± 1.35% (n = 3)) of methyl orange collected using a CMA/12 microdialysis probe at 1.0 µL/min and under the same conditions, the relative recovery of methyl orange from the device was very low. This indicates that the microfluidic device is collecting molecules, but still needs to be optimized. One of the sources of the devices poor performance could be the thickness of the PES membrane used. The thickness of the hollow fiber membrane used with commercial microdialysis probes are 50 µm (including support layer, ~45 µm) and the thickness of the flat PES membrane used for the device was ~150 µm. This difference in thickness could increase the resistance of the membrane during the experiments reducing the performance of the device. The influence of thickness on the performance of the microfluidic device was elucidated when push-pull experiments were conducted.

The optimal setting for the push-pull experiments was found to be push at 0.2 µL/min and pull at 1.0 µL/min. The push-pull results showed that the microfluidic device was able to perform at the same level than microdialysis probes without any optimization.

The relative recovery of methyl orange collected using the microfluidic device was 78.78% ± 2.46% (n = 3) and for the microdialysis probes was 89.38% ± 0.91% (n = 3) and 88.29 ± 2.88% (n = 3) for CMA/20 and CMA/12 respectively. The work shown on this chapter could be the first step into minimizing the need for microdialysis calibration methods. The microfluidic device developed for this dissertation could be further optimized to achieve the same or better performance as the microdialysis probes in series method. This could be done by using a thinner (4 µm) PES membrane for the microfluidic device and increasing the surface area of the membrane.

5.3 References

1. Tüdős, A. J.; Besselink, G. A.; Schasfoort, R. B., Trends in miniaturized total analysis systems for point-of-care testing in clinical chemistry. *Lab on a Chip* **2001,** *1* (2), 83-95.

2. Hsieh, Y.-C.; Zahn, J. D., Glucose recovery in a microfluidic microdialysis biochip. *Sensors and Actuators B: Chemical* **2005,** *107* (2), 649-656.

3. Kricka, L. J., Miniaturization of analytical systems. *Clinical Chemistry* **1998,** *44* (9), 2008-2014.
4. Varteresian, J., *Fabricating printed circuit boards*. Newnes: 2002.

5. Espinal Cabrera, R. F. Development of a microfluidic device coupled to microdialysis sampling for the pre-concentration of cytokines. M.S., University of Arkansas, United States -- Arkansas, 2012.

6. Corp., M. SU-8 3000 Permanent Epoxy Negative Photoresist Data Sheet.

7. Aran, K.; Sasso, L. A.; Kamdar, N.; Zahn, J. D., Irreversible, direct bonding of nanoporous polymer membranes to PDMS or glass microdevices. *Lab on a Chip* **2010,** *10* (5), 548-552.

8. Bhattacharya, S. Plasma bonding of poly (dimethyl) siloxane and glass surfaces and its application to microfluidics. Texas Tech University, 2003.

9. http://www.sterlitech.com/polyethersulfone-membrane-filter-pes019025.html.

10. Bungay, P. M.; Wang, T.; Yang, H.; Elmquist, W. F., Utilizing transmembrane convection to enhance solute sampling and delivery by microdialysis: Theory and in vitro validation. *Journal of membrane science* **2010,** *348* (1), 131-149.

11. R. K. Shah and A. L. London, Laminar Flow Forced Conv ection in Ducts, Academic Press, New York, 1978.

6   Chapter 6.   Conclusions and Future Work

6.1   Conclusions

The growing interest in developing microdialysis-based microfluidic devices, increasing the efficiency (relative recovery) of microdialysis sampling method, and eliminating the microdialysis sampling cumbersome and time-consuming calibration methods, were the main factors for the research work presented in this dissertation. A new sampling method coined "microdialysis probes in series" was developed using microdialysis sampling probes connected in series. The microdialysis probes in series method was devised after working with the recycling flow method previously used by several researchers.[1-3] The recycling flow method was described in detail in Chapter 2. The new method improved the efficiency of microdialysis sampling by 33% for methyl orange and 2% for FITC-40 when experiments were conducted at a pumping rate of 0.8 µL/min. The method was more effective for small molecules such as methyl orange (MW = 330 Da), FITC-4 (MW = 4,000 Da), and FITC-10 (MW = 10,000 Da). On the other hand, when larger molecules were collected using this method the efficiency was lower. For example, the efficiencies of FITC-20 (MW = 20,000 Da) and FITC-40 (MW = 40,000 Da) were 4% and 2% respectively when collected at 0.8 µL/min. The microdialysis sampling probes used for this work had a concentric semi-permeable polyethersulfone membrane of 10 mm in length and molecular weight cutoff of 100,000 Da. One of the reasons for the lower efficiencies could be that the molecular weight cutoff of the microdialysis probes used were either closer or over the recommend values. The Harvard Apparatus Company that makes the microdialysis probes used for this work recommend choosing the molecular weight cutoff based on the molecular weight of the target analyte. They suggest to use microdialysis probes having membranes with molecular weight cutoff of four times the molecular weight of the target analyte.[4] This means in order to efficiently collect a molecule of 40 kDa, a microdialysis sampling probe having a MWCO of 120 kDa should be chosen. However, the FITC-20 or 20 kDa molecule still within the MWCO of the microdialysis sampling probe used for this work (100 kDa). Molecular weight cut off alone cannot explain the poor efficiency of the microdialysis probes.

A mathematical model based on Bungay's and Jacobson's methods was used to estimate how many probes in series were necessary to reach equilibrium between the inner and outer concentrations of analyte in the microdialysis probes. For small molecules like methyl orange and FITC-4 the model was in close agreement with experiments (section 4.2), but for larger molecules like FITC-10, FITC-20, and FITC-40 the model started deviating from experiments. For instance, the model predicted a relative recovery of methyl orange collected using four probes in series at a flow rate of 0.8 µL/min to be 98.8% compared to 99.7% ± 0.9% obtained experimentally. On the other hand, for the same conditions the relative recovery of FITC-40 was predicted to be 21.4% compared to 7.7% ± 0.1% obtained experimentally. However, after taking into account the fluid loss the model predictions were in agreement with experiments (Figure 4.7). A better understanding of how osmotic, transmembrane, and hydraulic pressures influence the efficiency (RR) of the microdialysis probes in series method during collection of molecules, could be valuable to develop a microdialysis-based microfluidic device. If the balance of those forces is understood for the microdialysis probes in series method, a microfluidic device could be engineering taking advantage of them.

The microdialysis probes in series method was miniaturized into a PDMS microfluidic device. This microdialysis-based microfluidic system was able to mimic a regular microdialysis probes efficiency under certain conditions (e.g., push-pull). For example, the collections conducted at a pushing rate of 0.2 µL/min and pulling rate of 1.0 µL/min using methyl orange as analyte were 78.8% ± 2.5%, 88.3% ± 2.9%, and 89.4% ± 0.9% using the microdialysis-based microfluidic system, CMA/12, and CMA/20 microdialysis probes respectively. These results indicated that the microdialysis-based microfluidic device needs further optimization.

6.2 Future Work

One of the future work that could be done to elucidate the poor efficiency of the microdialysis sampling probes in series for large molecules is to study different compounds with uniform radius of gyration and different molecule weights. This would minimize the influence of the molecular conformation during the experiments. More experiments should to be done using the microdialysis probes in series method. One of the experiments that should be done is an experiment placing each microdialysis sampling probe in series (4) in separate vials.

This experiment would show the contribution of each connection to fluid loss or how much pressure is generated at each point. As mentioned before in Chapter 1 section 1.5.2.2, several researcher have devised methods to systematically regulate the pressure inside and outside of a microdialysis sampling probe to find optimal conditions, see Figure 1.15.[5] However, as far as this author knows, the same type of experiments have not be done using microdialysis probes in series. A similar experiment like Chu et al. could be performed using their chamber, but connecting four microdialysis probes in series. For their work, they did not connect each probe in series. Using a chamber like the one show on Figure 1.15 would simplify the study of how the osmotic, transmembrane, and hydraulic pressures influence the relative recovery of molecules. This would lead to the optimal conditions of the microdialysis probes in series for different molecules. The work done by Chu et al. showed how those forces influenced the relative recovery of one microdialysis probes. The information obtained about those forces during microdialysis probes in series, would lead to the design of a more efficient microdialysis-based microfluidic system.

6.3 References

1. Lerma, J.; Herranz, A. S.; Herreras, O.; Abraira, V.; Martin del Rio, R., In vivo determination of extracellular concentration of amino acids in the rat hippocampus. A method based on brain dialysis and computerized analysis. *Brain Res* **1986,** *384* (1), 145-55.

2. Sternberg, F.; Meyerhoff, C.; Mennel, F. J.; Hoss, U.; Mayer, H.; Bischof, F.; Pfeiffer, E. F., Calibration problems of subcutaneous glucosensors when applied \"in-situ\" in man. *Hormone and Metabolic Research* **1994,** *26* (11), 523-5.

3. Sternberg, F.; Meyerhoff, C.; Mennel, F. J.; Bischof, F.; Pfeiffer, E. F., Subcutaneous glucose concentration in humans: real estimation and continuous monitoring. *Diabetes Care* **1995,** *18* (9), 1266-1269.

4. www.microdialysis.com/us/basic-research/faq-basic-research.

5. Chu, J.; Hjort, K.; Larsson, A.; Dahlin, A. P. In *Consequence of static pressure on transmembrane exchanges during in vitro microdialysis sampling of proteins*, Monitoring Molecules in Neuroscience: 14th International Conference, September 16–20, London, UK, 2012.

CHAPTER 1

Permissions:

For Figure 1.4

ELSEVIER LICENSE
TERMS AND CONDITIONS

Apr 05, 2017

This Agreement between Randy Espinal ("You") and Elsevier ("Elsevier") consists of your license details and the terms and conditions provided by Elsevier and Copyright Clearance Center.

License Number	4045500948312
License date	
Licensed Content Publisher	Elsevier
Licensed Content Publication	Journal of Neuroscience Methods
Licensed Content Title	A survey on quantitative microdialysis: theoretical models and practical implications
Licensed Content Author	Jan Kehr
Licensed Content Date	July 1993
Licensed Content Volume	48
Licensed Content Issue	3
Licensed Content Pages	11
Start Page	251
End Page	261
Type of Use	reuse in a thesis/dissertation
Portion	figures/tables/illustrations
Number of figures/tables/illustrations	1
Format	both print and electronic
Are you the author of this Elsevier article?	No
Will you be translating?	No
Order reference number	
Original figure numbers	Figure 2
Title of your thesis/dissertation	Development of Microdialysis Probes in Series Approach Toward Eliminating Microdialysis Sampling Calibration: Miniaturization into a PDMS Microfluidic Device

Expected completion date	May 2017
Estimated size (number of pages)	140
Elsevier VAT number	GB 494 6272 12
	Randy Espinal University of Arkansas CHEM 119
Requestor Location	
	FAYETTEVILLE, AR 72701 United States Attn: Randy Espinal
Publisher Tax ID	98-0397604
Total	0.00 USD

For Figure 1.5

ELSEVIER LICENSE
TERMS AND CONDITIONS
Apr 10, 2017

This Agreement between Randy Espinal ("You") and Elsevier ("Elsevier") consists of your license details and the terms and conditions provided by Elsevier and Copyright Clearance Center.

License Number	4045491358853
License date	
Licensed Content Publisher	Elsevier
Licensed Content Publication	Journal of Membrane Science
Licensed Content Title	Effect of pumping methods on transmembrane pressure, fluid balance and relative recovery in microdialysis
Licensed Content Author	Zhaohui Li,David Hughes,Jill P.G. Urban,Zhanfeng Cui
Licensed Content Date	5 March 2008
Licensed Content Volume	310
Licensed Content Issue	1-2
Licensed Content Pages	9
Start Page	237
End Page	245
Type of Use	reuse in a thesis/dissertation
Portion	figures/tables/illustrations

Number of figures/tables/illustrations	1
Format	both print and electronic
Are you the author of this Elsevier article?	No
Will you be translating?	No
Order reference number	
Original figure numbers	Figure 2
Title of your thesis/dissertation	Development of Microdialysis Probes in Series Approach Toward Eliminating Microdialysis Sampling Calibration: Miniaturization into a PDMS Microfluidic Device
Expected completion date	May 2017
Estimated size (number of pages)	140
Elsevier VAT number	GB 494 6272 12
Requestor Location	Randy Espinal University of Arkansas CHEM 119 FAYETTEVILLE, AR 72701 United States Attn: Randy Espinal
Publisher Tax ID	98-0397604
Total	0.00 USD

For Figure 1.9

For Figure 1.10 (Original Source)

ELSEVIER LICENSE
TERMS AND CONDITIONS

Apr 11, 2017

This Agreement between Randy Espinal ("You") and Elsevier ("Elsevier") consists of your license details and the terms and conditions provided by Elsevier and Copyright Clearance Center.

License Number	4045520322733
License date	Feb 10, 2017
Licensed Content Publisher	Elsevier
Licensed Content Publication	Journal of Neuroscience Methods
Licensed Content Title	Mass transfer in brain dialysis devices—a new method for the estimation of extracellular amino acids concentration
Licensed Content Author	I. Jacobson,M. Sandberg,A. Hamberger
Licensed Content Date	November–December 1985
Licensed Content Volume	15
Licensed Content Issue	3
Licensed Content Pages	6
Start Page	263
End Page	268
Type of Use	reuse in a thesis/dissertation
Intended publisher of new work	other
Portion	figures/tables/illustrations
Number of figures/tables/illustrations	1
Format	both print and electronic
Are you the author of this Elsevier article?	No
Will you be translating?	No
Order reference number	
Original figure numbers	Figure 1
Title of your thesis/dissertation	Development of Microdialysis Probes in Series Approach Toward Eliminating Microdialysis Sampling Calibration: Miniaturization into a PDMS Microfluidic Device
Expected completion date	May 2017

Estimated size (number of pages)	140
Elsevier VAT number	GB 494 6272 12
	Randy Espinal University of Arkansas CHEM 119
Requestor Location	
	FAYETTEVILLE, AR 72701 United States Attn: Randy Espinal
Publisher Tax ID	98-0397604
Total	0.00 USD

For Figure 1.10 (Printed from)

ELSEVIER LICENSE
TERMS AND CONDITIONS
Sep 17, 2017

This Agreement between Randy Espinal ("You") and Elsevier ("Elsevier") consists of your license details and the terms and conditions provided by Elsevier and Copyright Clearance Center.

License Number	4093690942428
License date	Apr 21, 2017
Licensed Content Publisher	Elsevier
Licensed Content Publication	Elsevier Books
Licensed Content Title	Techniques in the Behavioral and Neural Sciences
Licensed Content Author	B.H.C. Westerink,J.B. Justice
Licensed Content Date	Jan 1, 1991
Licensed Content Volume	7
Licensed Content Issue	n/a
Licensed Content Pages	21
Start Page	23
End Page	43
Type of Use	reuse in a thesis/dissertation
Intended publisher of new work	other
Portion	figures/tables/illustrations
Number of figures/tables/illustrations	1
Format	both print and electronic

Are you the author of this Elsevier chapter?	No
Will you be translating?	No
Original figure numbers	figure 3
Title of your thesis/dissertation	Development of Microdialysis Probes in Series Approach Toward Eliminating Microdialysis Sampling Calibration: Miniaturization into a PDMS Microfluidic Device
Expected completion date	May 2017
Estimated size (number of pages)	140

For Figure 1.11

Licensed Content Publisher	Elsevier
Licensed Content Publication	Biosensors and Bioelectronics
Licensed Content Title	Natural and synthetic affinity agents as microdialysis sampling mass transport enhancers: Current progress and future perspectives
Licensed Content Author	Jia Duo,Heidi Fletcher,Julie A. Stenken
Licensed Content Date	15 September 2006
Licensed Content Volume	22
Licensed Content Issue	3
Licensed Content Pages	9
Start Page	449
End Page	457
Type of Use	reuse in a thesis/dissertation
Intended publisher of new work	other
Portion	figures/tables/illustrations
Number of figures/tables/illustrations	1
Format	both print and electronic
Are you the author of this Elsevier article?	No
Will you be translating?	No
Order reference number	
Original figure numbers	Figure 1
Title of your thesis/dissertation	Development of Microdialysis Probes in Series Approach Toward Eliminating Microdialysis Sampling Calibration: Miniaturization into a PDMS Microfluidic Device
Expected completion date	May 2017
Estimated size (number of pages)	140
Elsevier VAT number	GB 494 6272 12
Requestor Location	Randy Espinal University of Arkansas CHEM 119 FAYETTEVILLE, AR 72701 United States Attn: Randy Espinal
Publisher Tax ID	98-0397604
Total	0.00 USD

Figure 1.12

ELSEVIER LICENSE
TERMS AND CONDITIONS
Apr 10, 2017

This Agreement between Randy Espinal ("You") and Elsevier ("Elsevier") consists of your license details and the terms and conditions provided by Elsevier and Copyright Clearance Center.

License Number	4085661416860
License date	
Licensed Content Publisher	Elsevier
Licensed Content Publication	Brain Research
Licensed Content Title	In vivo determination of extracellular concentration of amino acids in the rat hippocampus. A method based on brain dialysis and computerized analysis
Licensed Content Author	J. Lerma, A.S. Herranz, O. Herreras, V. Abraira, R. Martin del Rio
Licensed Content Date	1 October 1986
Licensed Content Volume	384
Licensed Content Issue	1
Licensed Content Pages	11
Start Page	145
End Page	155
Type of Use	reuse in a thesis/dissertation
Intended publisher of new work	other
Portion	figures/tables/illustrations
Number of figures/tables/illustrations	1
Format	both print and electronic
Are you the author of this Elsevier article?	No
Will you be translating?	No
Order reference number	
Original figure numbers	Figure 1
Title of your thesis/dissertation	Development of Microdialysis Probes in Series Approach Toward Eliminating Microdialysis Sampling Calibration: Miniaturization into a PDMS Microfluidic Device
Expected completion date	May 2017

| Estimated size (number of pages) | 140 |

| Elsevier VAT number | GB 494 6272 12 |

Randy Espinal
University of Arkansas CHEM 119

Requestor Location

FAYETTEVILLE, AR 72701
United States
Attn: Randy Espinal

| Publisher Tax ID | 98-0397604 |
| Total | 0.00 USD |

For Figure 1.14

ELSEVIER LICENSE
TERMS AND CONDITIONS
Apr 10, 2017

This Agreement between Randy Espinal ("You") and Elsevier ("Elsevier") consists of your license details and the terms and conditions provided by Elsevier and Copyright Clearance Center.

License Number	4085681056635
License date	
Licensed Content Publisher	Elsevier
Licensed Content Publication	Journal of Membrane Science
Licensed Content Title	Utilizing transmembrane convection to enhance solute sampling and delivery by microdialysis: Theory and in vitro validation
Licensed Content Author	Peter M. Bungay,Tianli Wang,Hua Yang,William F. Elmquist
Licensed Content Date	15 February 2010
Licensed Content Volume	348
Licensed Content Issue	1-2
Licensed Content Pages	19
Start Page	131
End Page	149
Type of Use	reuse in a thesis/dissertation
Intended publisher of new work	other

Portion	figures/tables/illustrations
Number of figures/tables/illustrations	1
Format	both print and electronic
Are you the author of this Elsevier article?	No
Will you be translating?	No
Order reference number	
Original figure numbers	Figure 4
Title of your thesis/dissertation	Development of Microdialysis Probes in Series Approach Toward Eliminating Microdialysis Sampling Calibration: Miniaturization into a PDMS Microfluidic Device
Expected completion date	May 2017
Estimated size (number of pages)	140
Elsevier VAT number	GB 494 6272 12
Requestor Location	Randy Espinal University of Arkansas CHEM 119 FAYETTEVILLE, AR 72701 United States Attn: Randy Espinal
Publisher Tax ID	98-0397604
Total	0.00 USD

For Figure 1.15

For Figure 1.18

ROYAL SOCIETY OF CHEMISTRY LICENSE
TERMS AND CONDITIONS
Apr 10, 2017

This Agreement between Randy Espinal ("You") and Royal Society of Chemistry ("Royal Society of Chemistry") consists of your license details and the terms and conditions provided by Royal Society of Chemistry and Copyright Clearance Center.

License Number	4085691494159
License date	
Licensed Content Publisher	Royal Society of Chemistry
Licensed Content Publication	Lab on a Chip
Licensed Content Title	Membranes and microfluidics: a review
Licensed Content Author	J. de Jong,R. G. H. Lammertink,M. Wessling
Licensed Content Date	Jul 14, 2006
Licensed Content Volume	6
Licensed Content Issue	9
Type of Use	Thesis/Dissertation
Requestor type	academic/educational
Portion	figures/tables/images
Number of figures/tables/images	1
Format	print and electronic
Distribution quantity	1
Will you be translating?	no
Order reference number	
Title of the thesis/dissertation	Development of Microdialysis Probes in Series Approach Toward Eliminating Microdialysis Sampling Calibration: Miniaturization into a PDMS Microfluidic Device
Expected completion date	May 2017
Estimated size	140
	Randy Espinal University of Arkansas CHEM 119
Requestor Location	
	FAYETTEVILLE, AR 72701 United States Attn: Randy Espinal
Billing Type	Invoice

Randy Espinal
University of Arkansas CHEM 119

Billing Address

FAYETTEVILLE, AR 72701
United States
Attn: Randy Espinal

Total   0.00 USD

For Table 1.5

ROYAL SOCIETY OF CHEMISTRY LICENSE
TERMS AND CONDITIONS
Apr 10, 2017

This Agreement between Randy Espinal ("You") and Royal Society of Chemistry ("Royal Society of Chemistry") consists of your license details and the terms and conditions provided by Royal Society of Chemistry and Copyright Clearance Center.

License Number	4085700435426
License date	
Licensed Content Publisher	Royal Society of Chemistry
Licensed Content Publication	Lab on a Chip
Licensed Content Title	Trends in miniaturized total analysis systems for point-of-care testing in clinical chemistry
Licensed Content Author	Anna J. Tüdős,Geert A. J. Besselink,Richard B. M. Schasfoort
Licensed Content Date	Nov 27, 2001
Licensed Content Volume	1
Licensed Content Issue	2
Type of Use	Thesis/Dissertation
Requestor type	academic/educational
Portion	figures/tables/images
Number of figures/tables/images	1
Format	print and electronic
Distribution quantity	1
Will you be translating?	no
Order reference number	Table 4

Title of the thesis/dissertation	Development of Microdialysis Probes in Series Approach Toward Eliminating Microdialysis Sampling Calibration: Miniaturization into a PDMS Microfluidic Device
Expected completion date	May 2017
Estimated size	140
Requestor Location	Randy Espinal University of Arkansas CHEM 119 FAYETTEVILLE, AR 72701 United States Attn: Randy Espinal
Billing Type	Invoice
Billing Address	Randy Espinal University of Arkansas CHEM 119 FAYETTEVILLE, AR 72701 United States Attn: Randy Espinal
Total	0.00 USD

For Table 1.6 and Figure 1.19

ROYAL SOCIETY OF CHEMISTRY LICENSE
TERMS AND CONDITIONS
Apr 10, 2017

License Number	4085700790034
License date	
Licensed Content Publisher	Royal Society of Chemistry
Licensed Content Publication	Lab on a Chip
Licensed Content Title	Membranes and microfluidics: a review
Licensed Content Author	J. de Jong,R. G. H. Lammertink,M. Wessling
Licensed Content Date	Jul 14, 2006
Licensed Content Volume	6
Licensed Content Issue	9
Type of Use	Thesis/Dissertation

Requestor type	academic/educational
Portion	figures/tables/images
Number of figures/tables/images	2
Format	print and electronic
Distribution quantity	1
Will you be translating?	no
Order reference number	Table 1 and Figure 6
Title of the thesis/dissertation	Development of Microdialysis Probes in Series Approach Toward Eliminating Microdialysis Sampling Calibration: Miniaturization into a PDMS Microfluidic Device
Expected completion date	May 2017
Estimated size	140
Requestor Location	Randy Espinal University of Arkansas CHEM 119 FAYETTEVILLE, AR 72701 United States Attn: Randy Espinal
Billing Type	Invoice
Billing Address	Randy Espinal University of Arkansas CHEM 119 FAYETTEVILLE, AR 72701 United States Attn: Randy Espinal
Total	0.00 USD

For Figure 1.20

CHAPTER 5

Permissions:

For Figure 5.10

ROYAL SOCIETY OF CHEMISTRY LICENSE
TERMS AND CONDITIONS
Sep 17, 2017

This Agreement between Randy Espinal ("You") and Royal Society of Chemistry ("Royal Society of Chemistry") consists of your license details and the terms and conditions provided by Royal Society of Chemistry and Copyright Clearance Center.

License Number	4191611085735
License date	Sep 17, 2017
Licensed Content Publisher	Royal Society of Chemistry
Licensed Content Publication	Lab on a Chip
Licensed Content Title	Irreversible, direct bonding of nanoporous polymer membranes to PDMS or glass microdevices
Licensed Content Author	Kiana Aran,Lawrence A. Sasso,Neal Kamdar,Jeffrey D. Zahn
Licensed Content Date	Jan 7, 2010
Licensed Content Volume	10
Licensed Content Issue	5
Type of Use	Thesis/Dissertation
Requestor type	academic/educational
Portion	figures/tables/images
Number of figures/tables/images	1
Format	print and electronic
Distribution quantity	6
Will you be translating?	no
Order reference number	
Title of the thesis/dissertation	Development of Microdialysis Probes in Series Approach Toward Eliminating Microdialysis Sampling Calibration: Miniaturization into a PDMS Microfluidic Device
Expected completion date	May 2017
Estimated size	140
Requestor Location	Randy Espinal University of Arkansas CHEM 119

	FAYETTEVILLE, AR 72701
	United States
	Attn: Randy Espinal
Billing Type	Invoice
	Randy Espinal
	University of Arkansas CHEM 119
Billing Address	
	FAYETTEVILLE, AR 72701
	United States
	Attn: Randy Espinal
Total	0.00 USD